

SAR / Optical Applications to Ice and Snow

Gabriele SCHWAIZER

ENVEO Environmental Earth Observation IT GmbH

INNSBRUCK, AUSTRIA

ESA ECS Training Course on Earth Observation
Bratislava, Slovakia
21 September 2018

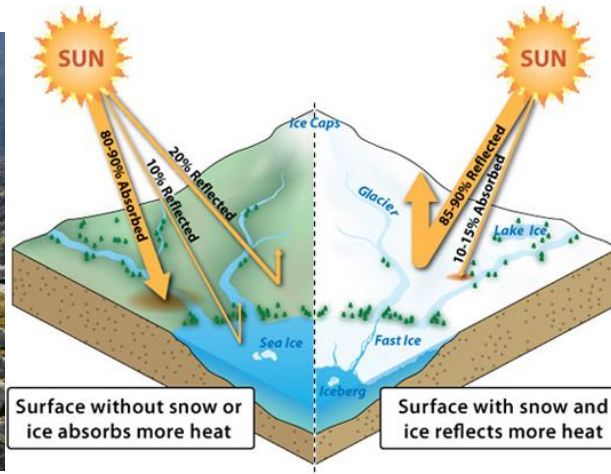
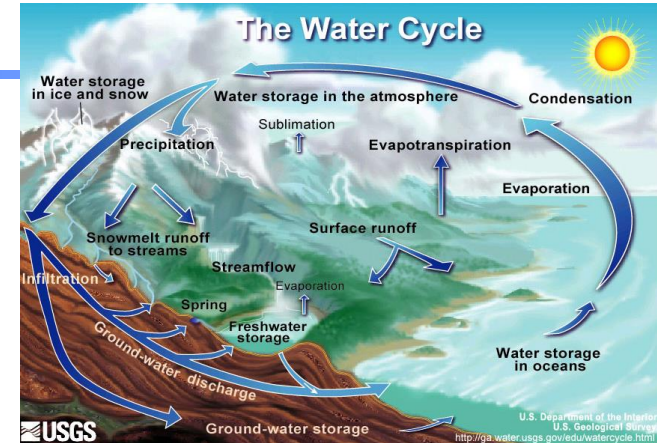


Ice in summer...



Why do we need information about snow and ice???

- Contribution to water cycle
- Water management (human consumption, agriculture, etc.)
- Hydropower generation
- Impact on the Earth's energy budget
- Input for hydrological / glacier mass balance / weather / climate / land surface models



... and because of...

- Impact on permafrost evolution and carbon exchange in high latitudes
- Natural hazards (avalanches, floods, ice jams, droughts, etc)
- Transportation, Housing
- Tourism, Sports



Content of Lecture

- A. General Characteristics of Ice and Snow**
- B. Remote Sensing of Snow and Ice**
- C. Snow and Ice from Radar Satellite data**
- D. Snow and Ice from Optical Satellite data**
- E. Concluding Remarks**

Practical Training – Schedule

2 Groups: execute each one main exercise:

- *Mapping snow from **Sentinel-2** optical data over the Alps*
- *Mapping wet snow from **Sentinel-1** SAR data over the Alps*

Timing:

13:30 – 15:00 & 15:15 – 16:30:

Process the data following the instructions of the exercises

You can either work alone or together with a colleague.

In case of any problems or questions, feel free to communicate with your colleagues, or just ask me!

16:30 – 17:00:

Interpretation of results (together)

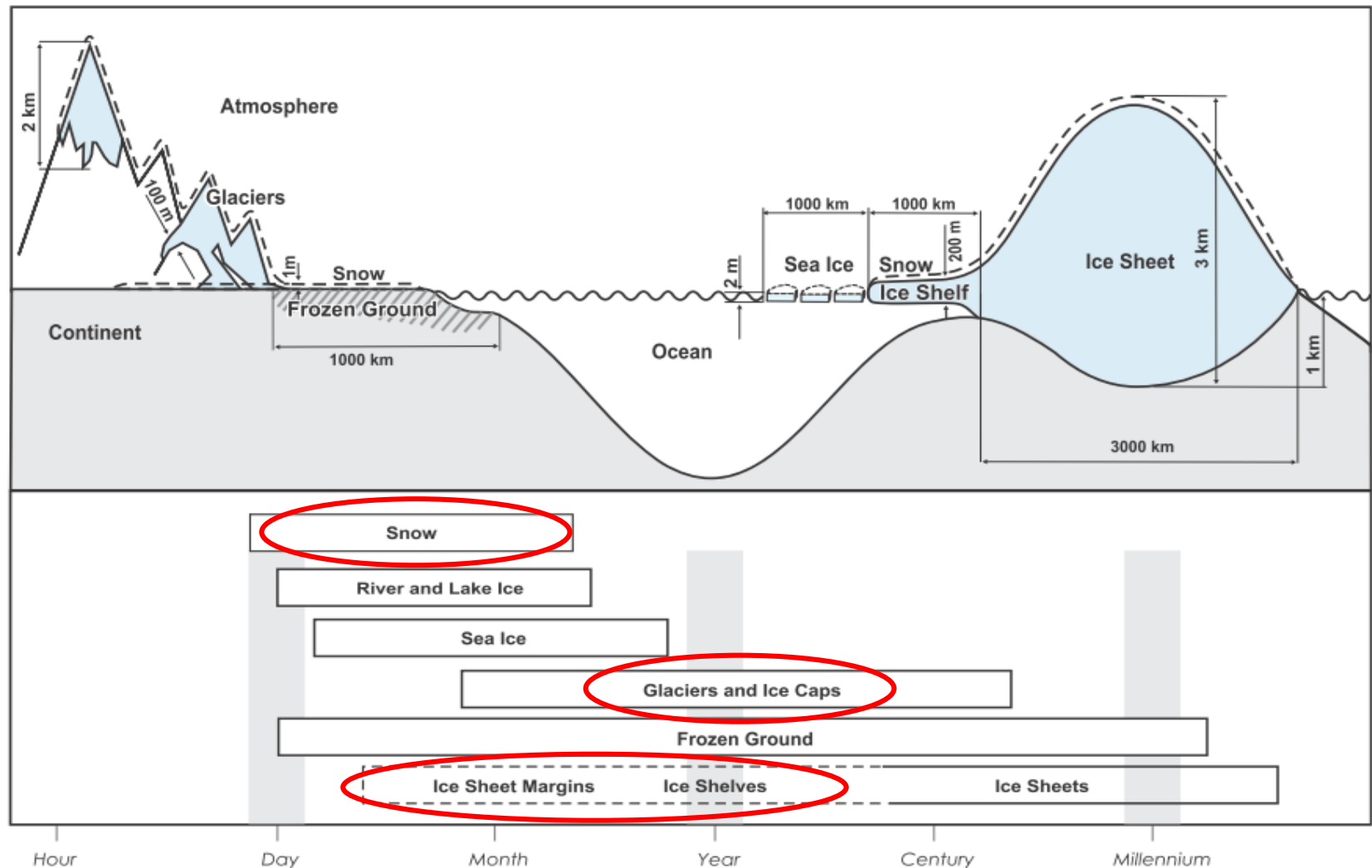
A. General characteristics of Ice and Snow



Part A – Contents

1. Components of the Cryosphere
2. Snow patterns in different environments
3. Types of ice sheets and glaciers
4. The physics of snow crystals
5. Transformation of snow to glacier ice
6. Typical densities of snow and ice

1. Components of the Cryosphere



Lemke et al., 2007

2. Examples of snow patterns in different environments...

Totally snow covered plains



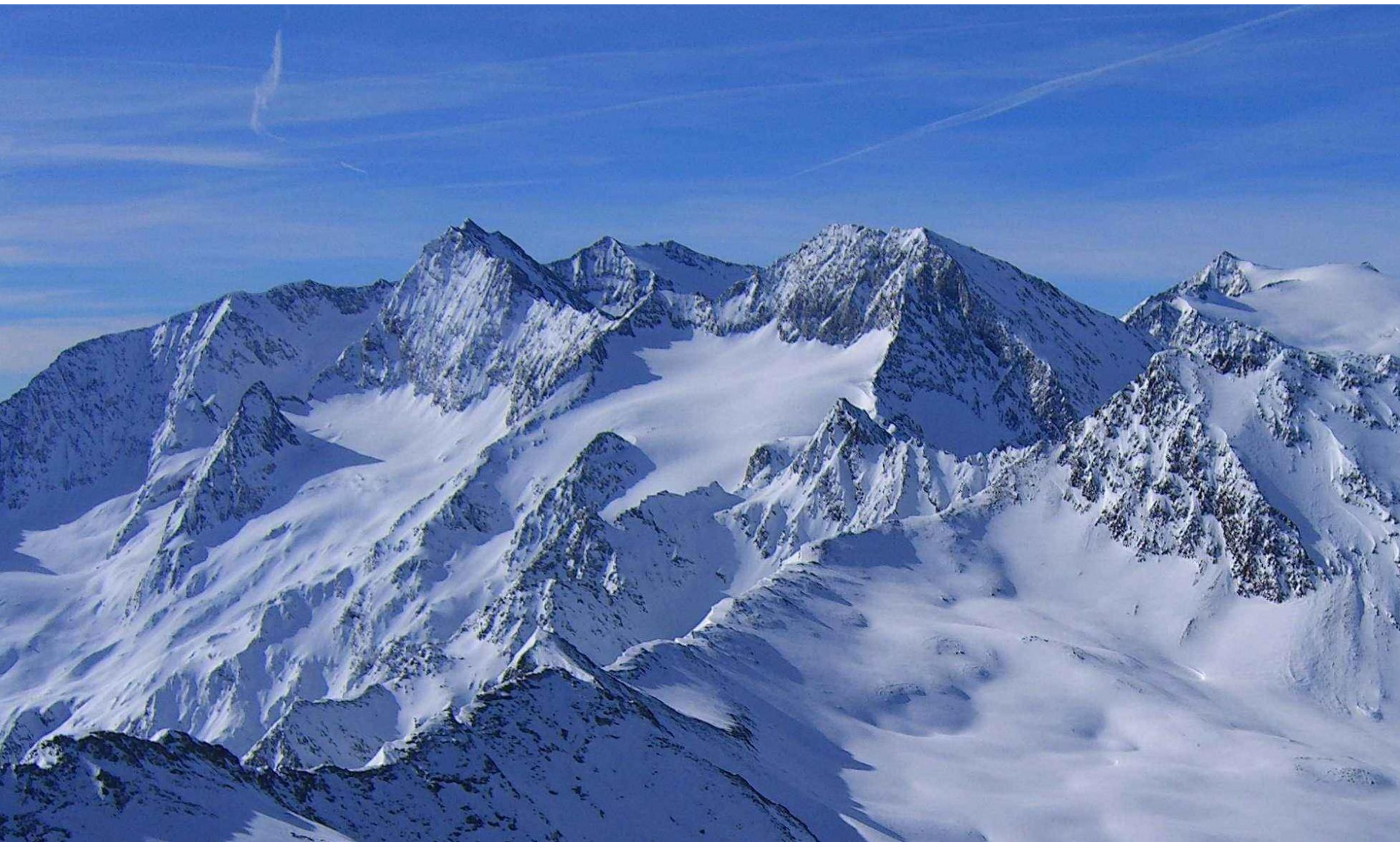
Totally snow covered sparse forest



Totally snow covered dense forest



Totally snow covered mountains



Patchy snow in mountains



Patchy snow cover in open land



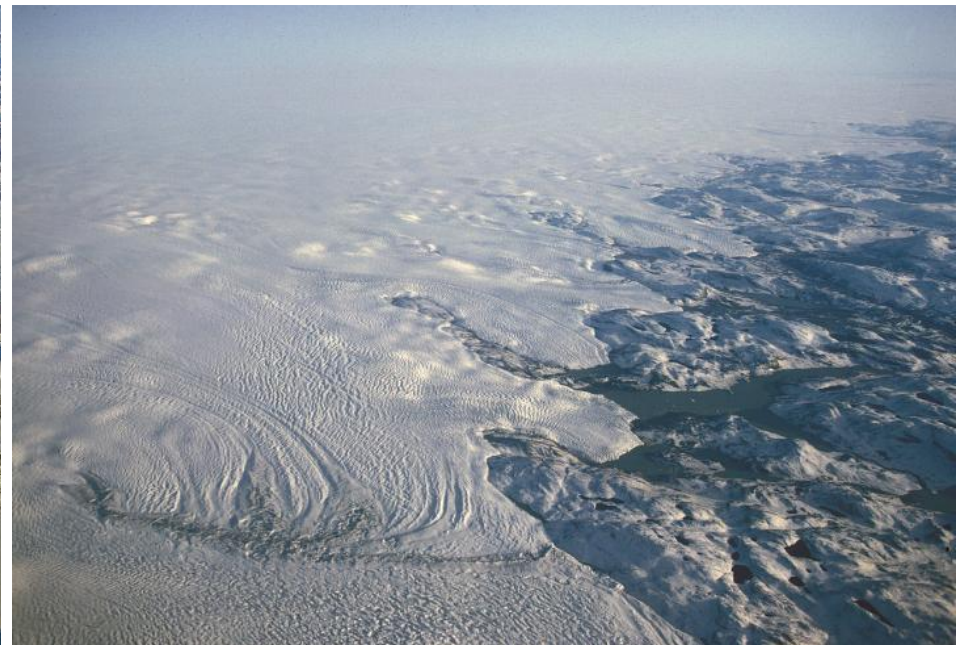
Patchy snow cover in forest



Snow in regions you wouldn't expect...



3. Types of ice sheets and glaciers – Greenland Ice Sheet



Antarctic Ice Sheet



Small mountain glaciers



Valley glacier with limited debris cover



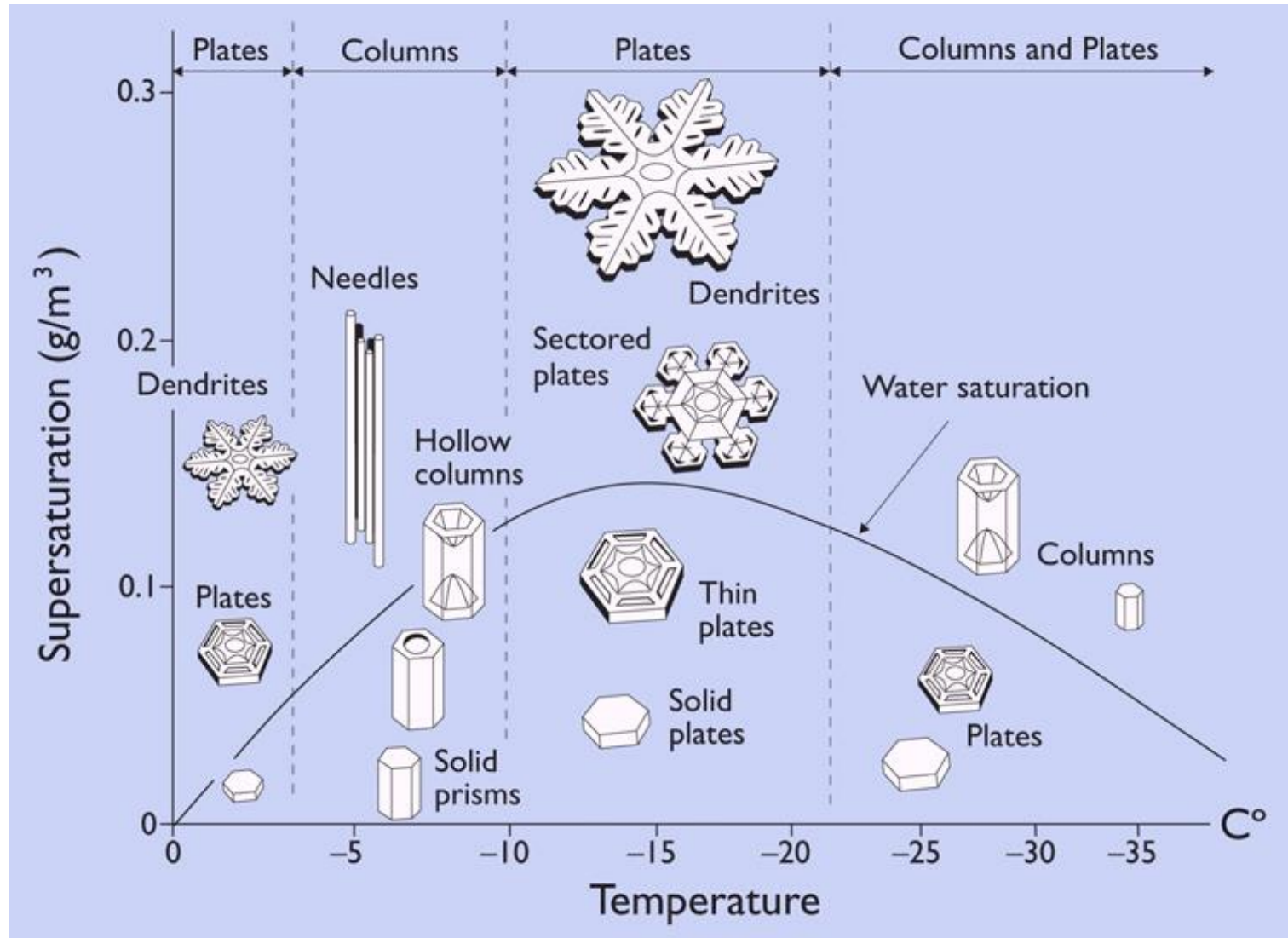
Valley glaciers with extensive debris cover



Calving glaciers



4. The physics of snow crystals



5. Transformation of snow to glacier ice

Definitions:

- *Snow*: seasonal snow that has not changed much since fell
- *Firn*: wetted snow that survived at least one summer season without being transformed into ice
- *Glacier ice*: crystals formed after sealing off all air passages between grains

Main processes to transform snow to glacier ice:

- Packing and/or settling
- Thermodynamic processes
- Deformation under load

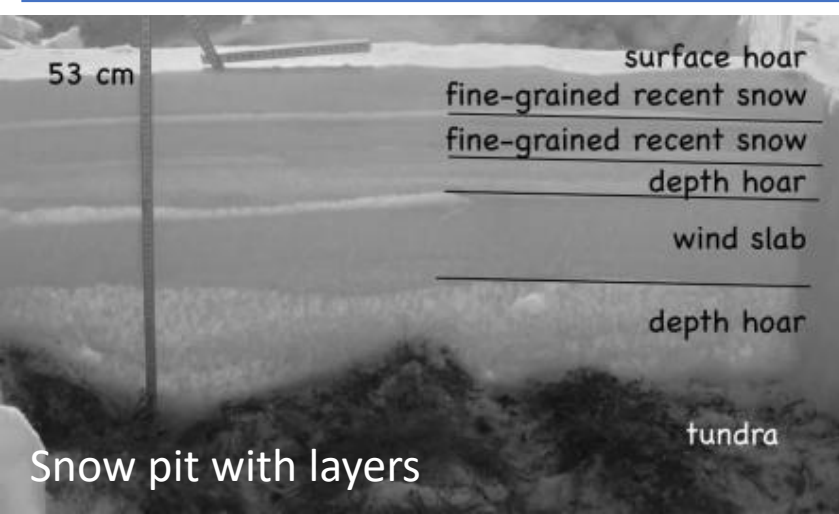
→ *About 80 cm new snow are needed to form 1 cm glacier ice*

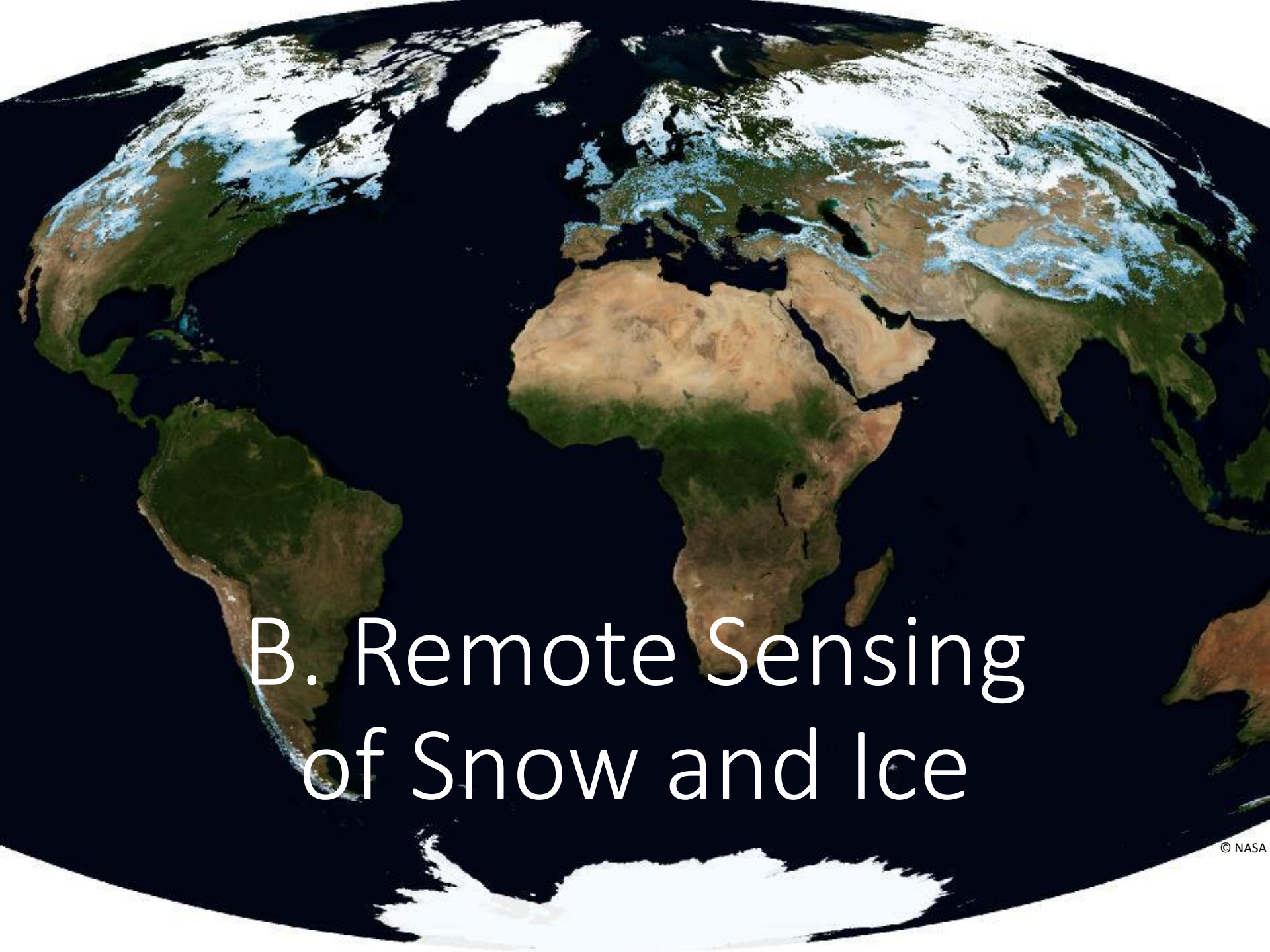


Glacier ice crystal

6. Typical densities of snow and ice

Type	(kg/m ³)	Fig.
New snow (immediately after falling in calm)	50 – 70	A
Damp new snow	100 – 200	
Settled snow	200 – 300	
Depth hoar	100 – 300	B
Wind packed snow	350 – 400	C
Firn (only when melting occurs)	400 – 830	D
Very wet snow and firn	700 – 800	
Glacier ice	830 – 917	E



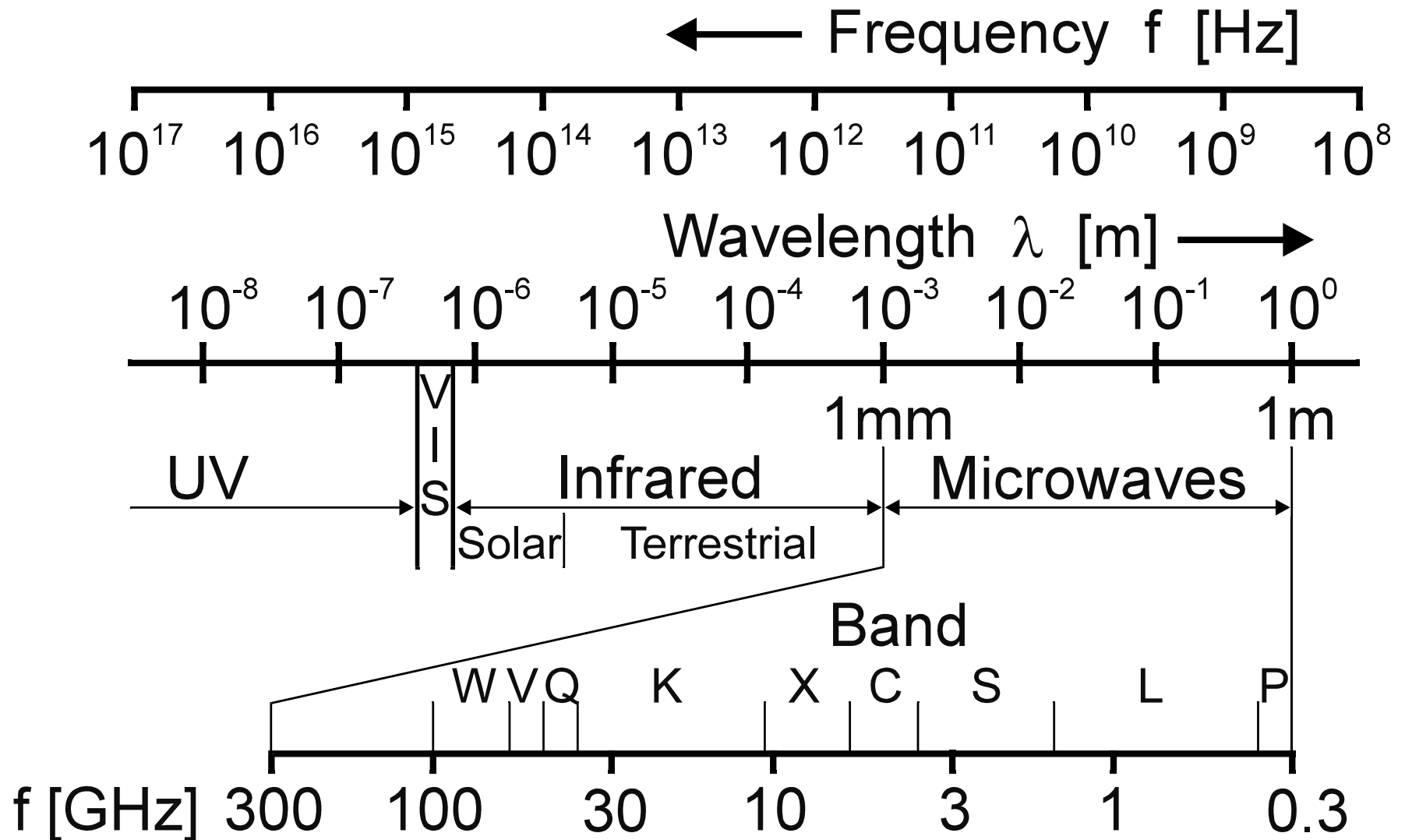
A satellite image of Earth showing the distribution of snow and ice. The image is a false-color composite where snow and ice are represented in bright white and light blue, contrasting with the green of vegetation and the brown/tan of bare land. Large white areas are visible in the Arctic region, Greenland, and parts of Antarctica. Smaller, more fragmented white patches are scattered across the mountainous regions of North America, Europe, and Asia. The oceans are shown in dark blue. The text "B. Remote Sensing of Snow and Ice" is overlaid in white on the lower half of the image.

B. Remote Sensing of Snow and Ice

Part B – Contents

1. The electromagnetic spectrum
2. Spectral regions for EO
3. Spectral Transmittance of the Atmosphere
4. Resolution of satellite data
5. Applications in Cryosphere

1. The electromagnetic spectrum



2. Spectral regions for Earth Observations

	<i>Wavelength</i>
Ultraviolet	10 nm – 380 nm
Visible	380 nm – 750 nm
Near Infrared*	0.75 μm – 3.0 μm (also: Shortwave IR)
Middle Infrared*	3.0 μm – 50 μm (also: Thermal IR)
Far Infrared*	50 μm – 1.0 mm
Microwaves	0.1 cm – 100 cm (300 GHz – 0.3 GHz)

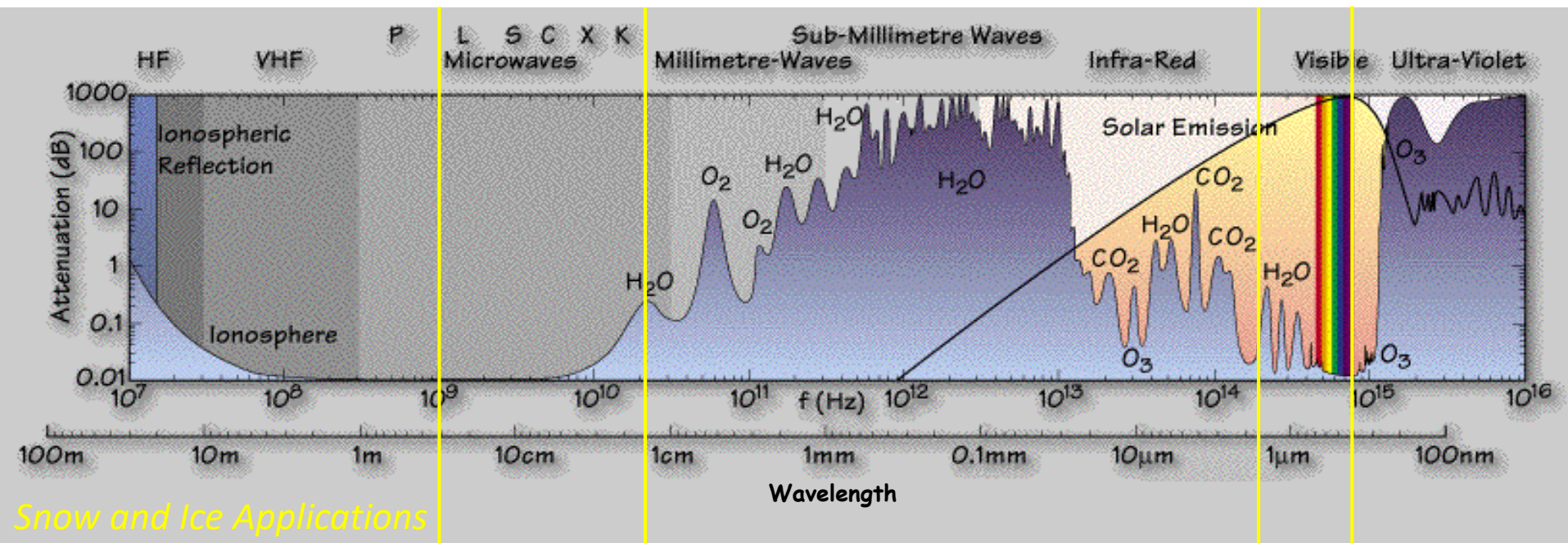
* ISO 20473

Other designations are in use; better specify wavelength directly.

Microwave (MW) Band Designations:

L-Band 0.39 – 1.55 GHz	X-Band 5.75 – 10.9 GHz
S-band 1.55 – 4.20 GHz	K _u -Band 10.90 – 22.0 GHz
C-Band 4.20 – 5.75 GHz	K _a -Band 22.00 – 36.0 GHz

3. Spectral Transmittance of the Atmosphere



Selected satellites used i.a. for cryospheric applications:

C-Band:	Sentinel-1 Envisat ASAR ERS-1/-2 Radarsat-1/-2	Local/regional:	Sentinel-2 MSI Landsat 4-8 TM/ETM+/OLI SPOT-5 – 7 HRV/NAOMI Terra ASTER
X-Band:	TerraSAR-X Cosmo-Skymed	Continental/global:	Sentinel-3 SLSTR/OLCI Aqua/Terra MODIS NPP VIIRS NOAA AVHRR

4. Resolution of Satellite data

Orthophoto – 0.5 m, true-color-composite



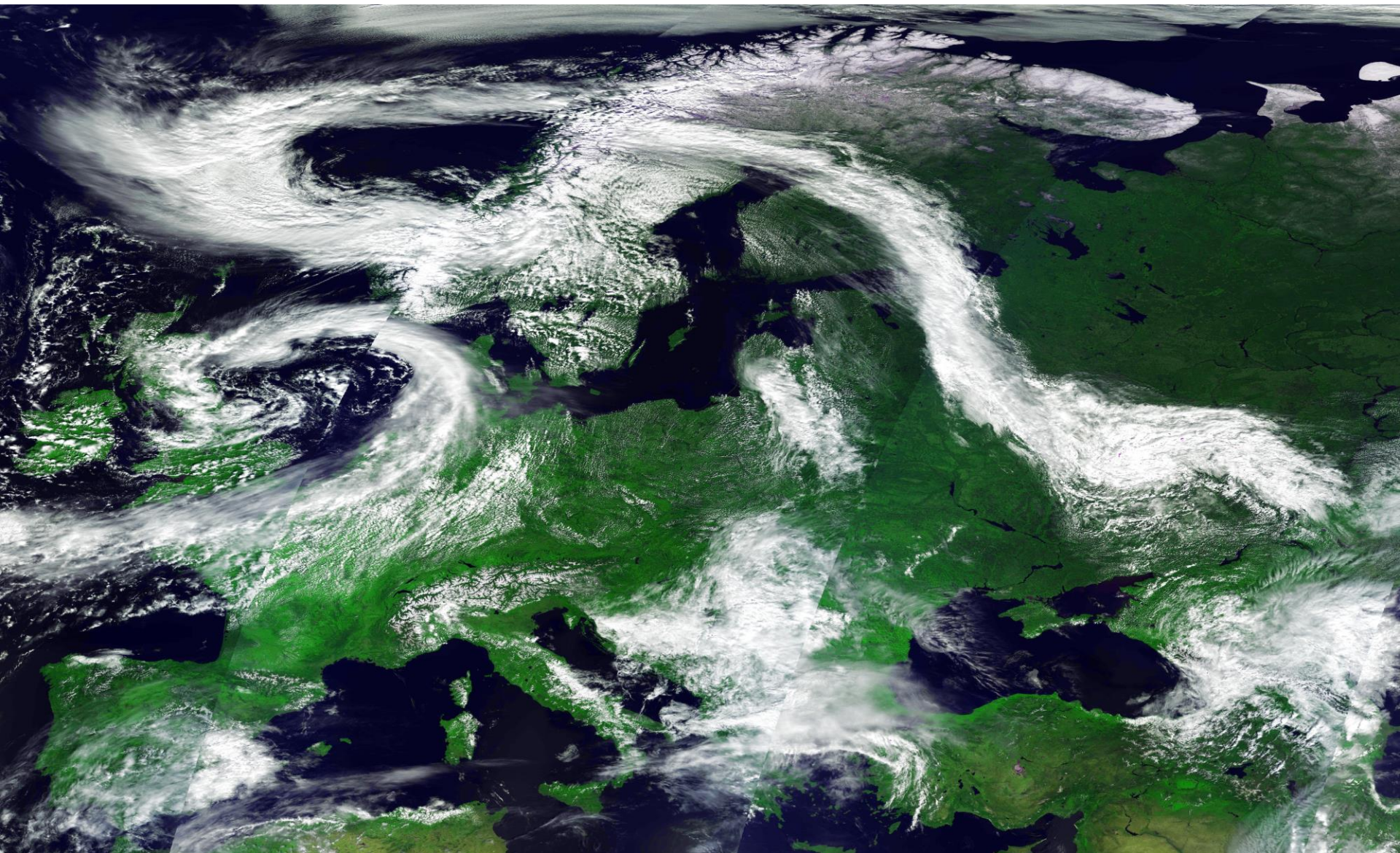
Sentinel-2, 10 m – single band



MODIS – 250 m, single band



MODIS – 500 m RGB123

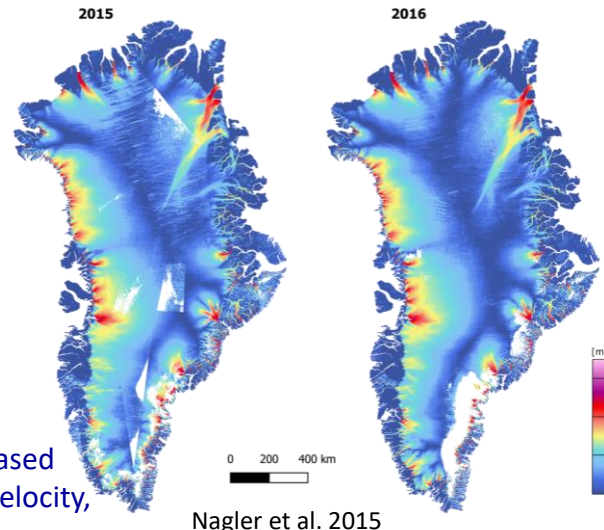
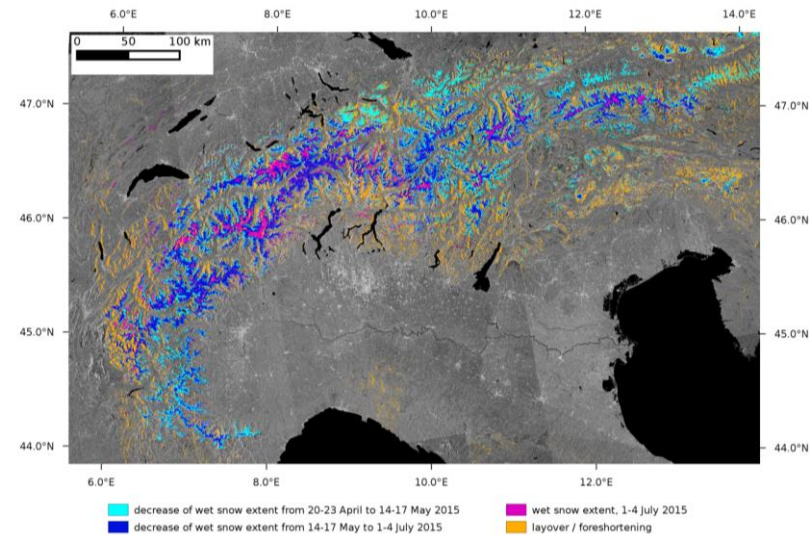


5. Applications in Cryosphere: Radar Sensors

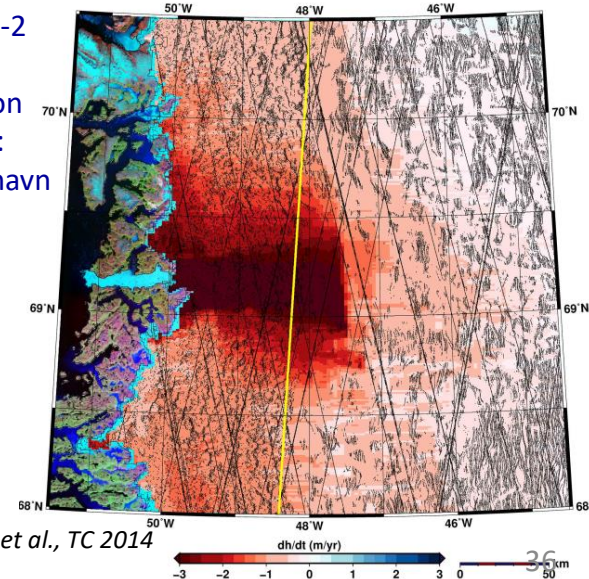
Monitoring of

- Melting snow
- Snow Water Equivalent (SWE)
- Glacier topography and volume change
- Dynamics and mass balances of ice sheets
- Glacier motion
- 3D ice surface deformation and glacier hydraulics
- River ice
- Sea ice

Sentinel-1 based melting snow extent, Alps Nagler et al. 2016



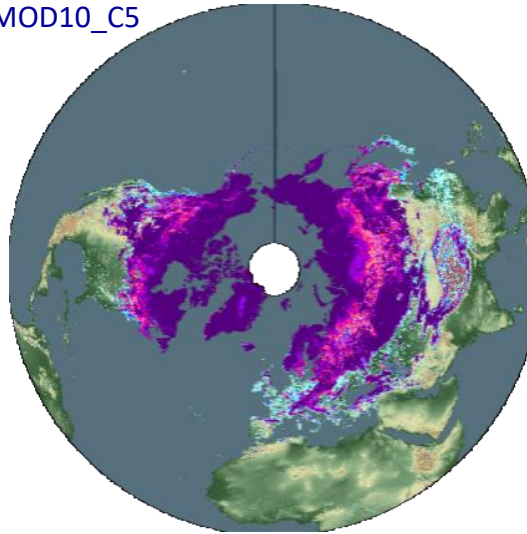
Cryosat-2 based Elevation change: Jakobshavn Glacier



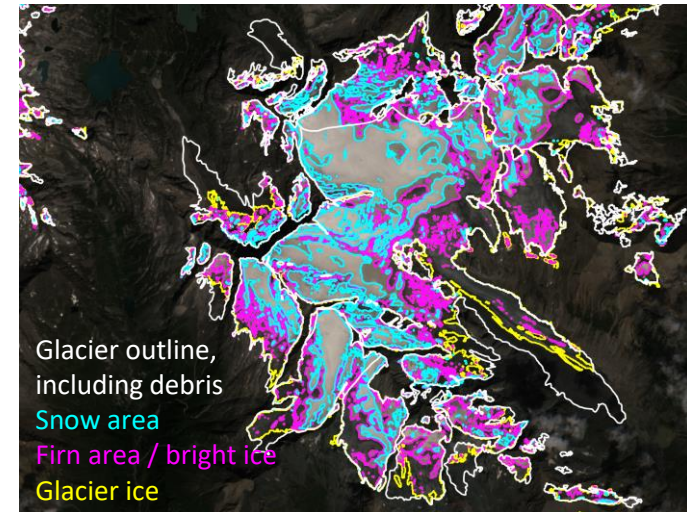
Applications in Cryosphere: Optical Sensors

- Snow mapping
- Lake ice monitoring
- Glacier mapping
- Albedo
- Glacier facies
- Snow and ice properties
- Ice motion
- Ice sheet boundaries
- Surface topography

MODIS based hemispheric snow extent, MOD10_C5

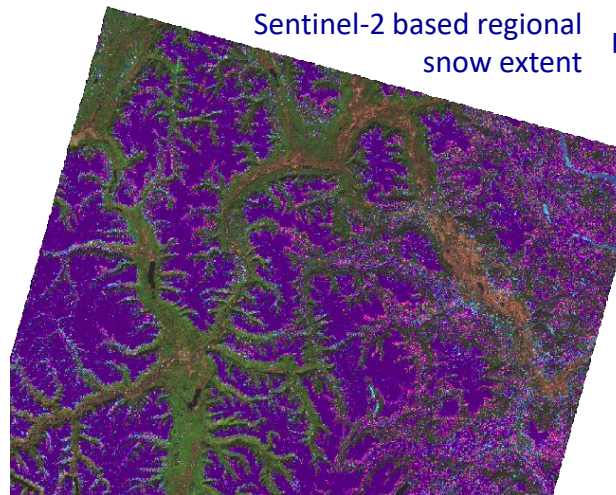


Sentinel-2 based glacier outlines and glacier facies, Alps

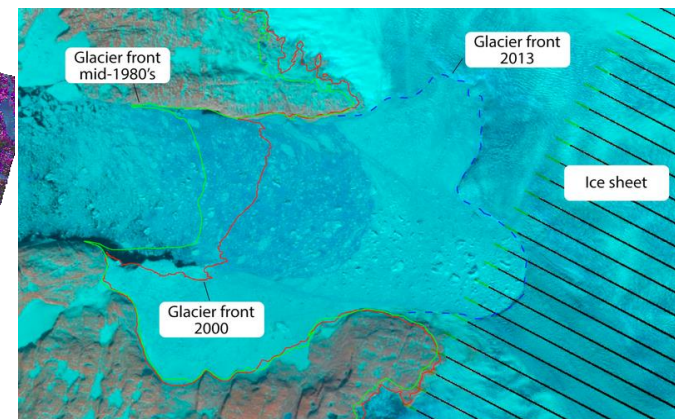


Schwaizer et al. 2017

Sentinel-2 based regional snow extent



Landsat based glacier fronts, Jakobshavn, Greenland



C. Snow and Ice from Radar Satellite data



X- & C- Band Radio-Scatterometer

Part C – Contents

1. Radar – Some Basics
2. Electric Properties in the Microwave Region – physical background
3. Dielectric Properties and Emissivity in the Microwave Region – Snow and Ice
4. Radar Scattering Signatures of Snow and Ice
5. SAR Application for Snowmelt Area Mapping
6. Interferometric Signals of Snow Cover
7. Glacier Motion by InSAR and Offset Tracking
8. InSAR Analysis of Glacier Topography & Volume Change
9. SAR Applications to Monitoring Dynamics and Mass Balance of Ice Sheets

1. RADAR – Some Basics

RADAR – Radar Detection And Ranging:

- emits electromagnetic (EM) waves and detects EM waves reflected from target
- Determines distance to target from the returning time of the EM waves

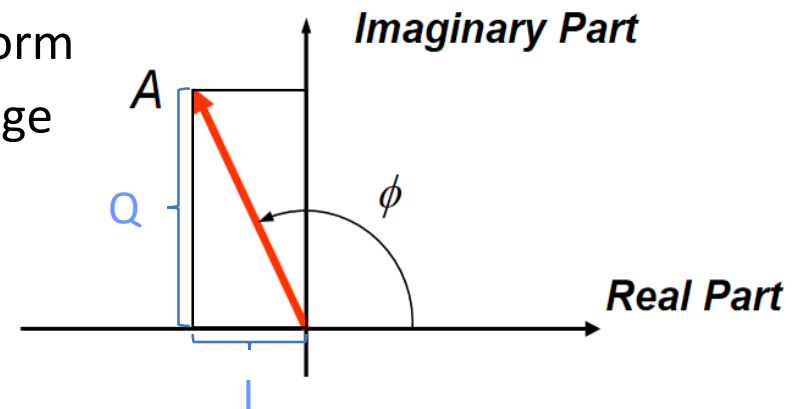
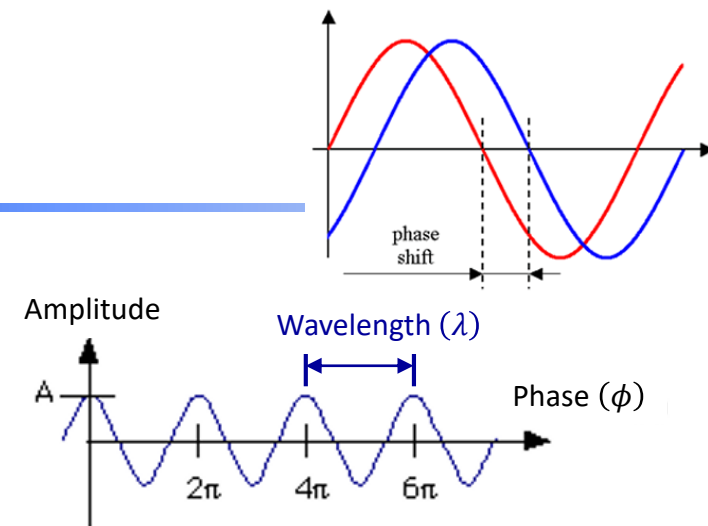
SAR – Synthetic Aperture Radar:

- Coherent imaging system on a moving platform
- emits Microwave to the surface on slant range and detects backscattering

Main image types:

Amplitude: A (measure of the strength or height of an EM wave)

Intensity: $I = A^2$ (proportion of microwave backscattered from target on ground to sensor)



$$A = \sqrt{Q^2 + I^2} \quad \tan(\phi) = Q/I$$

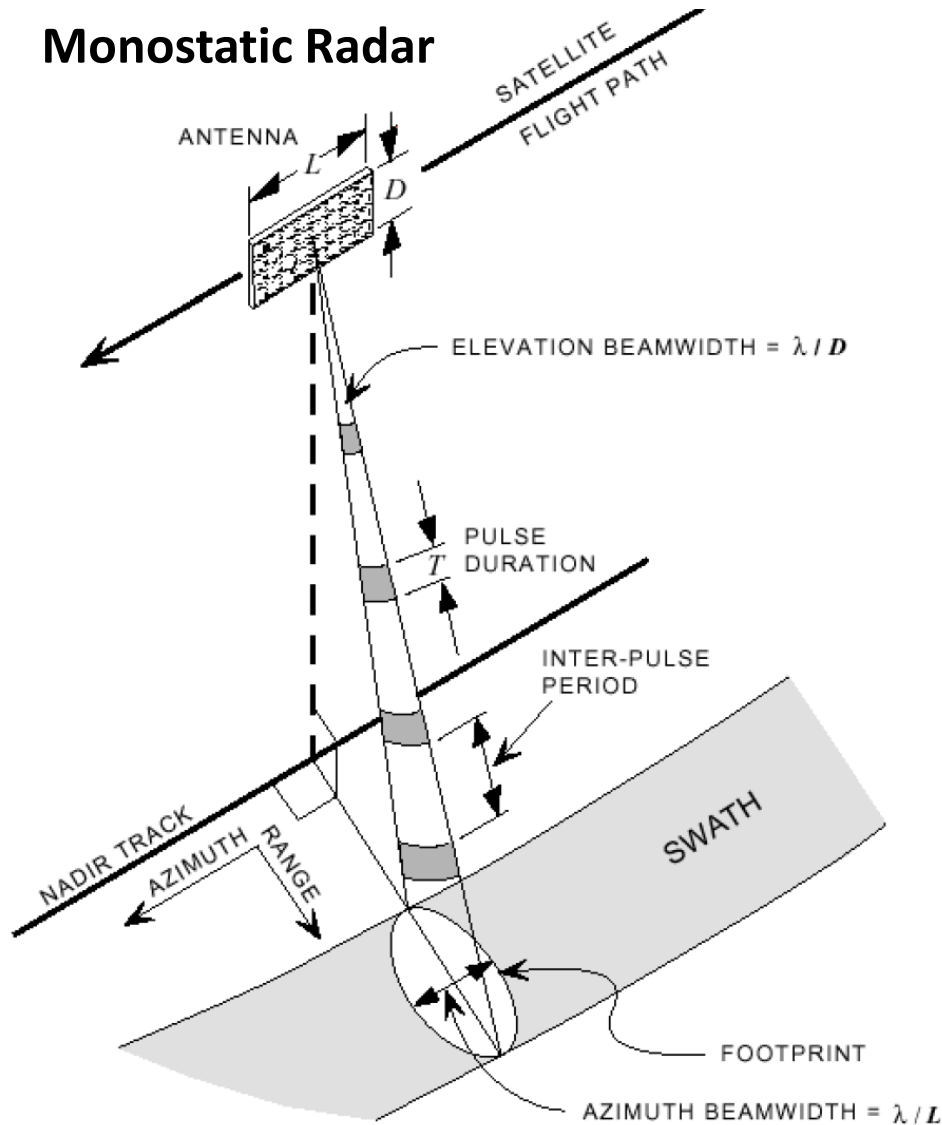
$\Phi = \text{Phase (oscillation of EM wave)}$

$$I = \text{In-Phase} = A * \cos(\Phi)$$

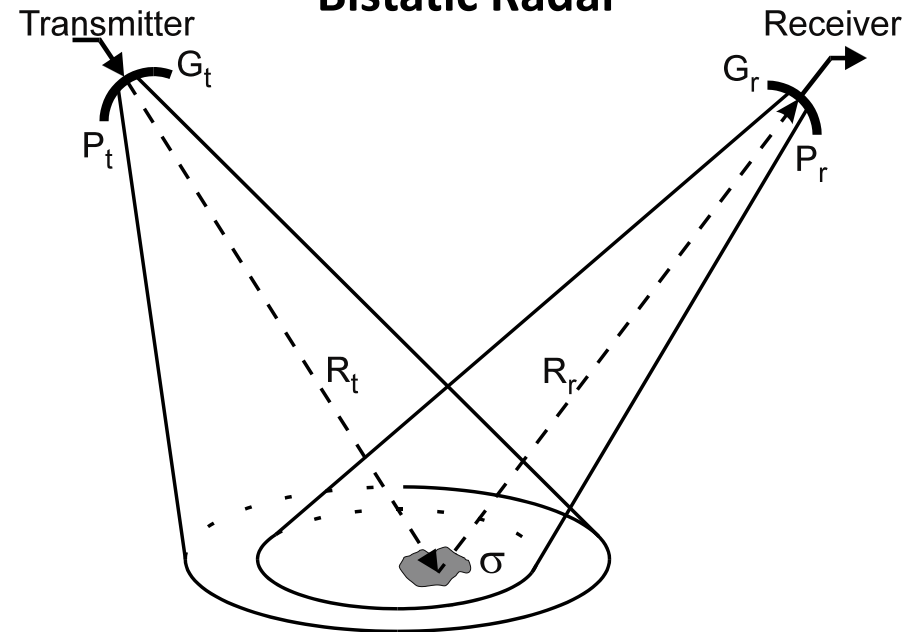
$$Q = \text{Quadrature} = A * \sin(\Phi)$$

Radar Acquisition Geometry

Monostatic Radar

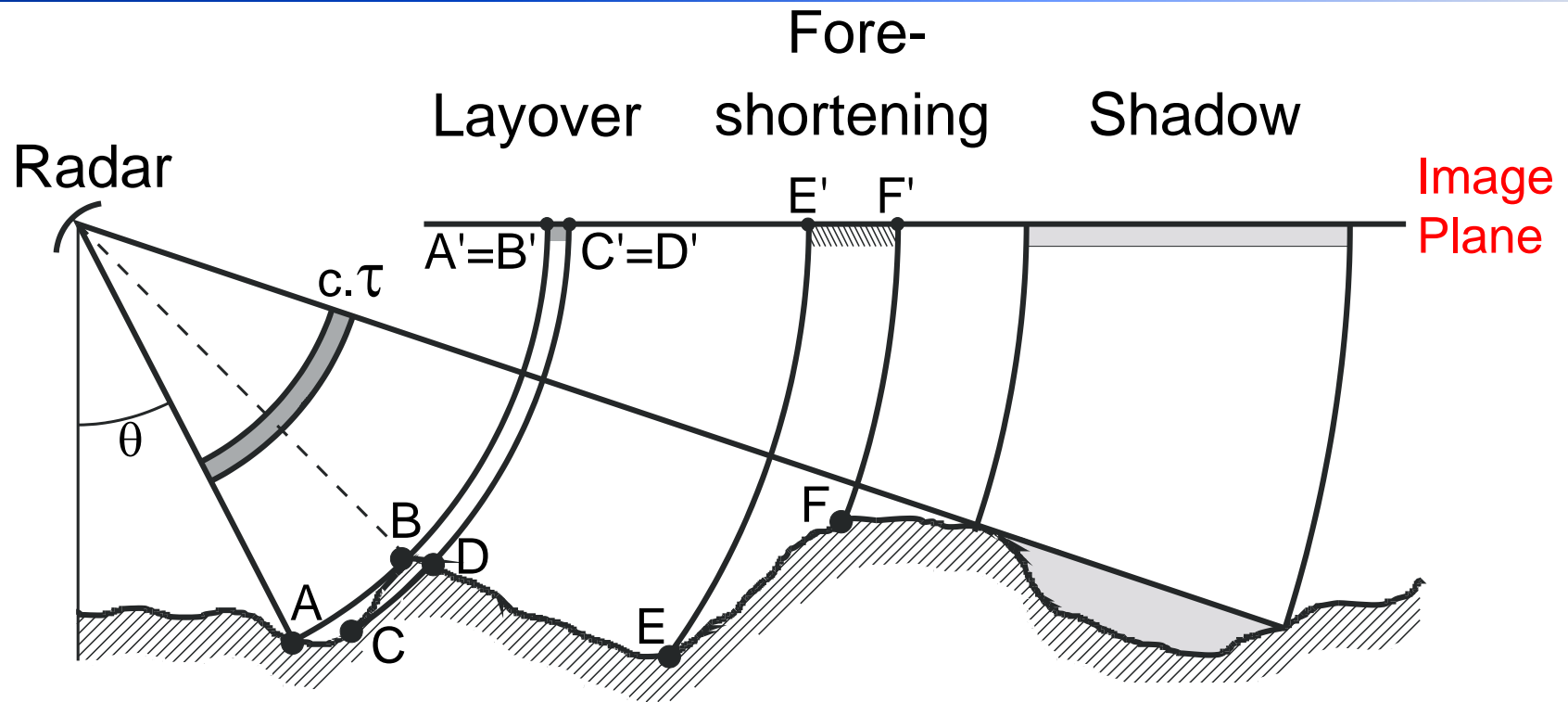


Bistatic Radar



P Power
A Antenna Gain
R Range
 σ Scattering Cross Section

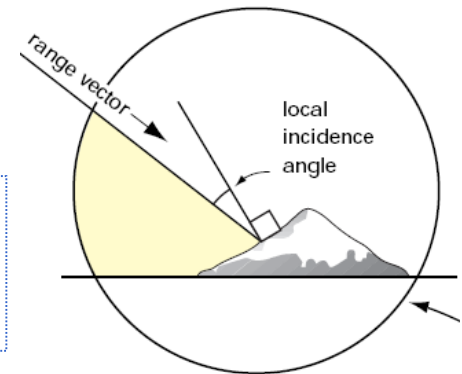
Across Track Radar Imaging Geometry



Topographic distortion depends on local incidence angle

Size of local range resolution:

$$\Delta r = c\tau / (2\sin\theta_{\text{inc}})$$



SAR Imaging Properties

Specifications for Sentinel-1 IW SAR:

Center frequency: $\nu = 5.405$ GHz

Polarization: VV+VH, HH+HV, HH, VV

Antenna Length: $L = 12.3$ m

Swath width: 250 km

Incidence angle range: $\theta_i = 20^\circ - 46^\circ$

Chirp Bandwidth: $B = 42.80 - 56.4$ MHz
(programmable)

Pulse Repetition Frequency:
1000 – 3000 Hz (programmable)

Pulse Width: $\tau = 5 - 100$ ns
(programmable)

Geometric resolution: $r_r = 5$ $r_a = 20$ m

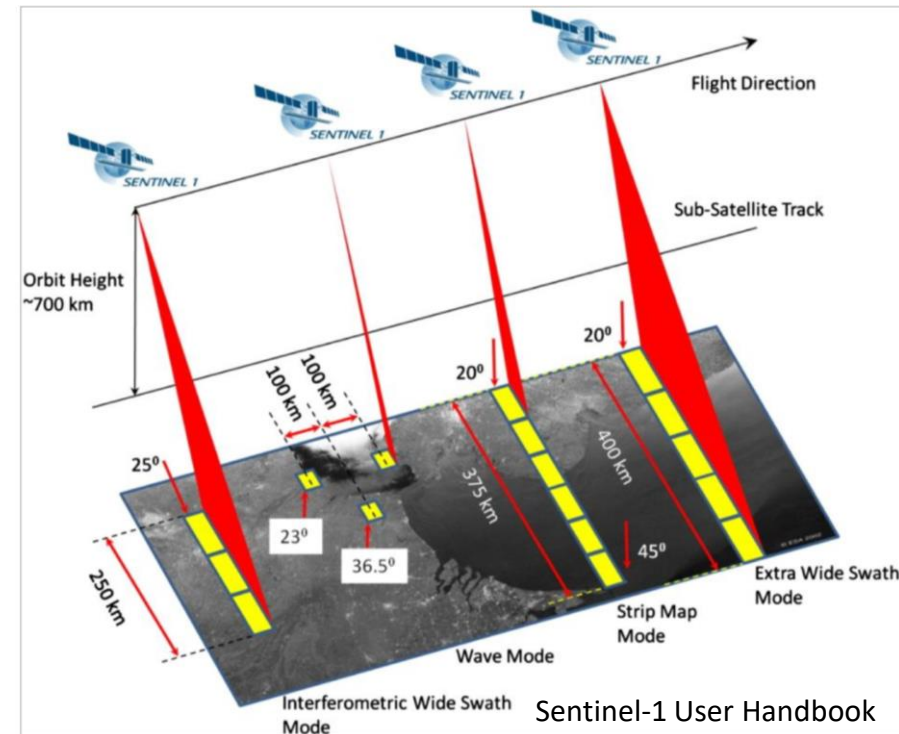
Spatial Resolutions

c = speed of light
 τ = Pulse duration

$r_a = L/2$ *azimuth resolution*

$r_r = c\tau/2$ *slant range resolution*

$r_g = r_r / \sin \theta_i$ *ground range resolution*



Satellite-borne SAR Systems (selection)

<i>Sensor</i>	<i>Satellite</i>	<i>[GHz].</i>	<i>Resolution/Swath</i>	<i>Repeat</i>
AMI	ERS-1,-2(1991-2011)	5.3 VV	25 m - 100 km	35d/1 d
SIR-C/X-SAR	Shuttle (1994)	1.2,5.3,9.6	25 m - 40 km	2 Campaigns
SIR-C/X-SAR	SRTM (Feb.2000)	5.3 & 9.6	50/100 m - 100/200 DEM	
Present				
SAR	Radarsat1(1995-)	5.3	10,30,100 m - 100-500 km	24 d
ASAR	Envisat (2002-12)	5.3	30,100,1000 - 100-400 km	35 d
PALSAR	ADEOS (2007-11)	1.2	15/100 m - 40-350 km	46 d
TerraSAR	TerraSAR-X(2007-)	9.6	1, 3,10 m - 10,30,100 km	11 d
TerraSAR2	TanDEM-X (2010-)	9.6	in Tandem with TerraSAR-X (InSAR)	
SAR	COSMO-SkyMed	9.6	1, 3,10 m - 10-100 km	16 d, 1d, 8d
SAR	Radarsat2 (2007-)	5.3	3, 10, 30 m, ≥20 km	24 d
SAR	Sentinel-1 (2013-)	5.3	10 m, 30 m 250, 400 km	12 d x 2 Sat.
Future				
SAR Constellation	Radarsat (2019 -)	5.3	3 m ...100m 30 ...500 km	16 d x 3 Sat.

SAR Signal & Imaging Characteristics

Radar Equations for Distributed Target

Monostatic

$$P_r = P_t \frac{\lambda^2 G^2}{(4\pi)^3 R^4} (\sigma^\circ A_0)$$

Bistatic

$$P_r = P_t \frac{\lambda^2 G_t G_r}{(4\pi)^3 R_t^2 R_r^2} (\sigma^\circ A_0)$$

Antenna gain:

$$G = \frac{4\pi A_a}{\lambda^2} ; \quad \sigma^\circ = \left\langle \frac{d\sigma_i}{dA_i} \right\rangle_{A_0}$$

P	Power	r	Receiver
R	Range	t	Transmitter

Radiometric Sensitivity

$$P_{noise} = k T_{sys} B_R ; \quad SNR = \frac{\overline{P_r}}{P_{noise}}$$

k – Boltzmann's constant [1.38E-23 J/K]

T_{sys} – Receiver noise temp. [K]

B_R – Range (chirp) bandwidth [Hz]

P_{noise} – Thermal noise power

SNR – Signal-to-noise ratio

σ° Radar cross section per unit area (for distributed targets), usually specified in dB

A_a Antenna area

σ_i Radar cross section of incremental scattering element

A_i Incremental surface element

A_0 Surface resolution cell

λ Wave length

SAR Image Characteristics - Speckle

Interference of the signals from many individual scatterers in a distributed target results in **Speckle**

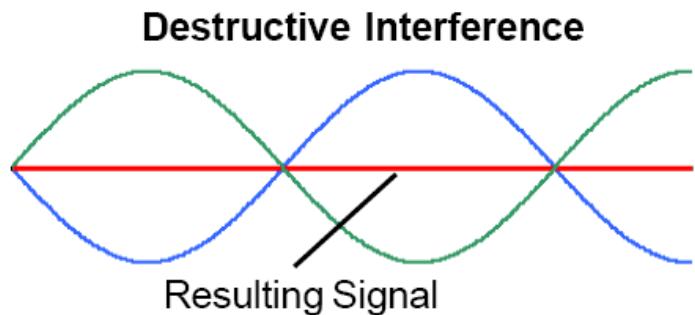
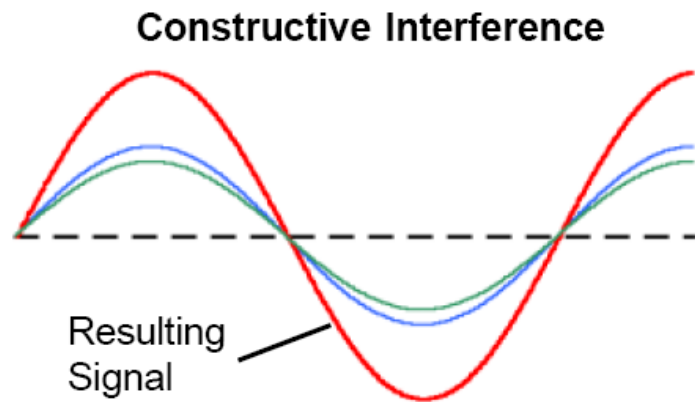
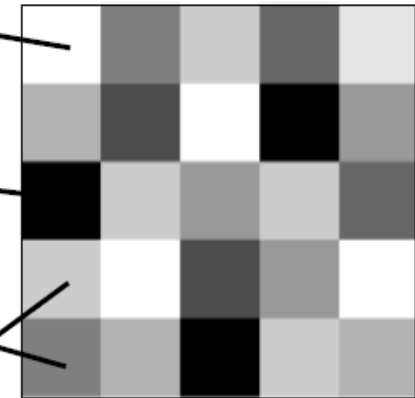


Fig. Micro-images

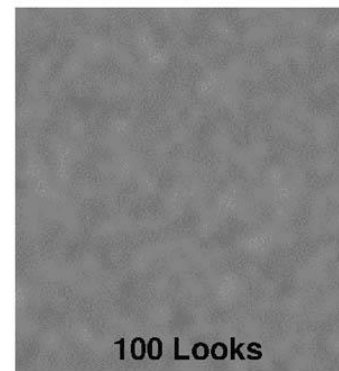
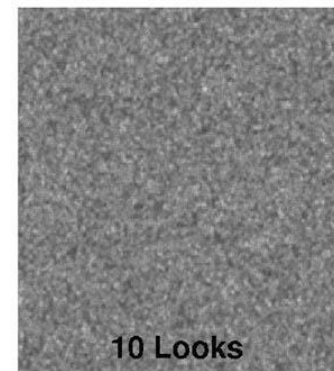
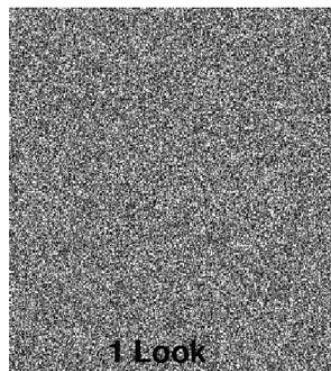
Full constructive interference

Full destructive interference

Varying degrees of interference



Pixels (backscattered power) from a point target with homogeneous scattering properties



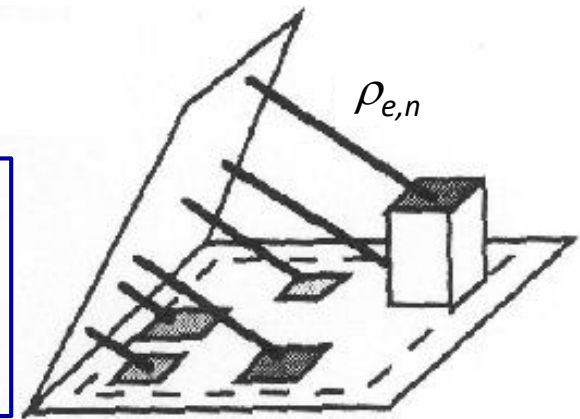
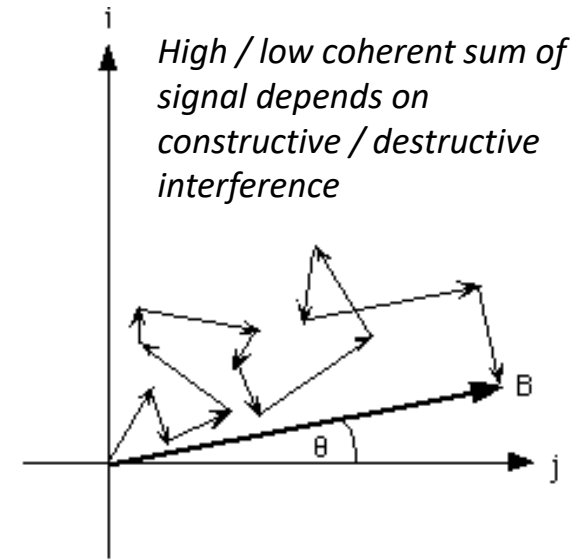
SAR Image Characteristics - Speckle

The backscattered signal at the surface for a SAR resolution element is:

$$S_0 = A_b \exp[i\psi_b]$$
$$= \sum_n A_{e,n} \exp[i\psi_{e,n}] \exp\left[-i \frac{4\pi}{\lambda} \rho_{e,n}\right]$$

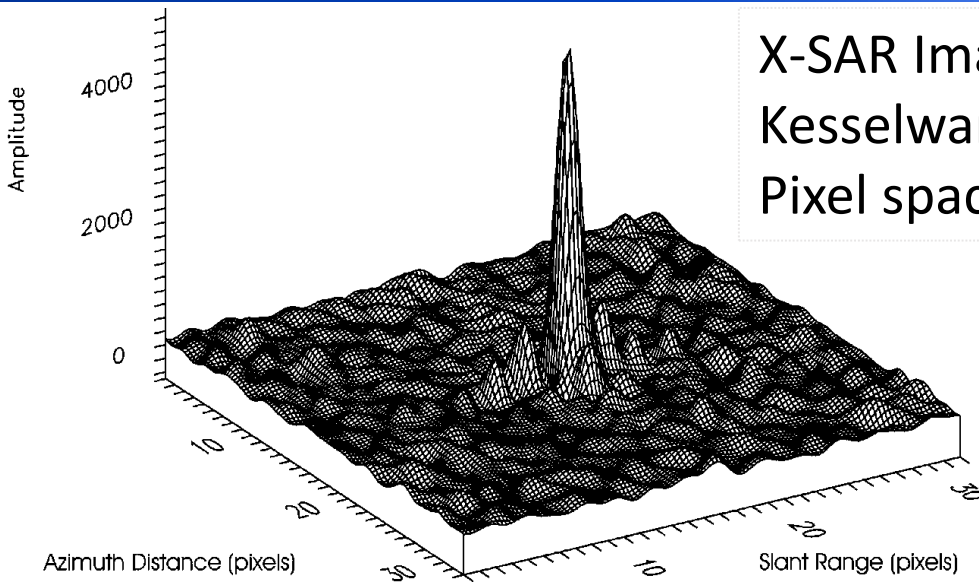
The signal is the **coherent sum** of contributions from all (n) elemental scatterers in the resolution cell $A_{e,n} \exp[i\psi_{e,n}]$ and their differential path delays $\rho_{e,n}$ between the scatterer and the wave front.

For natural targets many scatterers contribute to the signal of a resolution cell. *The resulting Amplitude of a single pixel is randomly distributed: **Speckle***



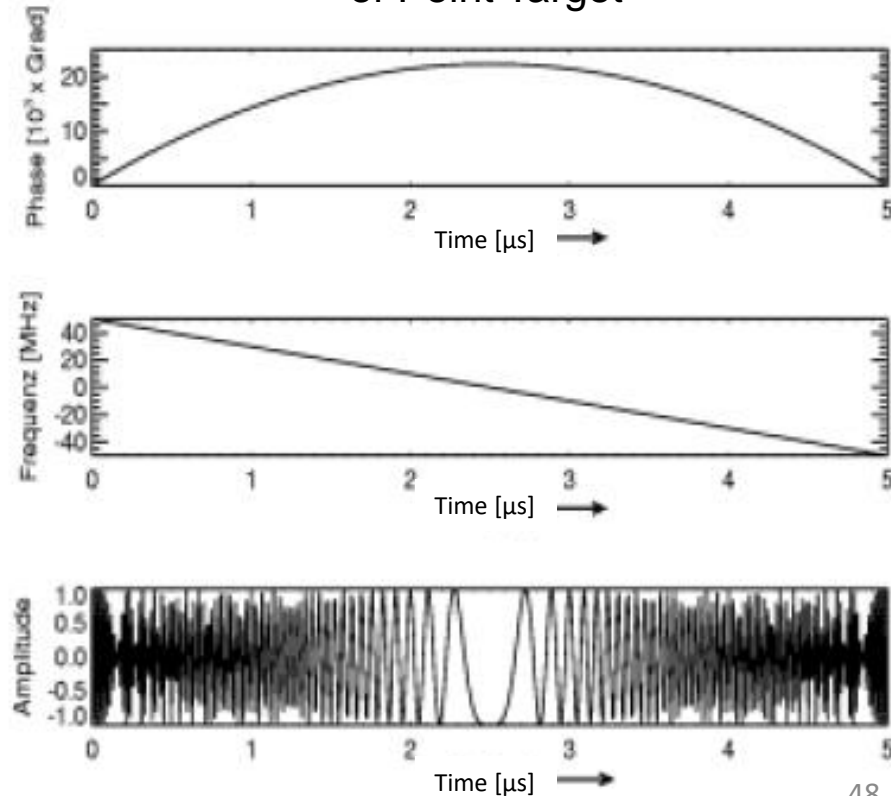
Speckle is not noise \Rightarrow InSAR utilizes speckle

Point Spread Function of Corner Reflector



X-SAR Image of Corner Reflector on Kesselwandferner, with size $L = 1.8$ m.
Pixel spacing (range, azimuth) 6.66m , 4.88 m

Phase, Frequency, and Amplitude of Point Target



Radar back-scatter signal depends on

- **Physical factors:** dielectric constant of the surface materials (depends strongly on the moisture content)
- **Geometric factors:** surface roughness, slopes, shape and orientation of the objects relative to the radar beam direction
- **The types of landcover:** soil, vegetation, man-made objects
- **Sensor characteristics:** Microwave frequency, polarisation and incident angle

2. Electrical properties in the Microwave Region – Physical background

We consider non-magnetic media

Permittivity, dielectric constant & dielectric loss factor:

$$\epsilon_r = \epsilon' - i\epsilon'' = \epsilon_r (1 - i \tan \delta)$$

***Complex
relative
permittivity***

$$i = \sqrt{-1}$$

Dielectric constant (real part, represents stored energy when the material is exposed to an electric field)

Dielectric loss factor (imaginary part, influences energy absorption and attenuation), is proportional to changes in temperature

***Tangent of
loss factor***

Tangent of loss factor: $\tan \delta = \frac{\epsilon''}{\epsilon'}$

Electrical properties – physical background (cont.)

Penetration depth: depth where the power of the signal is reduced to $1/e$ of the power entering the surface

The wave velocity v and the refractive index n in a medium with electric permittivity ε and magnetic permeability μ are:

$$v = \frac{c_0}{\sqrt{\varepsilon_r \mu_r}} \quad n = n' - in'' \quad n^2 = \varepsilon_r$$

$e \simeq 2.71828$ Base for natural logarithm
 $c_0 = 2.9979 \text{ E}8 \text{ m/s}$
 $\varepsilon_0 = 8.8554 \text{ E-}12 \text{ [As/Vm]}$
 $\varepsilon_r = \varepsilon/\varepsilon_0$ Relative permittivity
 $\delta = \varepsilon''/\varepsilon'$ Loss tangent
 κ_a Absorption coefficient
 κ_e Extinction coefficient
 κ_s Scattering coefficient

Penetration depth in an **absorbing** (non-scattering) medium (for $\tan \delta \ll 1$):

$$d_p = \frac{1}{\kappa_a} = \frac{\lambda_0}{2\pi} \frac{\sqrt{\varepsilon'}}{\varepsilon''}$$

Penetration depth (intensity) in an **absorbing and scattering** medium:

$$d_p = \frac{1}{\kappa_e} ; \quad \kappa_e = \kappa_a + \kappa_s$$

3. Dielectric Properties and Emissivity in the Microwave Region – Snow and Ice

Microwave Permittivity

Ice:

$$\epsilon' = 3.15$$

$$\epsilon'' = 0.001 \text{ to } 0.0001 \text{ f } (\nu, T)$$

$$\nu_0 (-0.1^\circ\text{C}) = 7.3 \text{ KHz}$$

Dry snow:

$$\epsilon' = 1.0 + 1.7 \rho + 0.7 \rho^2$$

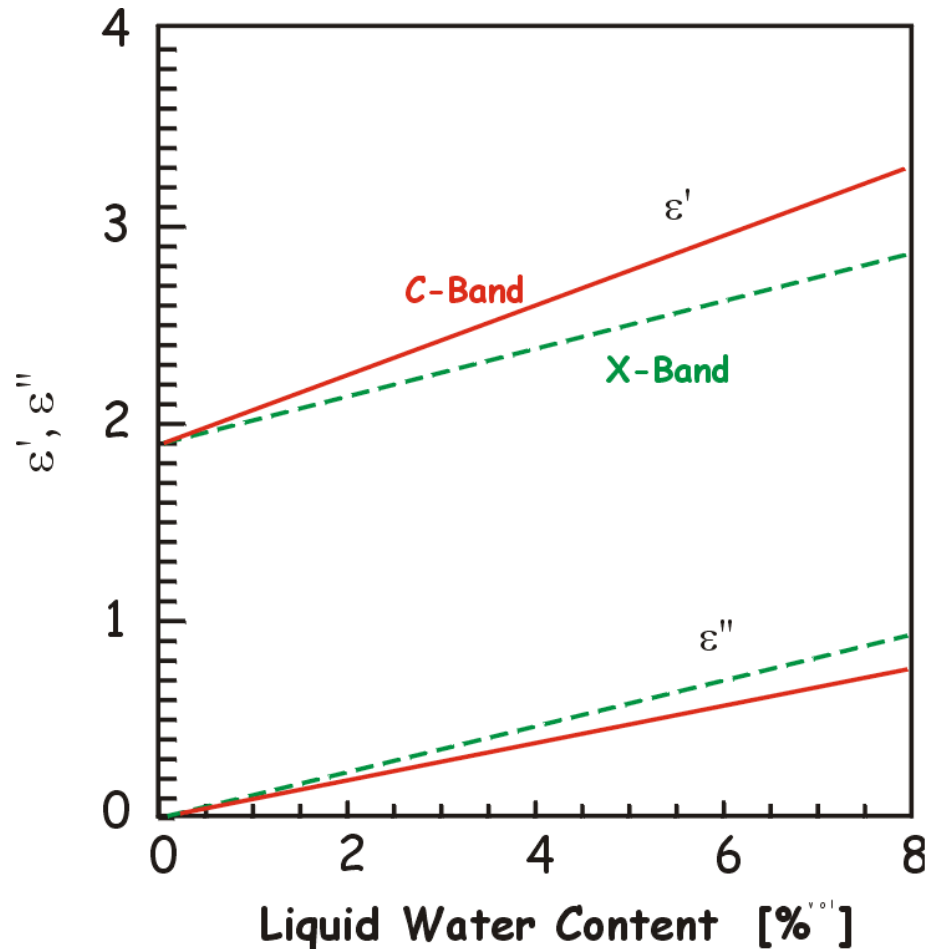
Wet snow:

$$\epsilon' = \epsilon' (\text{dry}) + \Delta \epsilon$$

$$\Delta \epsilon = 0.23 V_w / [1 - i(\nu / \nu_0)]$$

$$V_w [\% \text{ volume}]$$

ν_0 relaxation frequency for wet snow (ca. 10 GHz)



For snow density $\rho = 0.45 \text{ g/cm}^3$

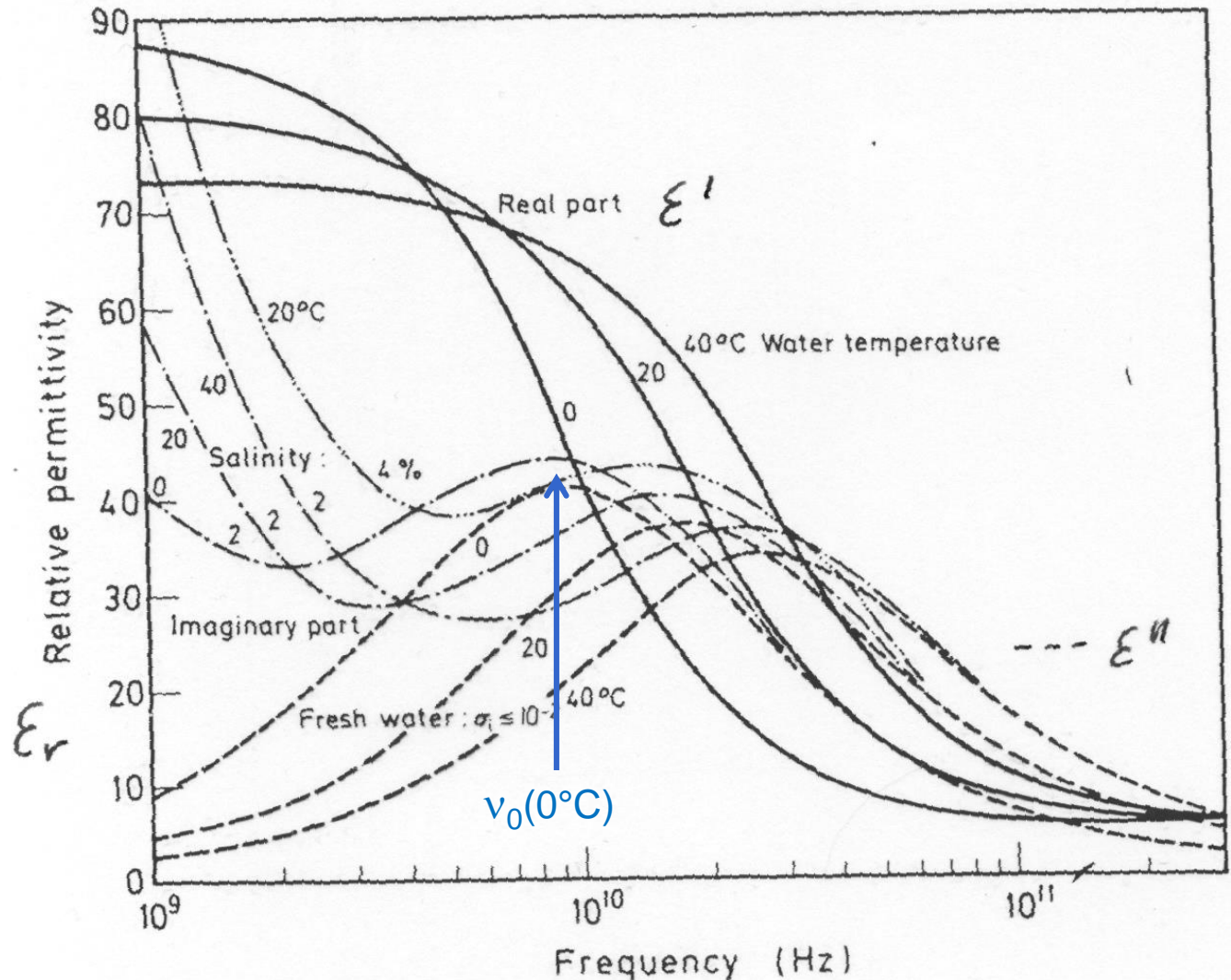
Microwave Permittivity of Water

$$\epsilon = f(\nu, T)$$

$$\nu_0(0^\circ\text{C}) = 8.84 \text{ GHz}$$

Debye
Relaxation

Relevant for
dielectric mixing
in wet snow and
sea ice

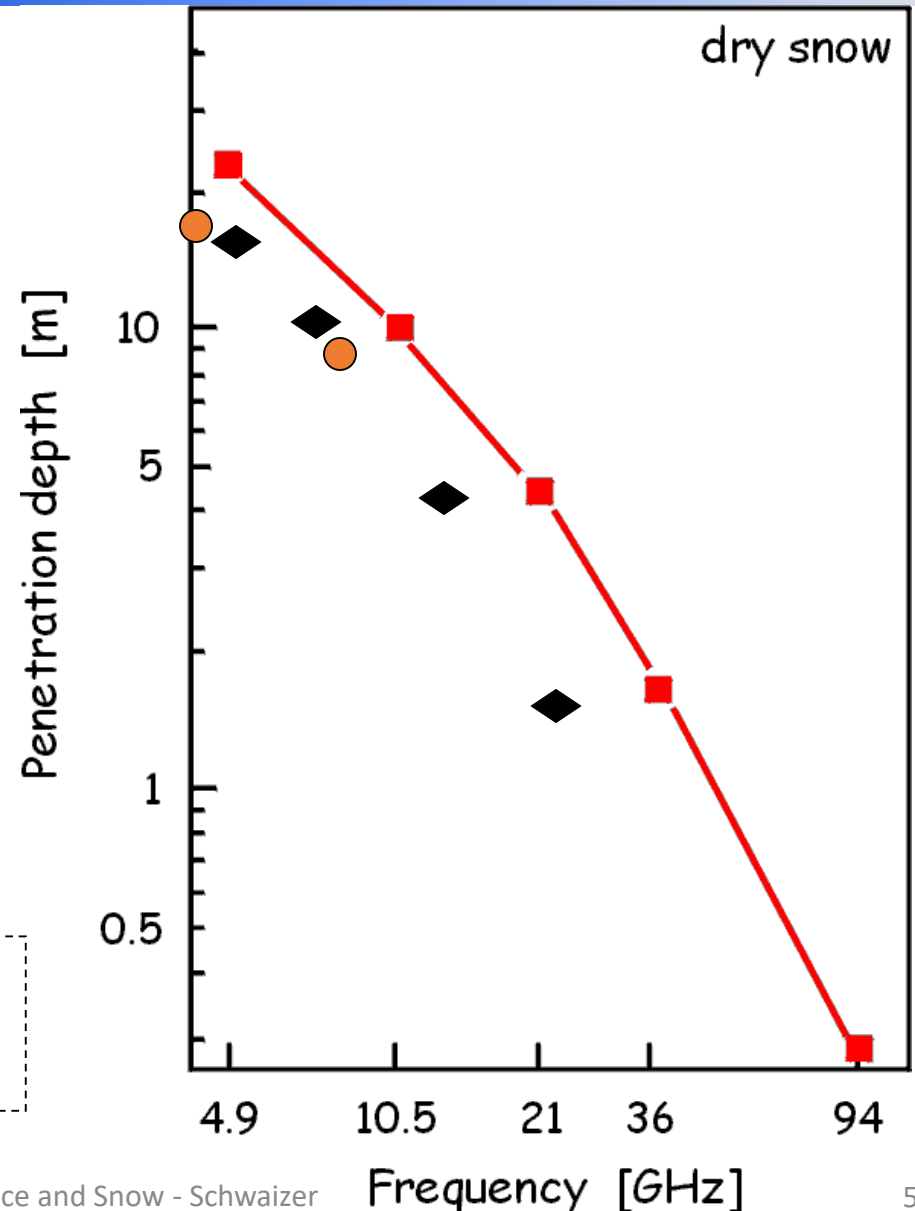


Microwave Penetration Depth in Dry Snow

Measured by microwave radiometry:

- Alpine snowpack (Mätzler, 1987)
- Antarctic snow (Rott, 1993)
- ◆ Retrieved by inversion of satellite MW radiometry (SMMR) data, Antarctic Plateau (Rott, 1993)

Dry snow: *Attenuation dominated by scattering losses*



Microwave Penetration Depth in Wet Snow

Penetration depth:
$$d_p = \frac{\lambda_o}{2\pi} \frac{\sqrt{\epsilon'}}{\epsilon''}$$

Permittivity:

Dielectric mixture of air, ice, water

Ice: $\epsilon' = 3.15$

$\epsilon'' < 0.001$ f (ν , T)

Wet snow:

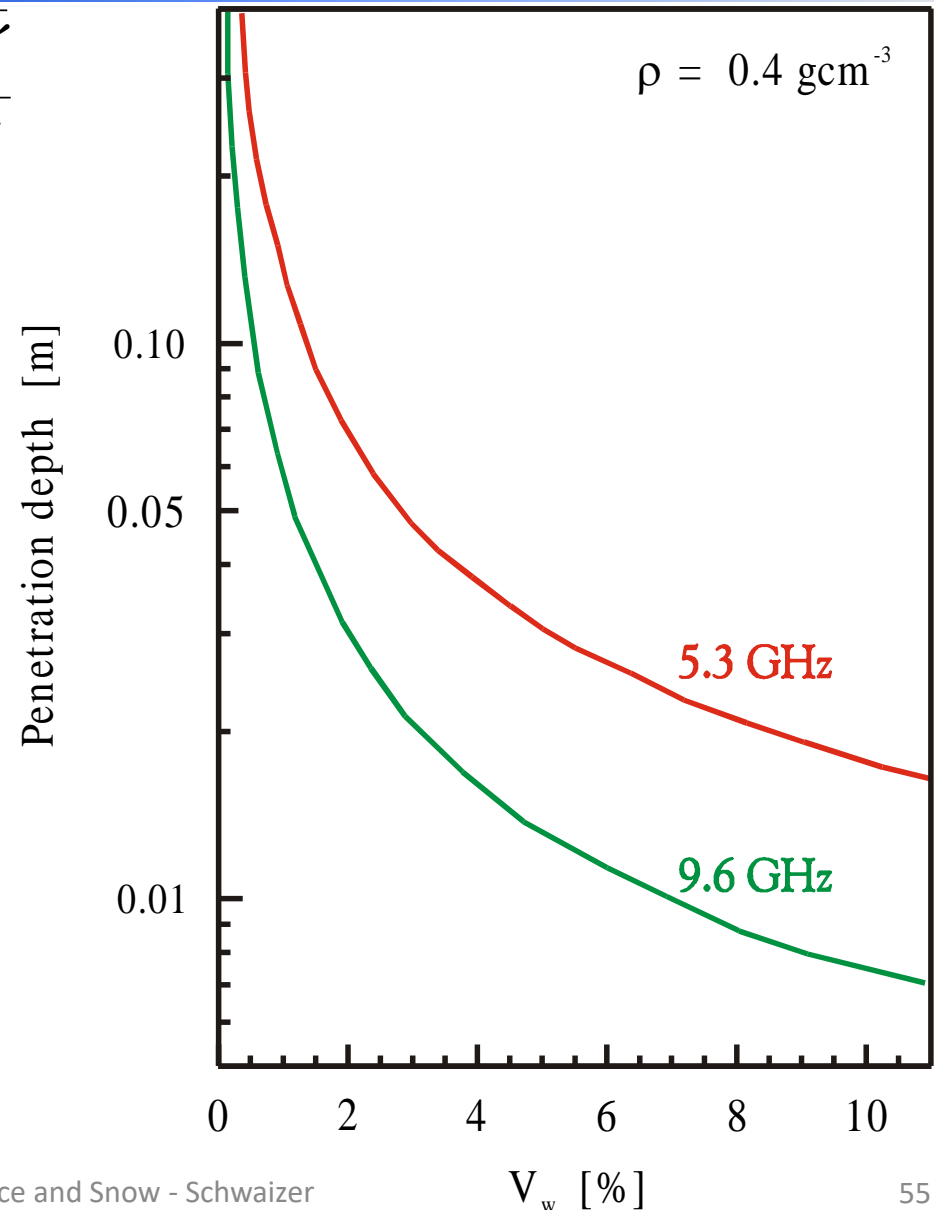
$$\epsilon' = \epsilon'(\text{dry}) + \Delta \epsilon$$

$$\Delta \epsilon = 0.23 V_w / [1 - i(\nu / \nu_0)]$$

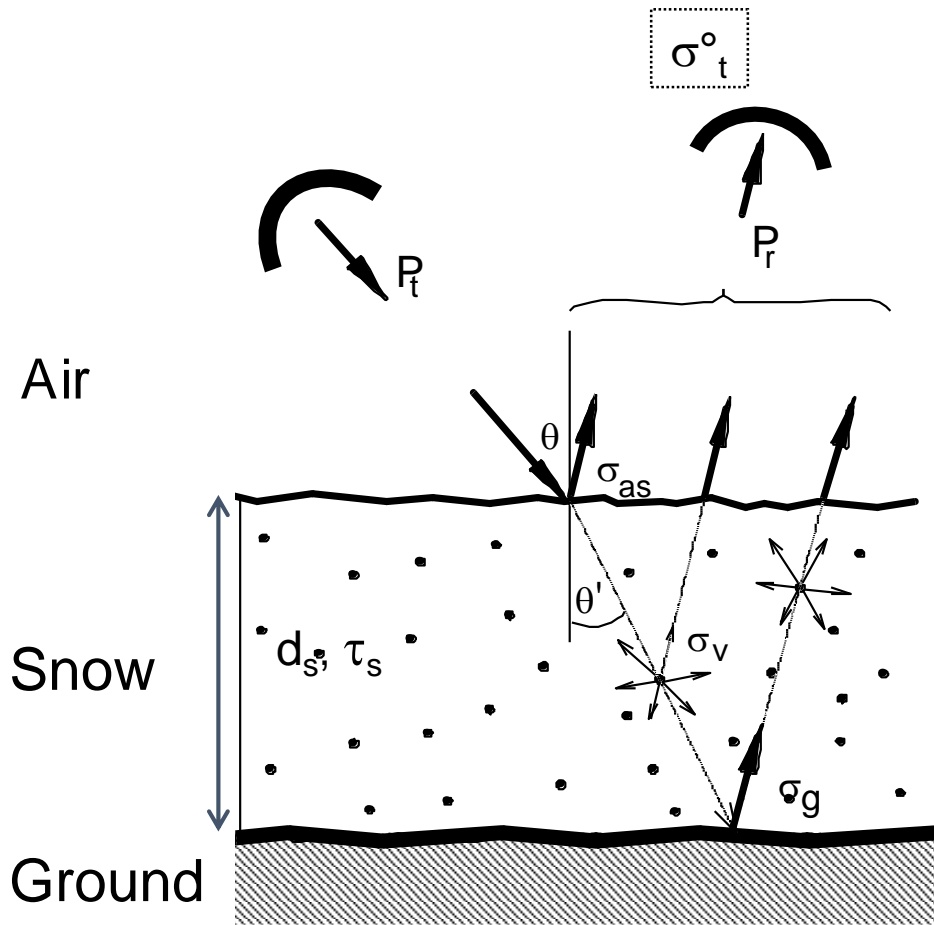
V_w [% volume], $\nu_0 \approx 10$ GHz

$\epsilon'' \approx 0.5$ in C-band

(for snow at $V_w = 6$ %)



4. Radar Scattering Signatures of Snow and Ice



Radiative Transfer (RT) Formulation

$$\sigma^{\circ}_t = \sigma^{\circ}_{as} + \sigma^{\circ}_v + \Upsilon^2_{as}(\sigma^{\circ}_g \tau_s^2)$$

$$\sigma^{\circ}_v = \Upsilon^2_{as}[\cos(\theta')(1 - \tau_s^2) k_s / (k_a + k_s)]$$

- Υ Transmission coefficient of air/snow interface
- σ°_{as} backscattering coefficient of air/snow interface
- σ°_t target backscattering coefficient
- σ°_v volume backscattering coefficient
- σ°_g backscattering coefficient ground
- k_a volume absorption coefficient
- k_s volume scattering coefficient
- d_s snow depth

$$k_e = k_a + k_s \text{ volume extinction coefficient}$$

$$\tau_s = \exp(-k_e d_s / \cos \theta') \text{ transmissivity of snow layer}$$

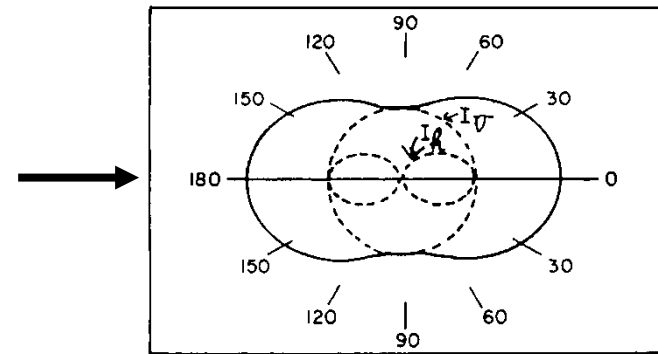
Rayleigh Scattering for independent Spherical Scatterers

Scattering and absorption cross section of a single particle:

$$\sigma_s = \frac{128\pi^5 r^6}{3\lambda^4} \left| \frac{\epsilon_r - 1}{\epsilon_r + 2} \right|^2$$

Approach valid for $r \ll \lambda$.

$$\sigma_a = \frac{2\pi}{\lambda} \left| \frac{3}{\epsilon_r + 2} \right| \frac{4r^3\pi}{3}$$



Scattering coefficient for the volume:

Scattering phase function

$$\sigma_v = \rho_n \langle \sigma_s \rangle = \frac{128\pi^5}{3\lambda^4} \left| \frac{\epsilon_r - 1}{\epsilon_r + 2} \right|^2 \int_0^\infty r^6 N(r) dr$$

in dense medium (dry snow pack) :

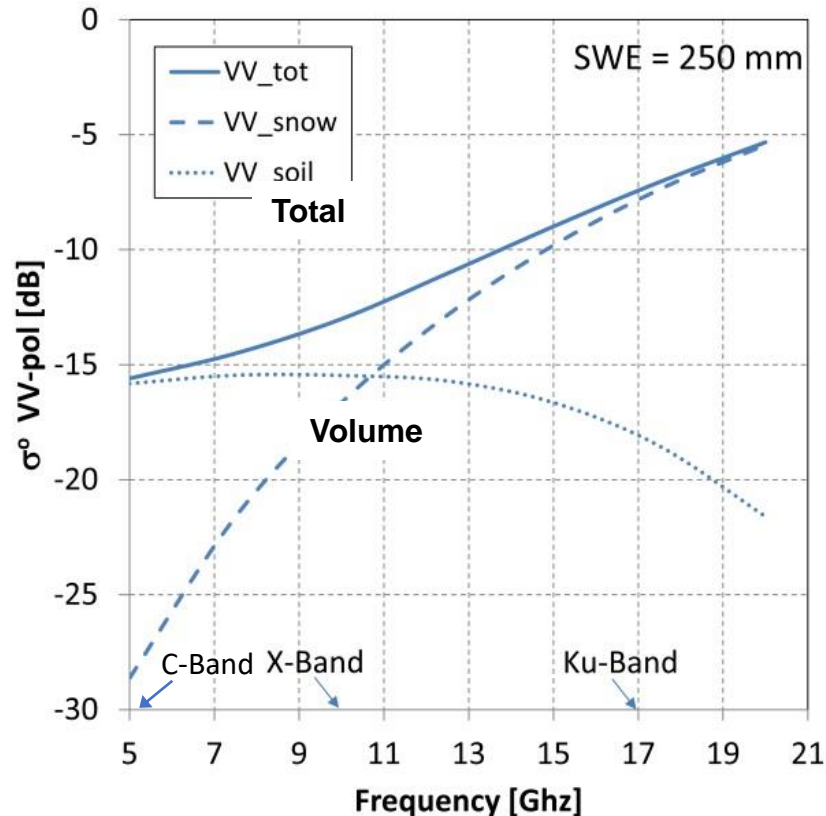
$$\rho_n = 1/r^3 \Rightarrow \rho_n \langle \sigma_s \rangle \propto r^3$$

ρ_n - Nr of particles/unit volume

$\langle \sigma_s \rangle$ - mean scattering coeff.

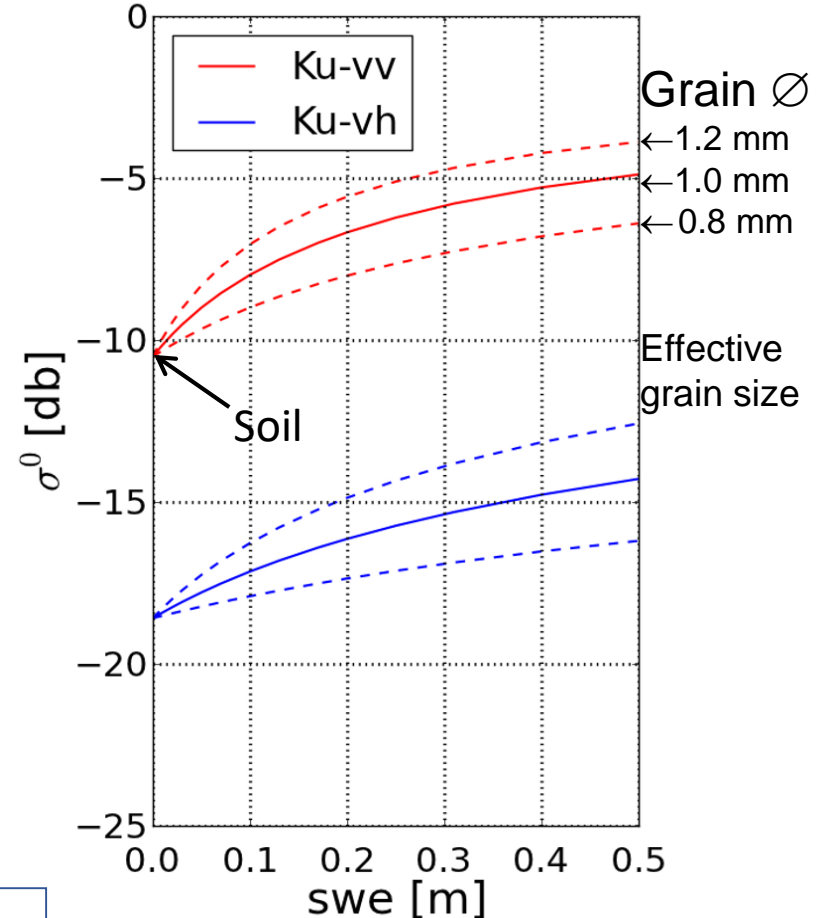
Backscatter Contributions of Dry Snow over Ground

Backscatter contributions in dependence of radar frequency (RT model)



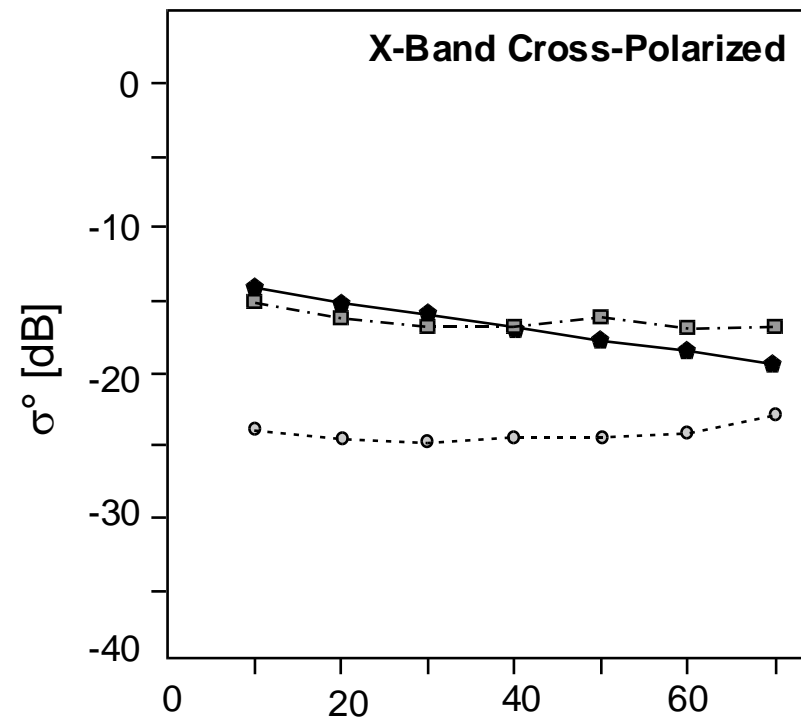
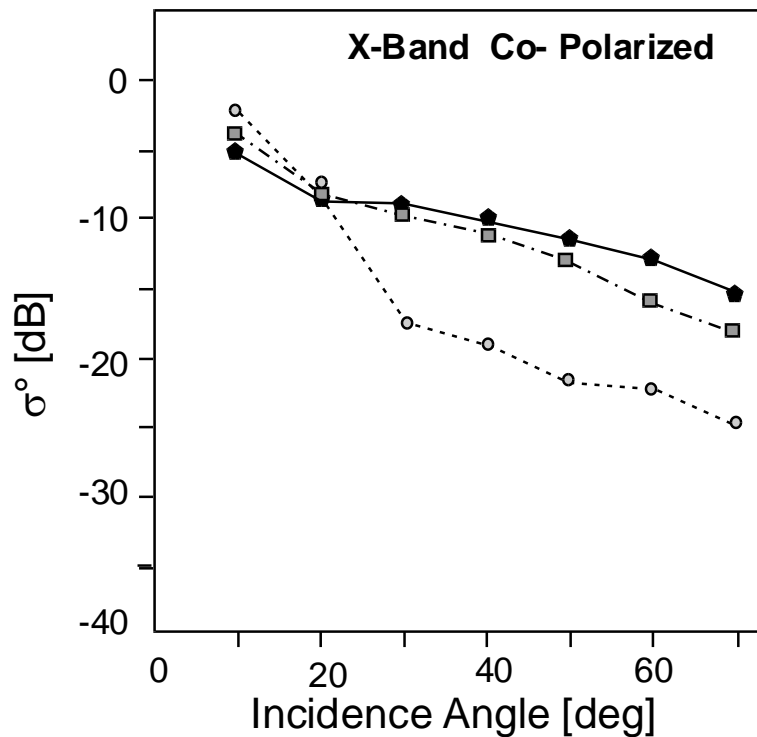
For VV pol, $\theta = 40^\circ$, snow grain \varnothing 1.0 mm
 Snow mass (SWE): 250 mm (~120 cm depth)

Ku-Band – 17.2 GHz



σ° of volume for different grain size

X-Band Backscattering Measurements Snow Covered Ground, Leutasch, Austria



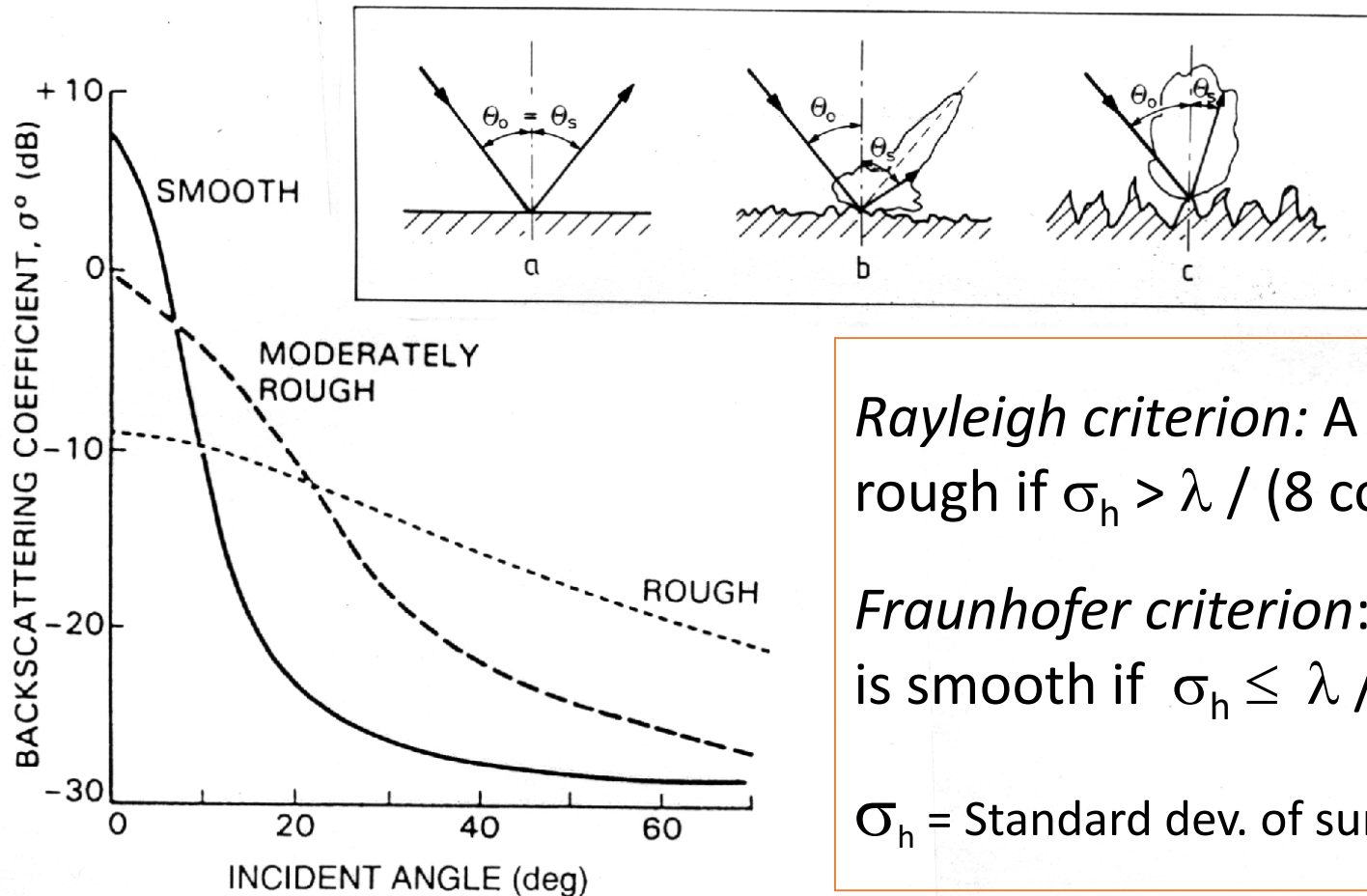
- ◆ snow-free (meadow) □ dry snow
○ wet snow → low σ^o (absorption)

Ground-based Scatterometry

Test site: Leutasch, Tyrol
Background target: Meadow



Backscattering from a Rough Surface



Rayleigh criterion: A surface is rough if $\sigma_h > \lambda / (8 \cos \theta_0)$

Fraunhofer criterion: A surface is smooth if $\sigma_h \leq \lambda / (32 \cos \theta_0)$

σ_h = Standard dev. of surface height

Surface scattering contribution dominates for wet snow, glacier ice, soil, ...

Angular Dependence of Backscattering from Alpine Snow

X-band

Measurements

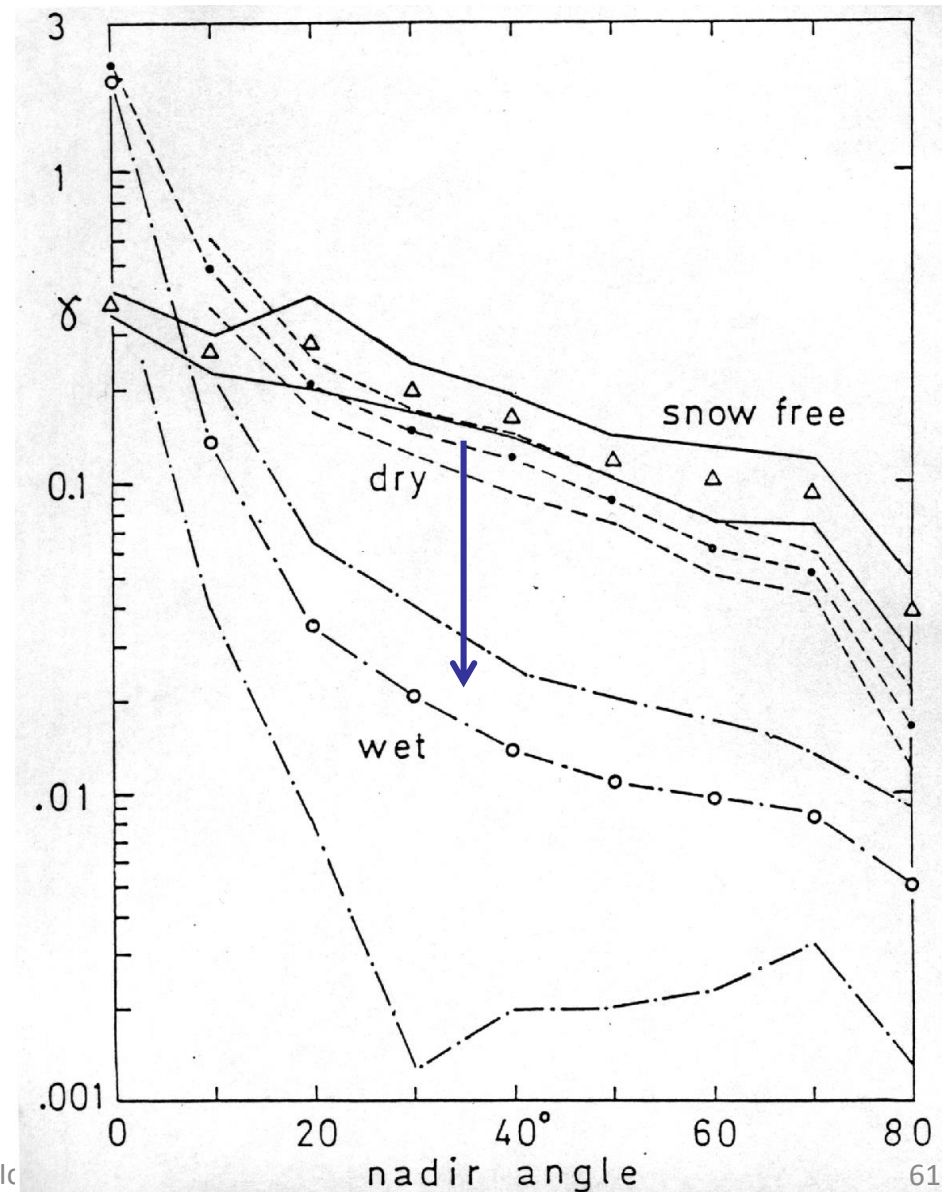
10.4 GHz co-pol

at Davos-Weissfluhjoch

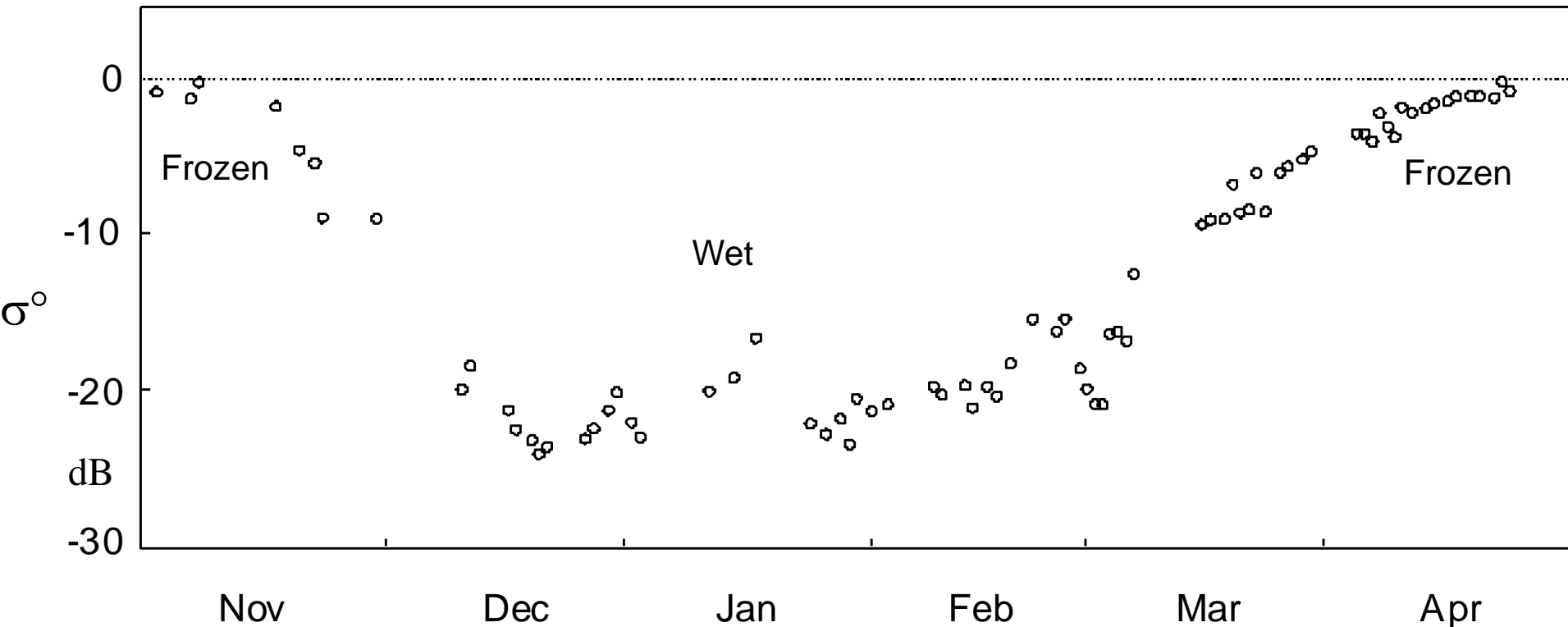
by C. Mätzler, Univ. Bern

**Backscattering
coefficient**

$$\gamma = \sigma^\circ / \cos\theta$$



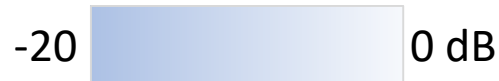
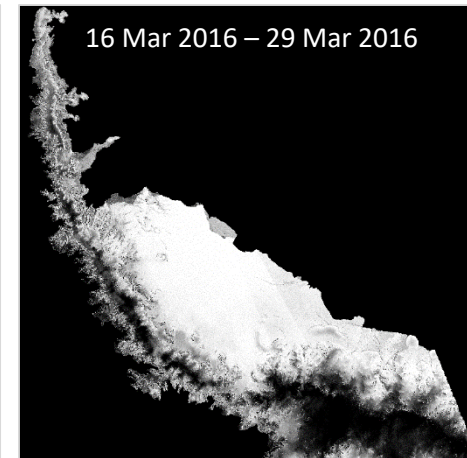
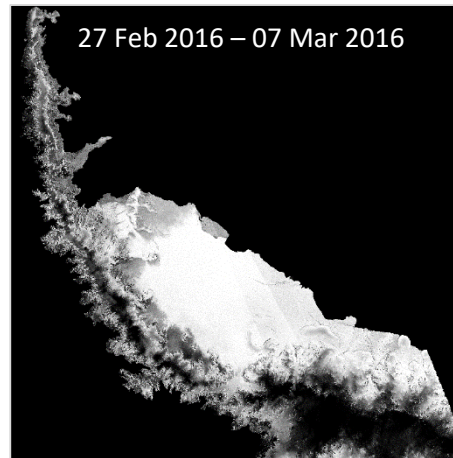
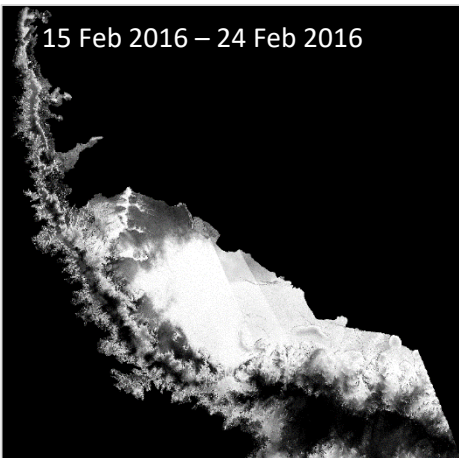
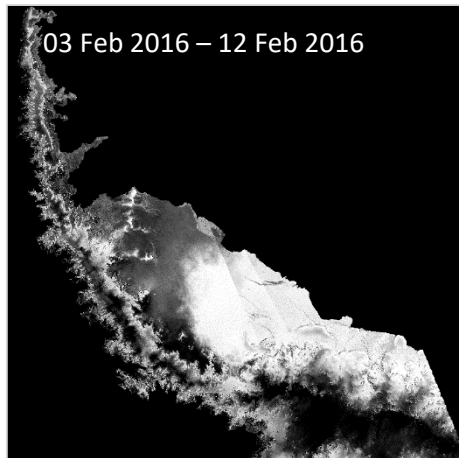
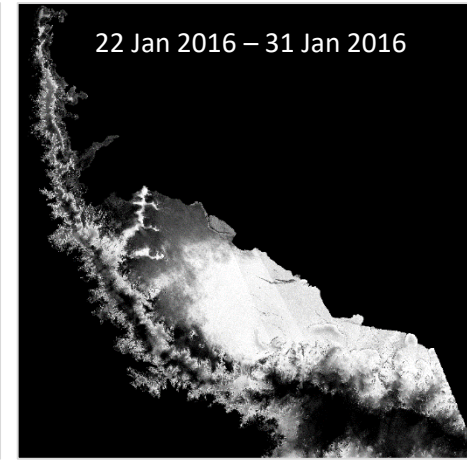
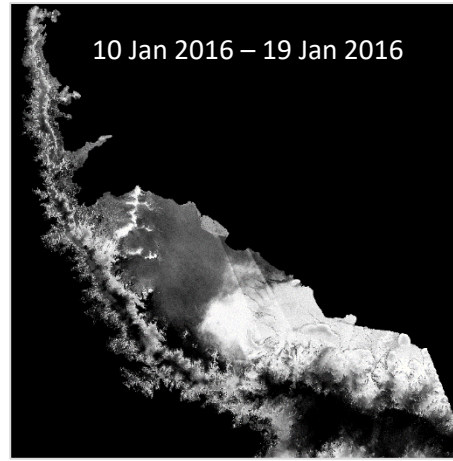
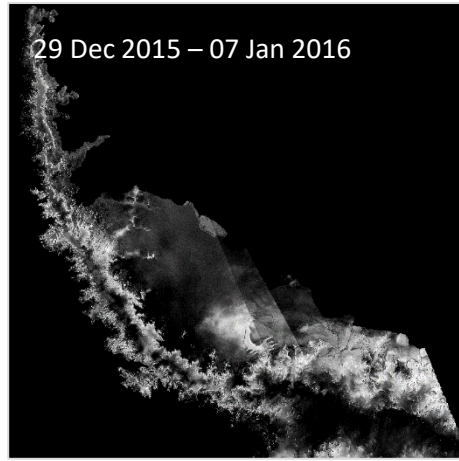
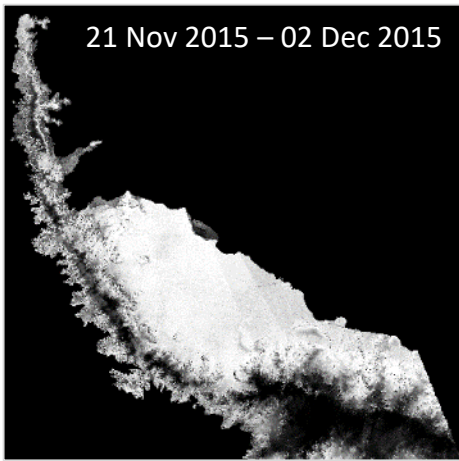
Observation of Seasonal Melt-Freeze Cycle on Ice Shelf



Site: Antarctic Peninsula, Larsen Ice Shelf (67°S), Firn

Sensor: ERS Scatterometer Data, 5.3 GHz (C-band)

Monitoring Melt Extent by means of Sentinel-1 backscatter



Factors for Backscattering of Snow (Ku to L-Band)

WET SNOW *Dominant Scattering Mechanism: Surface Scattering*

- Liquid water content *dominant factor*
- Surface roughness *important*
- Grain size *small effect*

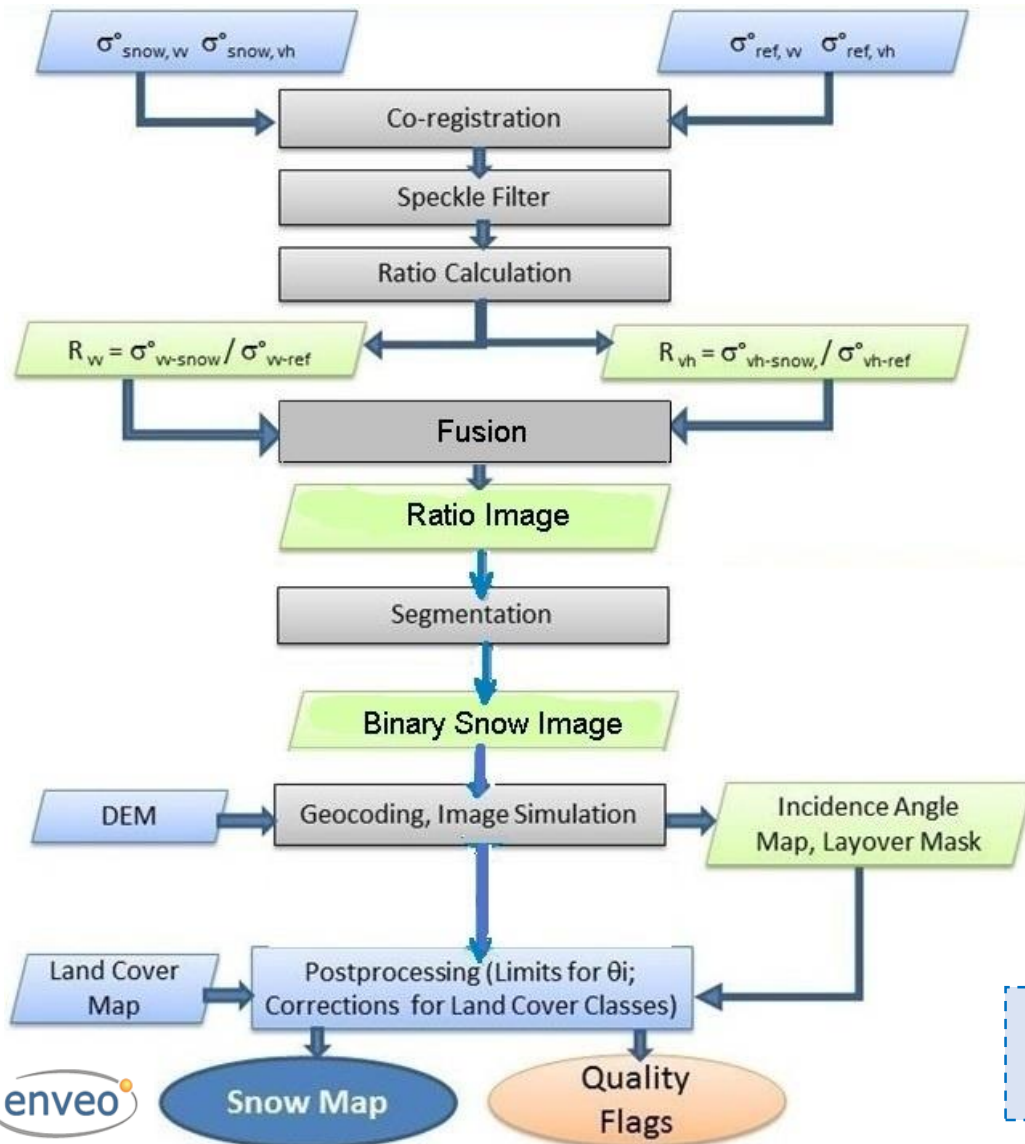
DRY SEASONAL SNOW: *Scattering in the Volume and/or at Lower Interface*

- σ° of medium below snow *dominating for seasonal snow at $f < \sim 10$ GHz*
- Grain size *important for $f > \sim 10$ GHz*
- *Snow Mass (snow water equivalent, SWE) → Little sensitivity of σ° at X- to L-band; Ku-band sensitive to SWE, but ambiguity with grain size*

REFROZEN SNOW (e.g. firn area on glaciers) *Volume Scattering*

- Volume inhomogeneities (grains, grain clusters, ice lenses, ice pipes, ..)
- Internal interfaces between snow layers of different density

5. SAR Application for Snowmelt Area Mapping



Basic Concept:

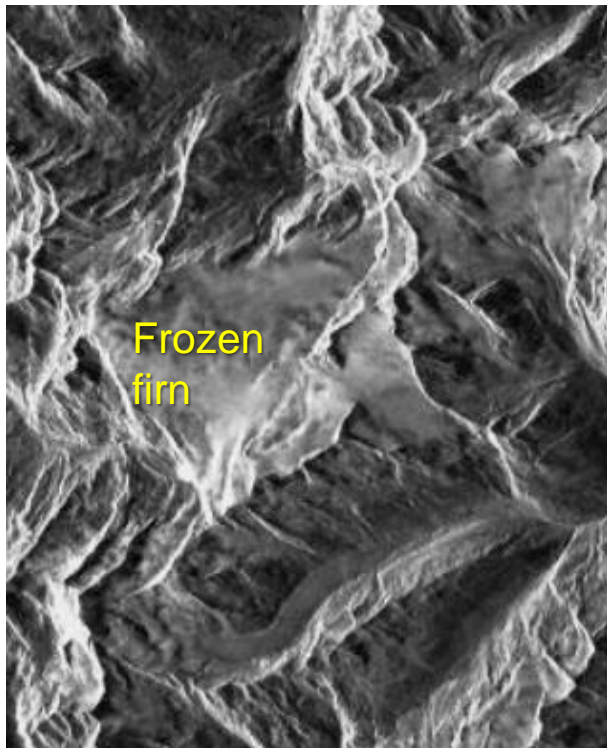
- Uses C-band or X-band SAR data
- Exploits the contrast of backscatter between wet snow and snow-free (resp. dry snow) reference conditions
- Applies the backscatter ratio ($\sigma^{\circ}_{\text{wetsnow}} / \sigma^{\circ}_{\text{reference}}$) to compensate for topographic effects
- Applies a segmentation procedure for separating the two surface types in σ° -ratio images



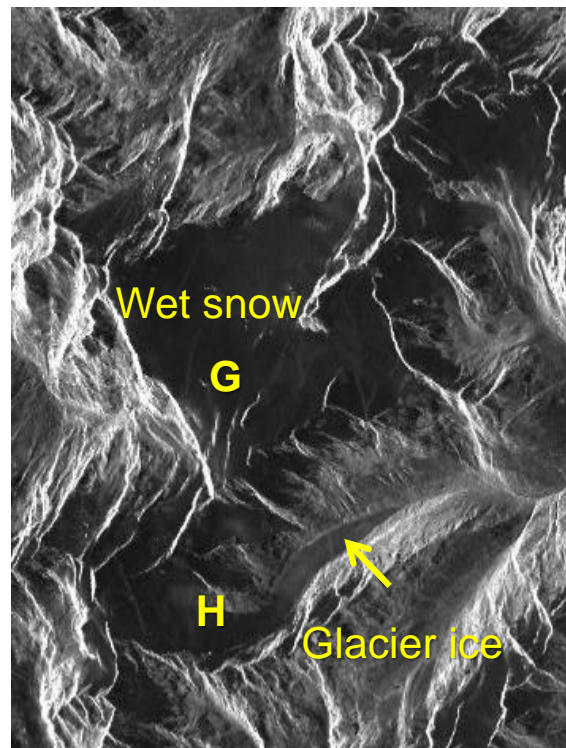
← Processing line for Sentinel-1 IW mode data (C-band, VV and VH polarization)

Wet Snow Area on Glaciers, from TerraSAR-X Data

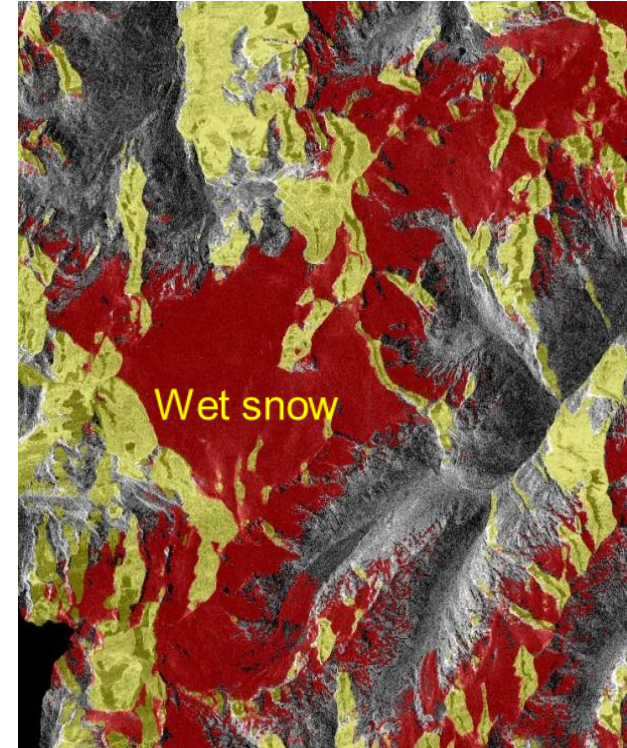
Reference image:
(Dry snow)
25 Dec 2008



Wet snow on glaciers:
Low σ°
10 July 2009



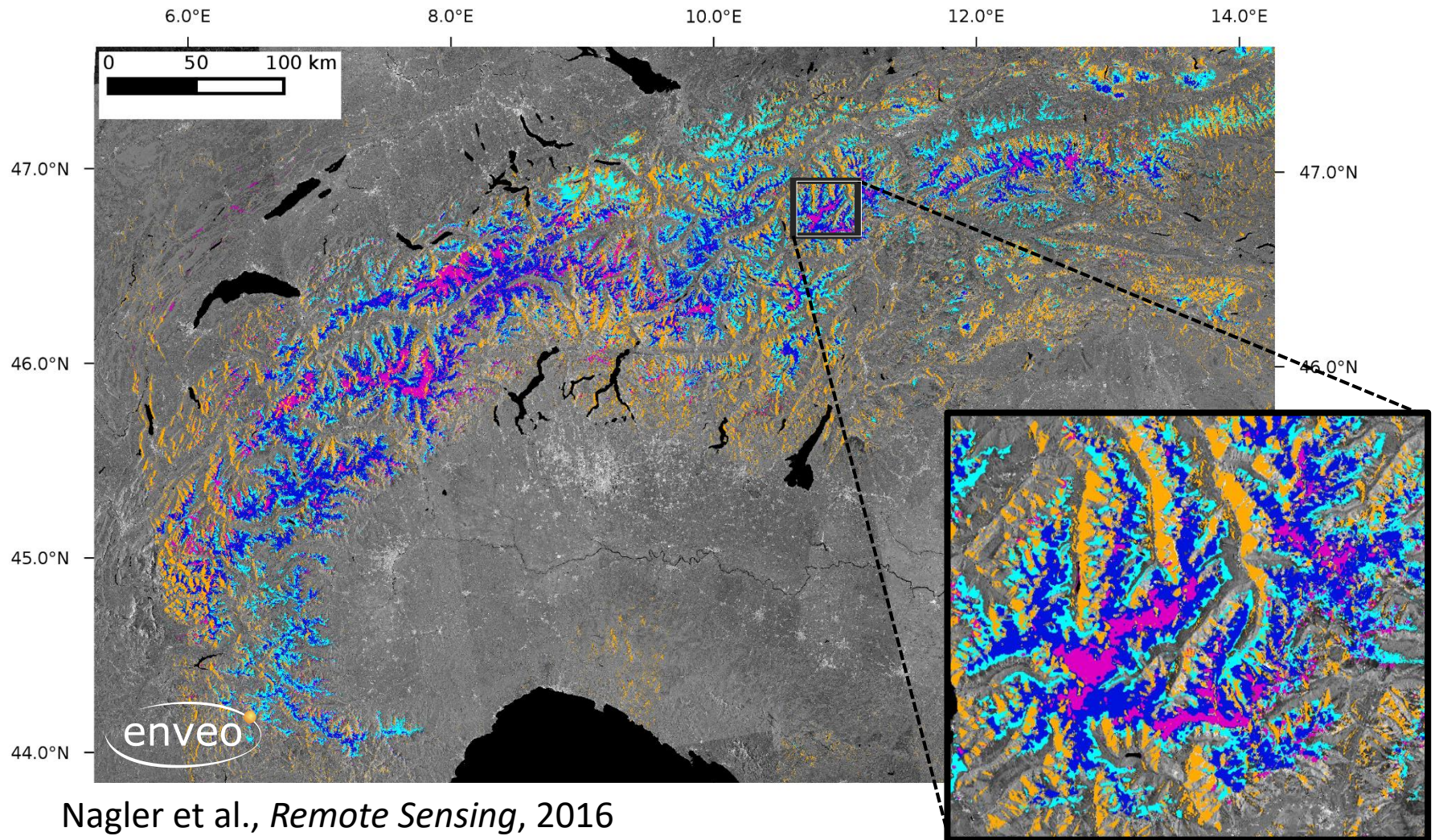
Snowmelt area 10 July 09:
Red – wet snow
Yellow - layover



G – Gepatsch Glacier, H – Hintereis Glacier (Ötztal, Austria)



Monitoring Snowmelt Area by Sentinel-1 SAR IW Mode Data



Nagler et al., *Remote Sensing*, 2016

- decrease of wet snow extent from April 20-23 to May 14-17, 2015
- decrease of wet snow extent from May 14-17 to July 1-7, 2015

- wet snow extent, July 1-4, 2015
- layover / foreshortening

6. Interferometric Signals of Snow Cover

Degree of coherence:

$$\gamma_{\text{total}} = \gamma_{\text{SNR}} \cdot \gamma_{\text{surface}} \cdot \gamma_{\text{volume}} \cdot \gamma_{\text{temporal}}$$

$$\gamma = \frac{|E\{V_1 V_2^*\}|}{\sqrt{E\{V_1\}^2 E\{V_2\}^2}}$$

Time dependent factors for decorrelation γ_{temporal} :

- Surface melt
- Snowfall
- Snow drift (wind erosion and deposition)

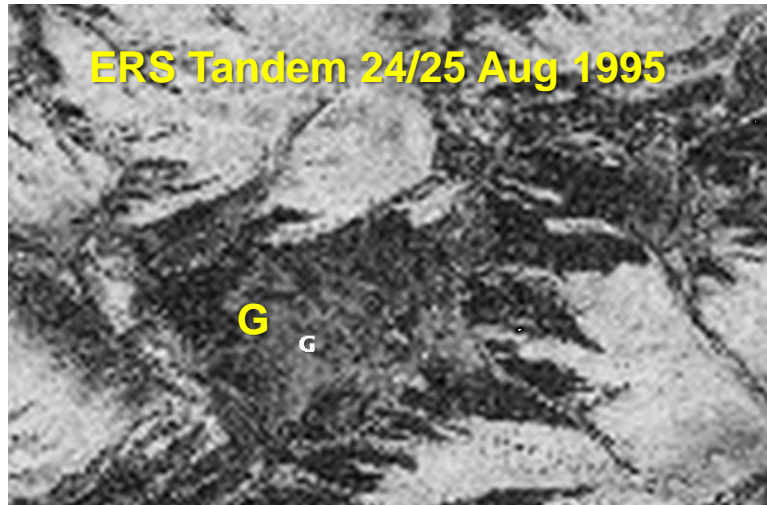
These are main obstacles for repeat-pass InSAR over snow and ice

Other factors

- Volume wavenumber shift (volume decorrelation in dry, deep snow; dependent on baseline and penetration depth) γ_{volume}
- Surface wavenumber shift (dependent on baseline) γ_{surface}
- Thermal noise (relevant for low σ°) γ_{SNR}

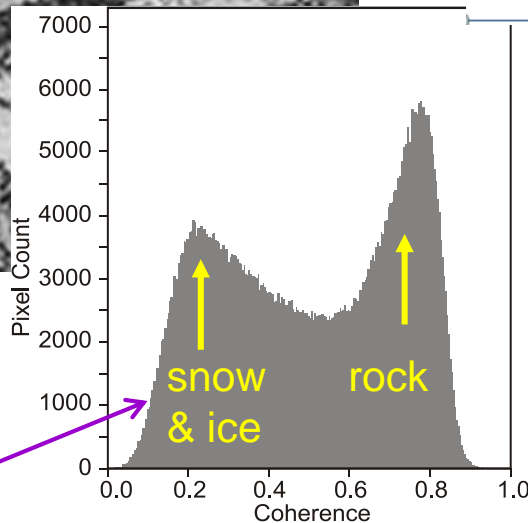
InSAR Coherence of Snow and Ice

Decorrelation due to melting

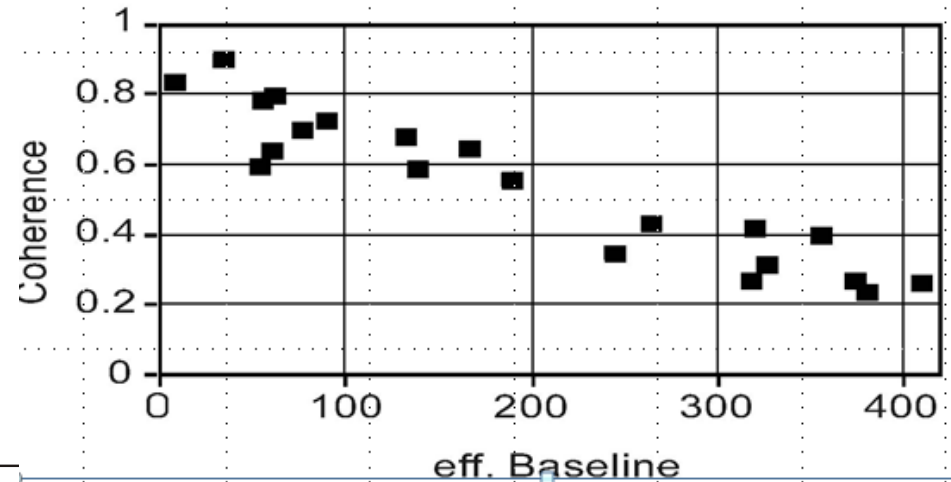


Ötztal Glaciers

Wet snow



Volume Decorrelation in **dry snow**



Coherence decreases with increasing length of InSAR baseline
From 3-day repeat pass ERS-1 SAR data, Antarctic inland ice (Dronning Maud Land)

Change of Propagation Path Length in Dry Snow Pack

Total interferometric phase difference of repeat-pass InSAR:

$$\phi = \phi_{flat} + \phi_{topo} + \phi_{dis} + \phi_{atm} + \phi_{snow} + \phi_{noise}$$

Phase shift due to accumulation of dry snow

related to SWE (Gunteriusen et al., 2001)

$$\Delta\phi_{snow} = -2k \Delta d_s \left(\cos \theta_i - \sqrt{\epsilon - \sin^2 \theta_i} \right)$$

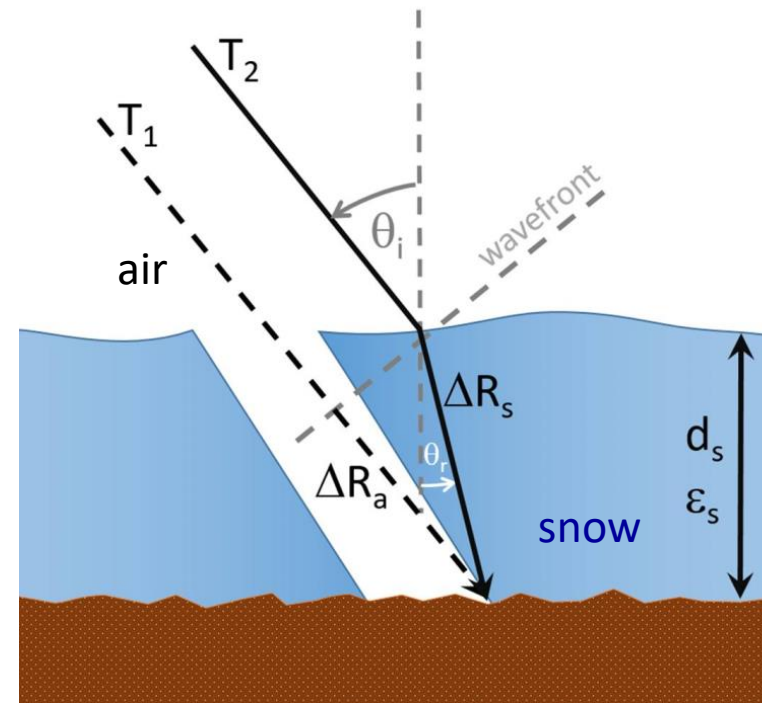
$$|k| = (2\pi)/\lambda \quad \lambda = 2\pi/\sqrt{\epsilon}$$

$$\epsilon' = 1 + 1.5995 \rho_s + 1.86 \rho_s^3 \text{ [g cm}^{-3}\text{]}$$

$$SWE = d_s \langle \rho_s \rangle$$

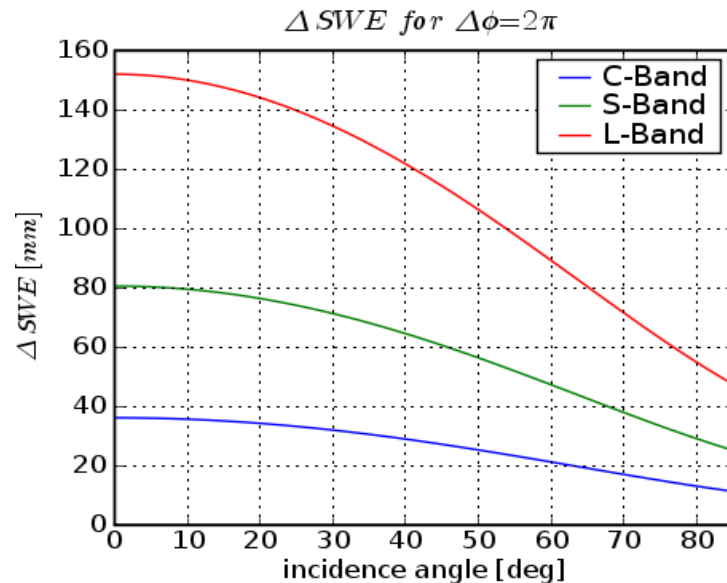
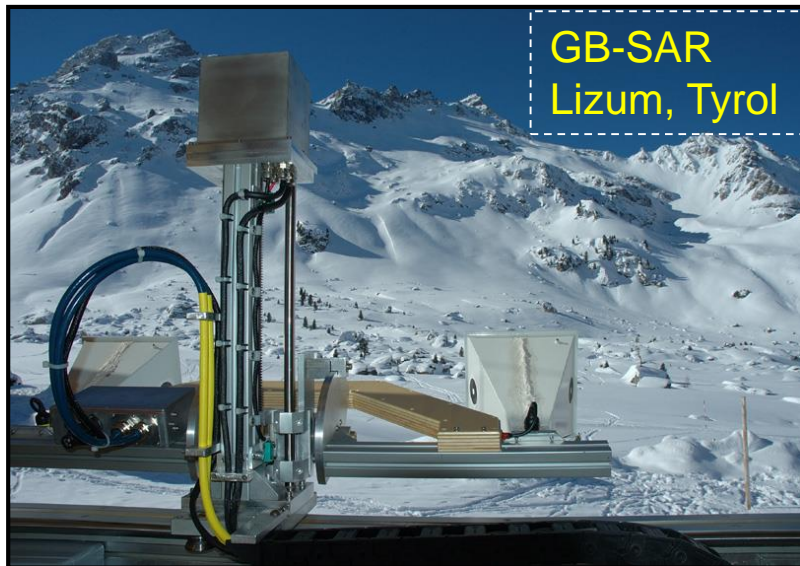
Linear approximation for incidence angles $\theta < \sim 40^\circ$:

$$\Delta\phi_{snow} = \frac{1.6k}{\cos \theta_i} \Delta SWE$$



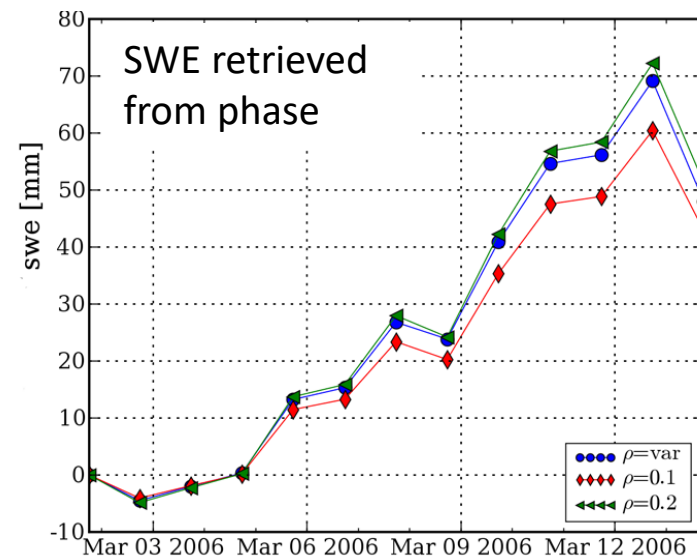
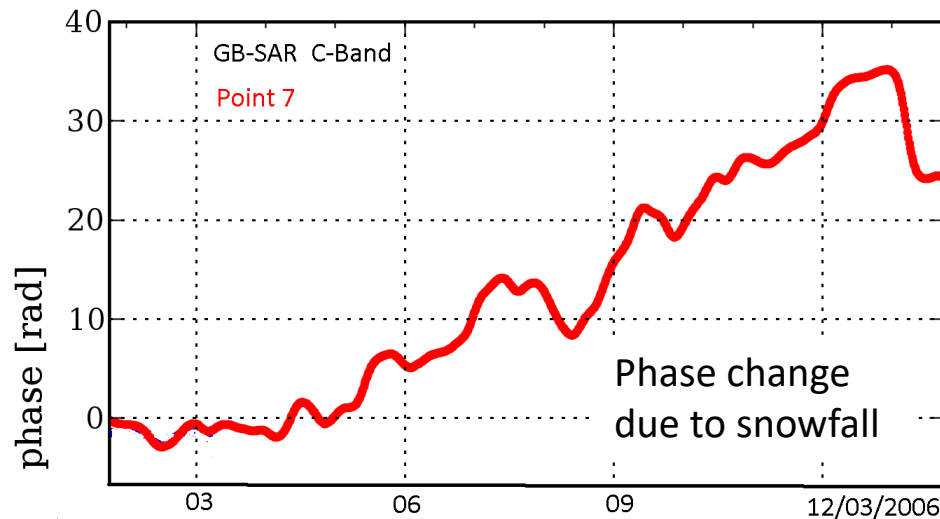
$$\Delta\phi_{snow} = 2\pi \Rightarrow \Delta SWE = 3.2 \text{ cm (C-band at } \theta=23^\circ) \quad \text{for one fringe}$$

SWE Retrieval by Means of Interferometric Phase Change



2π phase ambiguity for SWE

Luzi et al., 2009

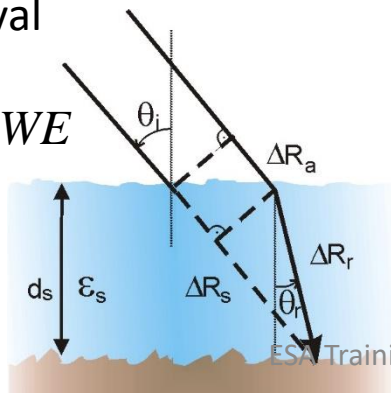


EO Concepts for SWE Monitoring

Approach	Strengths	Weaknesses
Passive MW 18.7 & 37 GHz 10.6 & 32 GHz	sensitive to SWE & melt; global daily coverage; independent of clouds/illumination; very long record	Coarse resolution, not suitable for mountains and forests, saturation at higher SWE
Radar (Scat or SAR): Dual: Ku & Ka Single: Ku, Ka	sensitive to SWE & melt; high resolution; independent of clouds/illumination	algorithm maturity, coverage, SWE saturation, forests
InSAR L- , C-Band	direct SWE sensitivity; high resolution avoids volume scattering issues	forests, complexity; requires advanced acquisition plan
LIDAR	direct observation of snow depth; very high resolution, minor forests and topographic issues	SWE retrieval requires snow density; No Sensor

InSAR SWE Retrieval

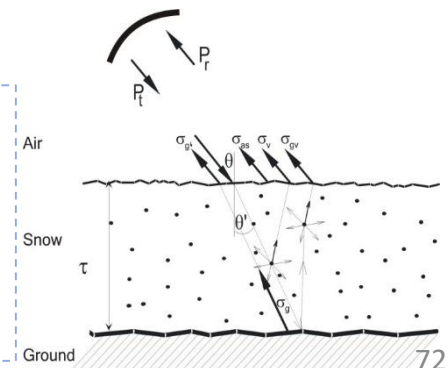
$$\Delta\phi_{snow} = \frac{1.6k}{\cos\theta_i} \Delta SWE$$



Radar (Scat or SAR)

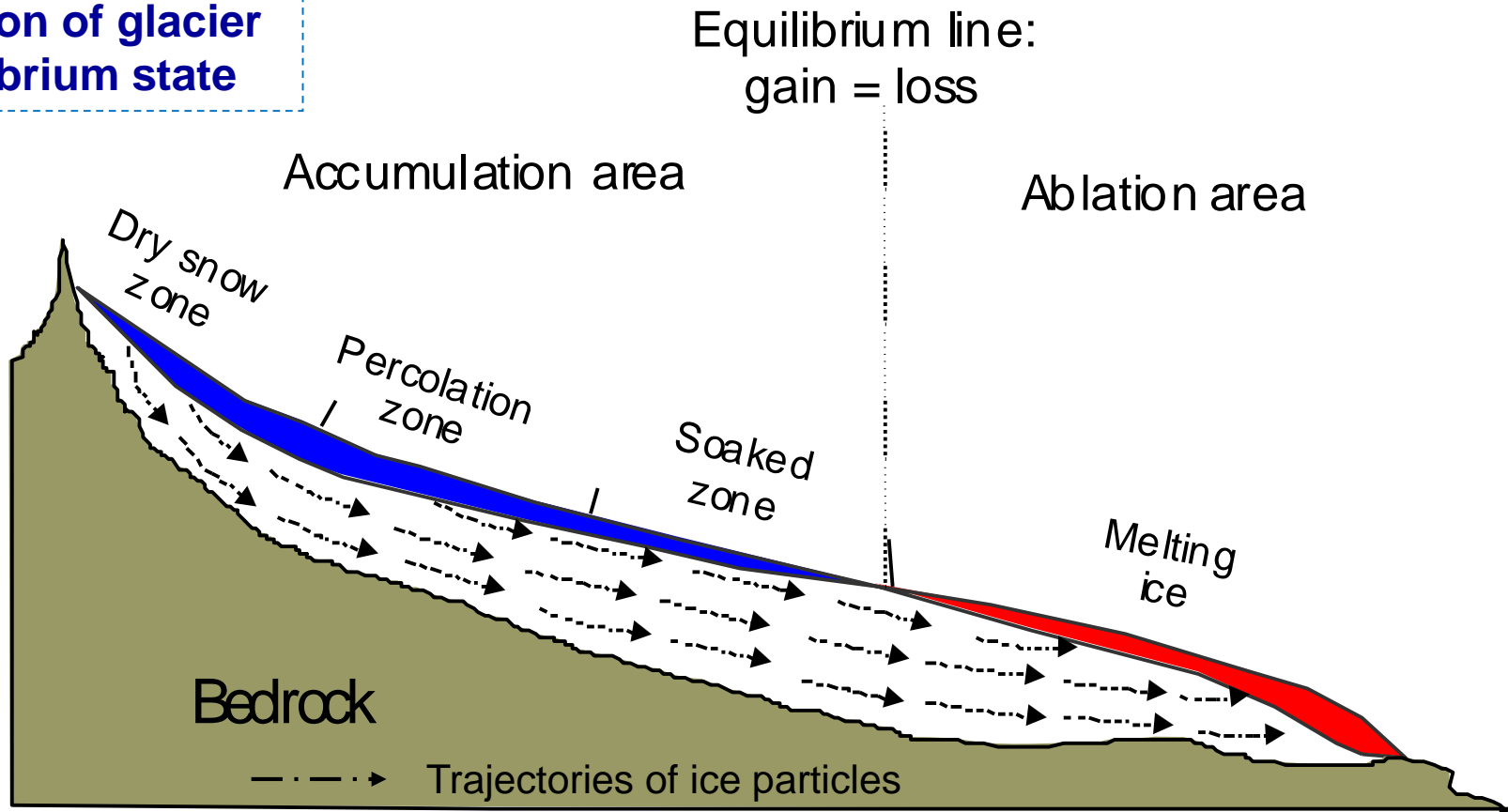
Sensitivity of backscatter
to SWE depends on
scattering albedo:

Dual F: Ku + Ka
Single F: Ku, Ka



7. Glacier Motion by InSAR and Offset Tracking

Ice motion of glacier in equilibrium state



Objectives for mapping Ice Motion:

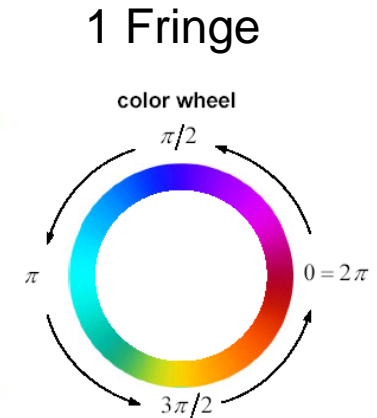
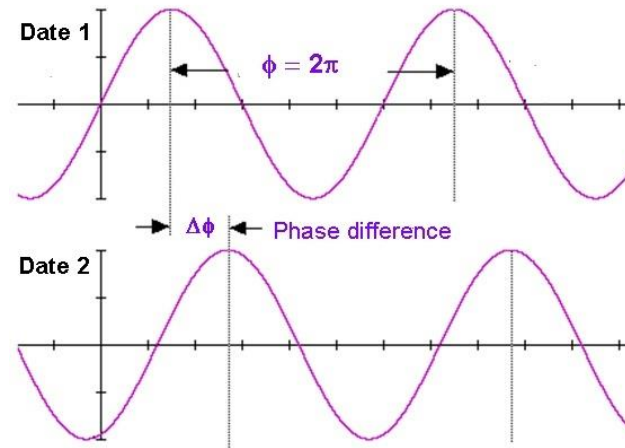
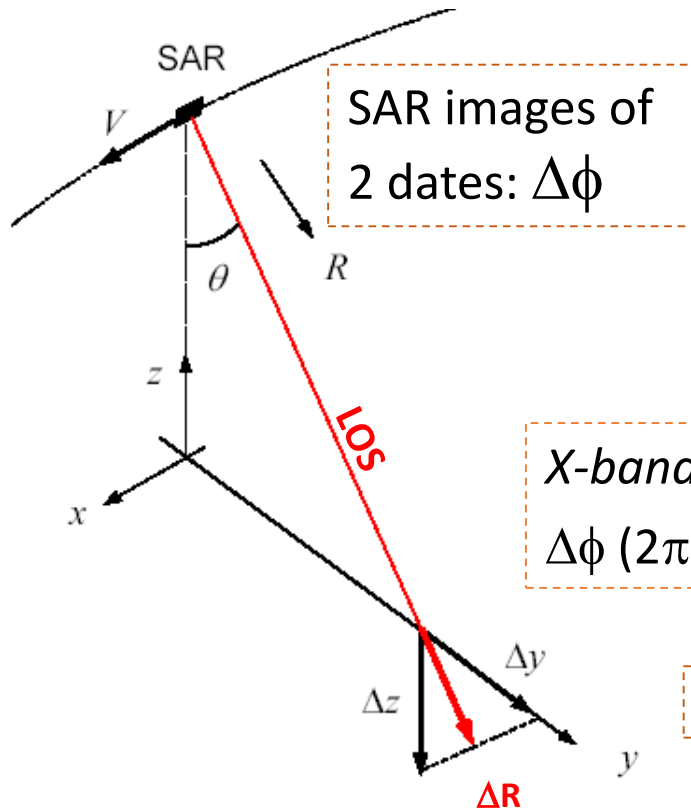
- Analyzing and predicting glacier response to climate change
- Retrieving ice export by calving (Input/Output method for mass balance)

Ice Motion: Repeat-Pass InSAR vs. Offset Tracking

	INSAR	OFFSET TRACKING
Velocity component	LOS motion only	2 motion components LOS (range) and along track
Accuracy of displacement for ERS , TerraSAR-X)	≤ 5 mm LOS (ERS, S-1) (with 1day repeat ~ 1.8 m/a)	~ 1.5 m, \sim 0.2 m slant range ~ 1.0 m, \sim 0.2 m along track
Typical time interval (Δt)	1, 3 days (ERS), 11 days TSX; 12 (6) d. Sentinel-1 (several weeks coherent in central Antarctica)	11, 22,.. days for TerraSAR-X 35 days for ERS, ASAR 6, 12, ... days for Sentinel-1
Main constraints	Temporal decorrelation (lack of coherence) No sensitivity to motion along track Unwrapping problem	Lack of stable amplitude features (for amplitude corr.) Coherence (speckle tracking) Lower sensitivity than InSAR (compensated by longer Δt) Less spatial detail

Interferometric measurement of Motion and Topography

Measurement of Displacement

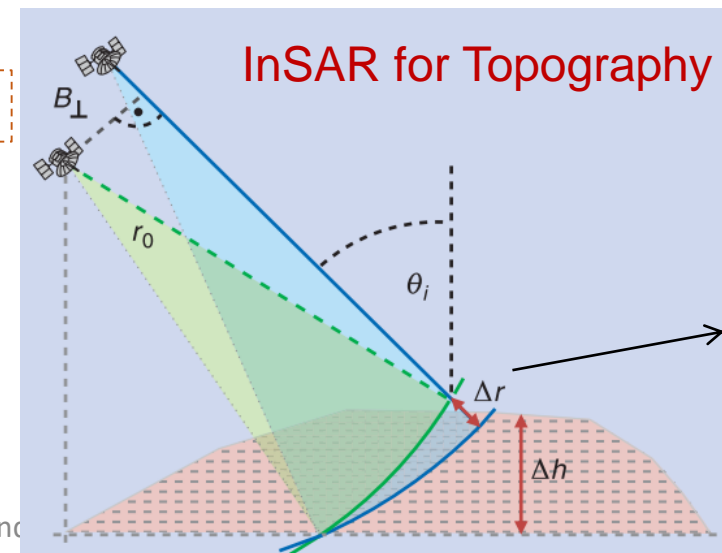


X-band SAR ($\lambda = 3.12 \text{ cm}$) *C-band SAR* ($\lambda = 5.66 \text{ cm}$)
 $\Delta\phi (2\pi) \Rightarrow \Delta R = 1.56 \text{ cm}$ $\Rightarrow \Delta R = 2.83 \text{ cm}$

TanDEM-X

InSAR repeat track measures displacement ΔR in Line-of-Sight

Requires temporal stability of radar signal phase (coherence)



$\Delta r \sim \Delta\phi$

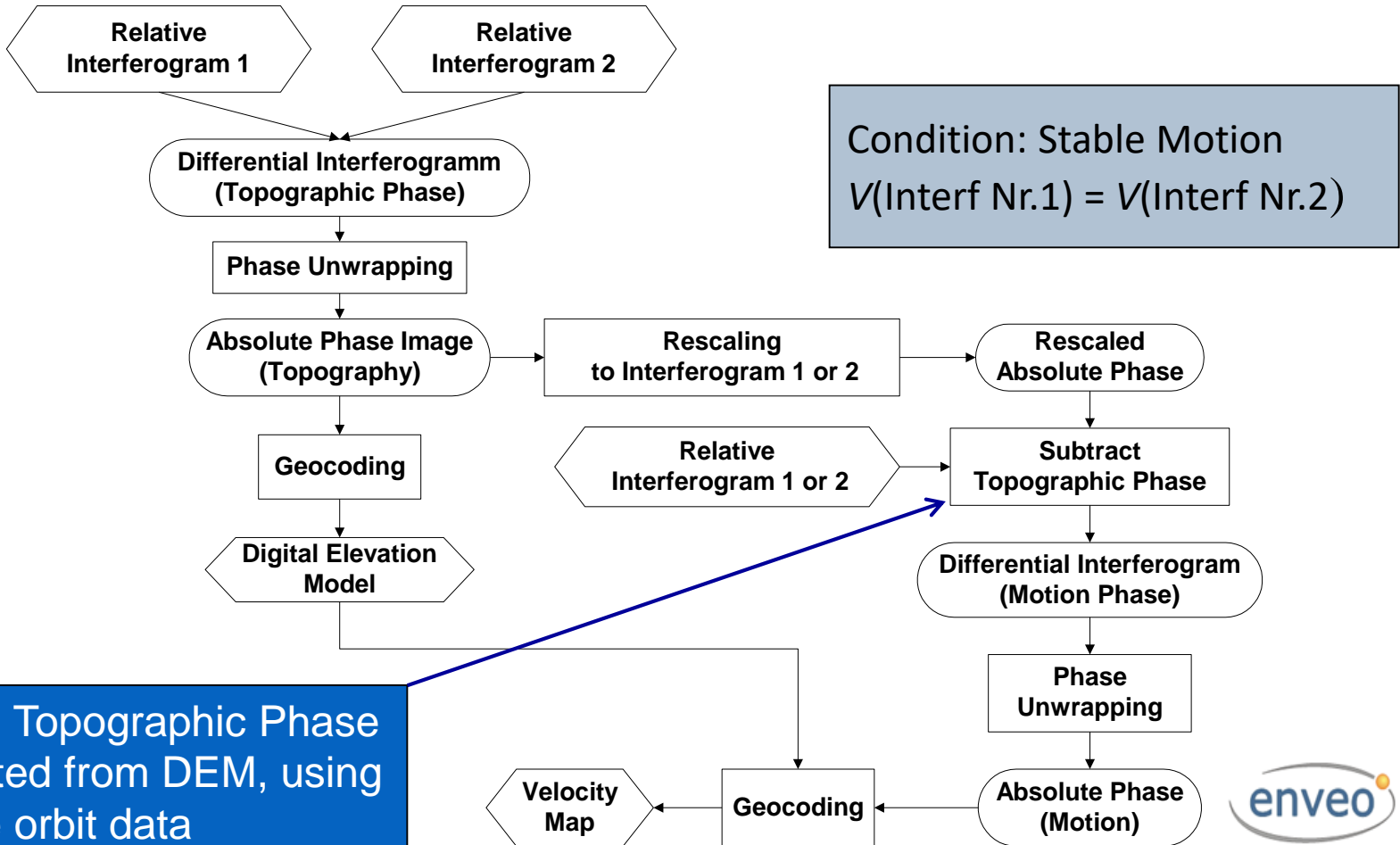
Ice and

Differential InSAR (DInSAR) Processing of Ice Motion

Repeat-pass InSAR Phase:
$$\Delta\phi = \Delta\phi_{flat} + \Delta\phi_{topo} + \Delta\phi_{dis} + \Delta\phi_{atm}$$

Derived from orbit data

Separated by DInSAR processing

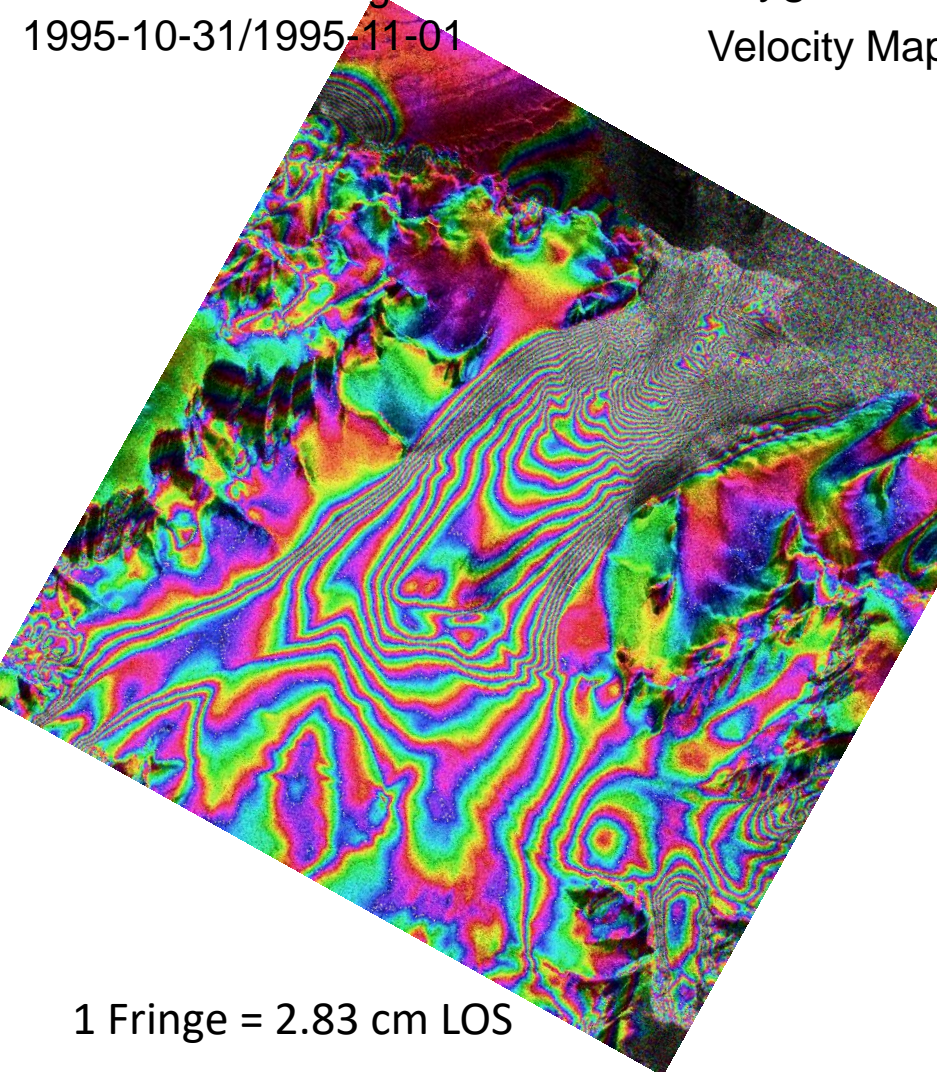


Glacier Velocity Map from ERS InSAR Data

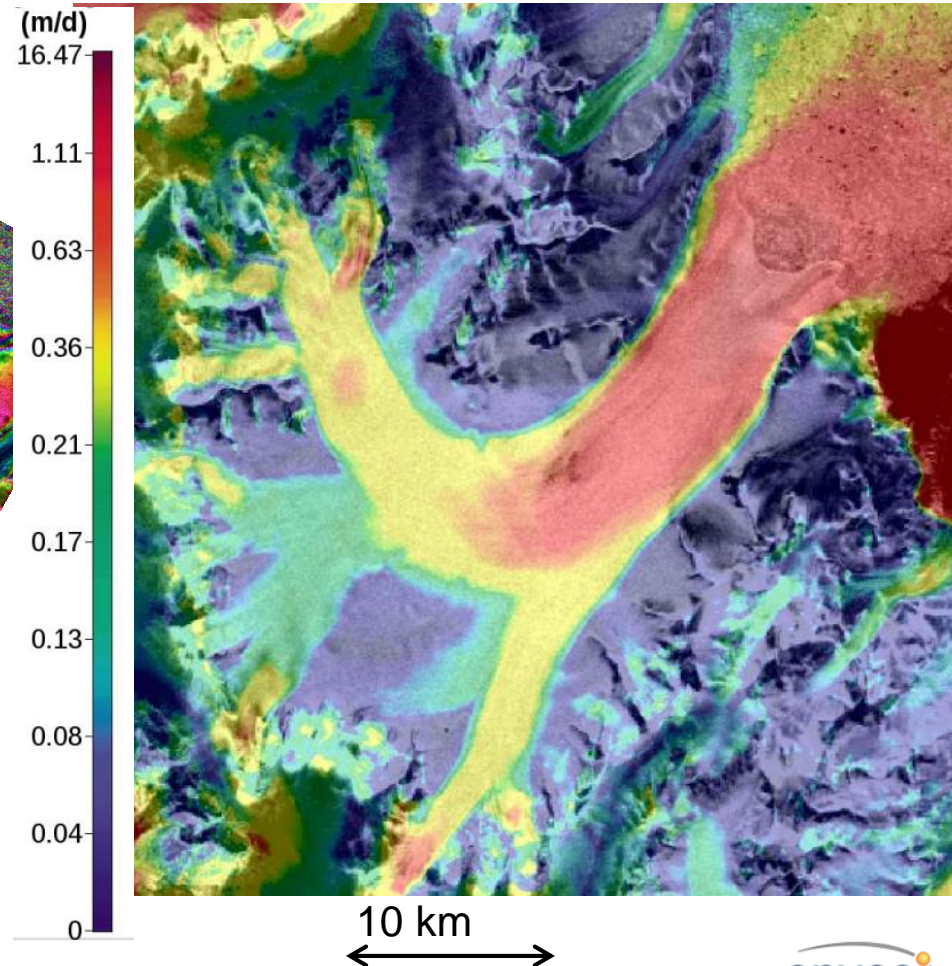
ERS-1/-2 Interferogram
1995-10-31/1995-11-01

Drygalski Glacier, Antarctic Peninsula

Velocity Map (magnitude) from InSAR data of **crossing orbits**



1 Fringe = 2.83 cm LOS





Drygalski Glacier

Sea Ice

SAR Offset Tracking Techniques for Ice Motion

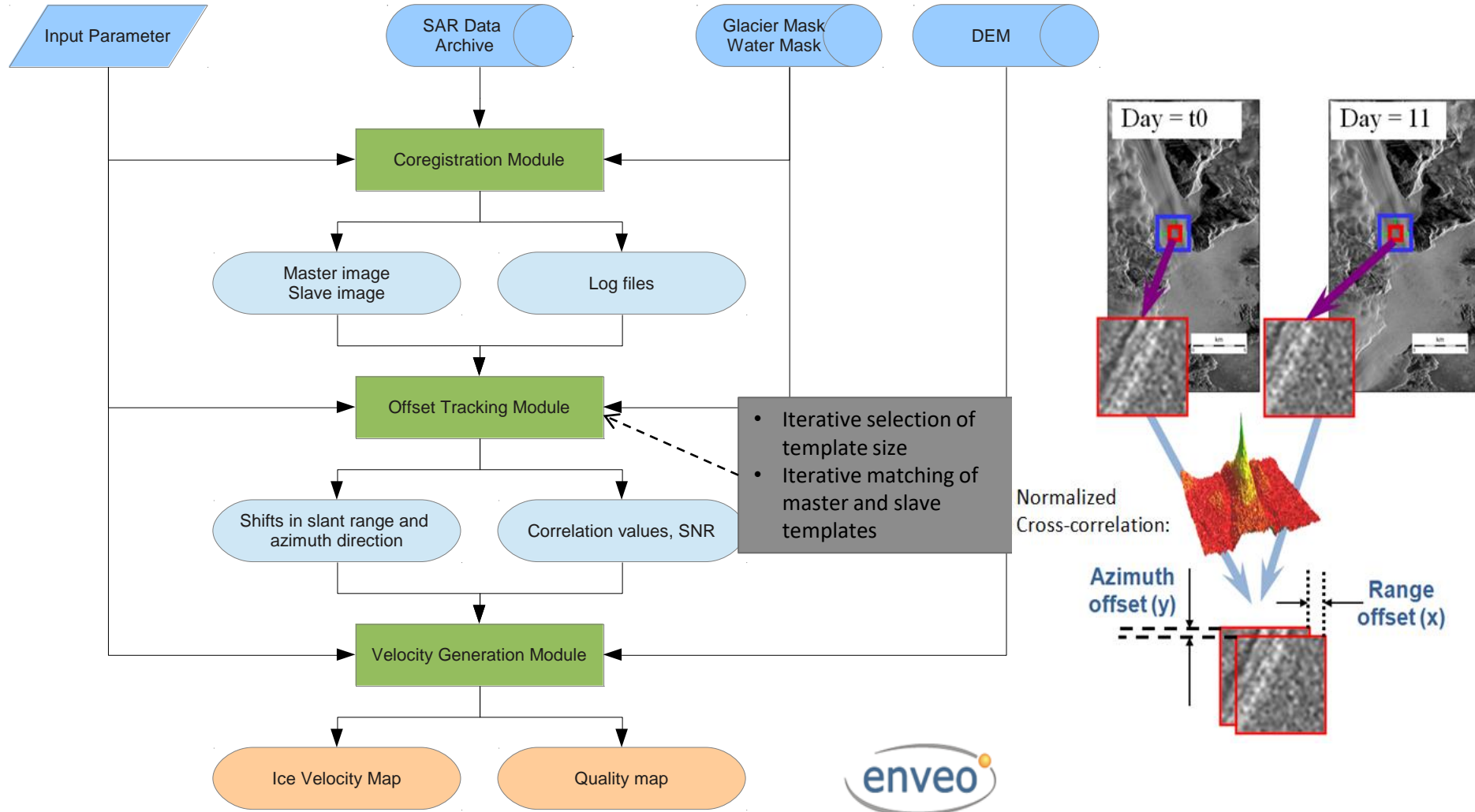
Basic principle: Matching of image templates by cross correlation (along track and in range) in co-registered SAR images.

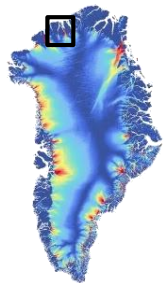
Possibilities for features to be tracked:

- 1. Amplitude correlation:** Uses persistent features in backscattering amplitude images (e.g. crevasses, drainage features). Advantage: Coherence not required. Disadvantage: Lack of features in accumulation areas of glaciers (snow areas) prohibits application.
- 2. Speckle tracking:** Uses coherent amplitude data (complex or magnitude). *Advantage:* Works also where no obvious amplitude features exist. No need for unwrapping. *Disadvantage:* Coherence required, but gaps due to lack of coherence can be bridged.
- 3. Coherence tracking:** Uses templates in coherence images and looks for maximum value. Method and possibilities similar to method (2).

*Typical achievable accuracy in displacement: ~ 0.2 pixels in x and y .
Errors depend on co-registration, type of features, quality of matching.*

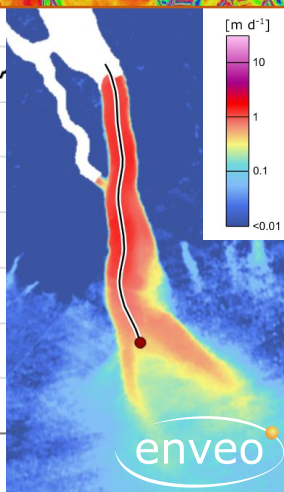
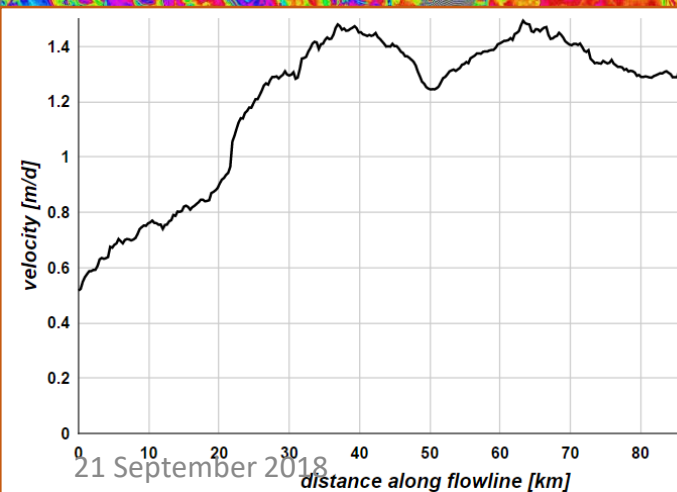
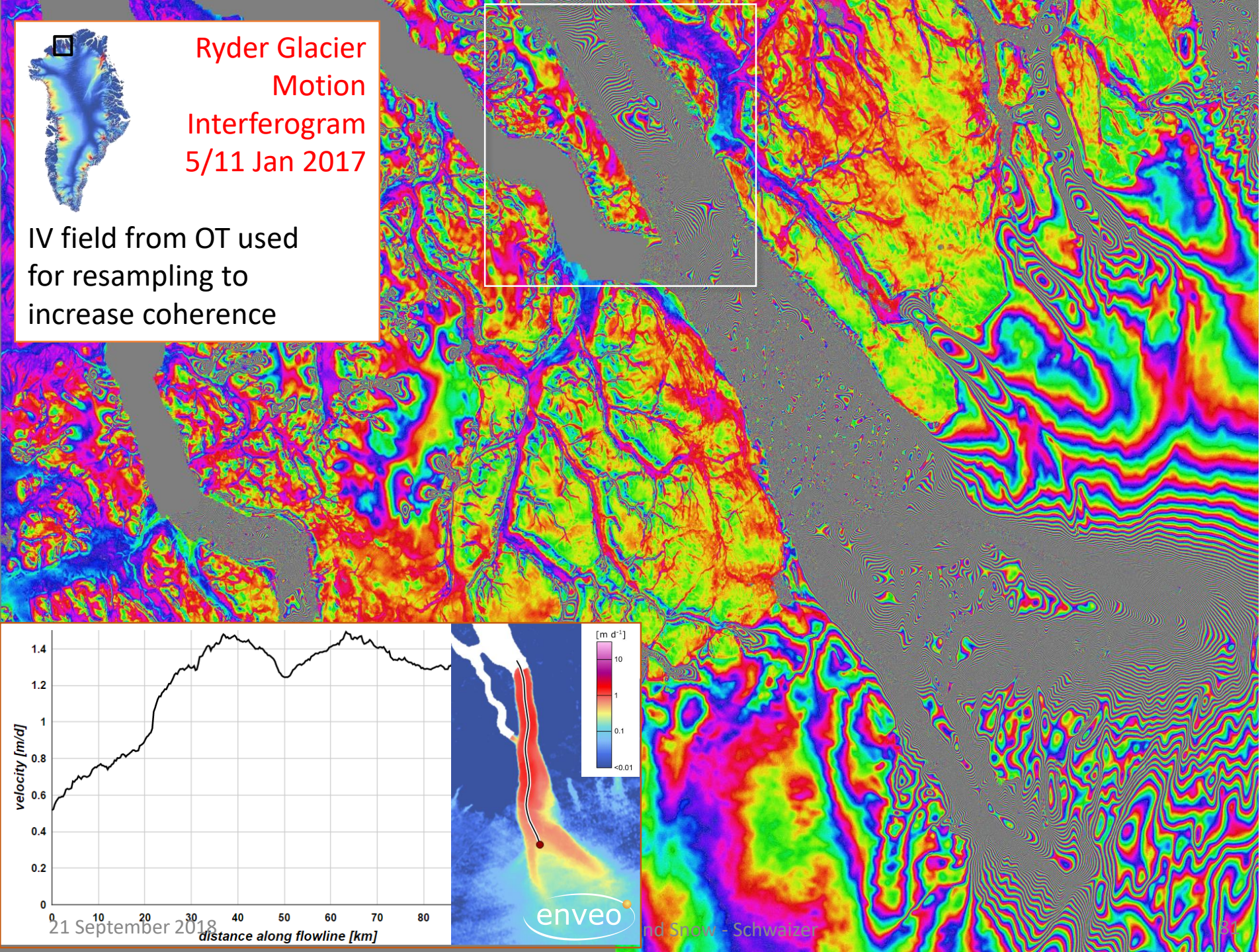
Processing Algorithm for SAR Offset Tracking





Ryder Glacier
Motion
Interferogram
5/11 Jan 2017

IV field from OT used
for resampling to
increase coherence



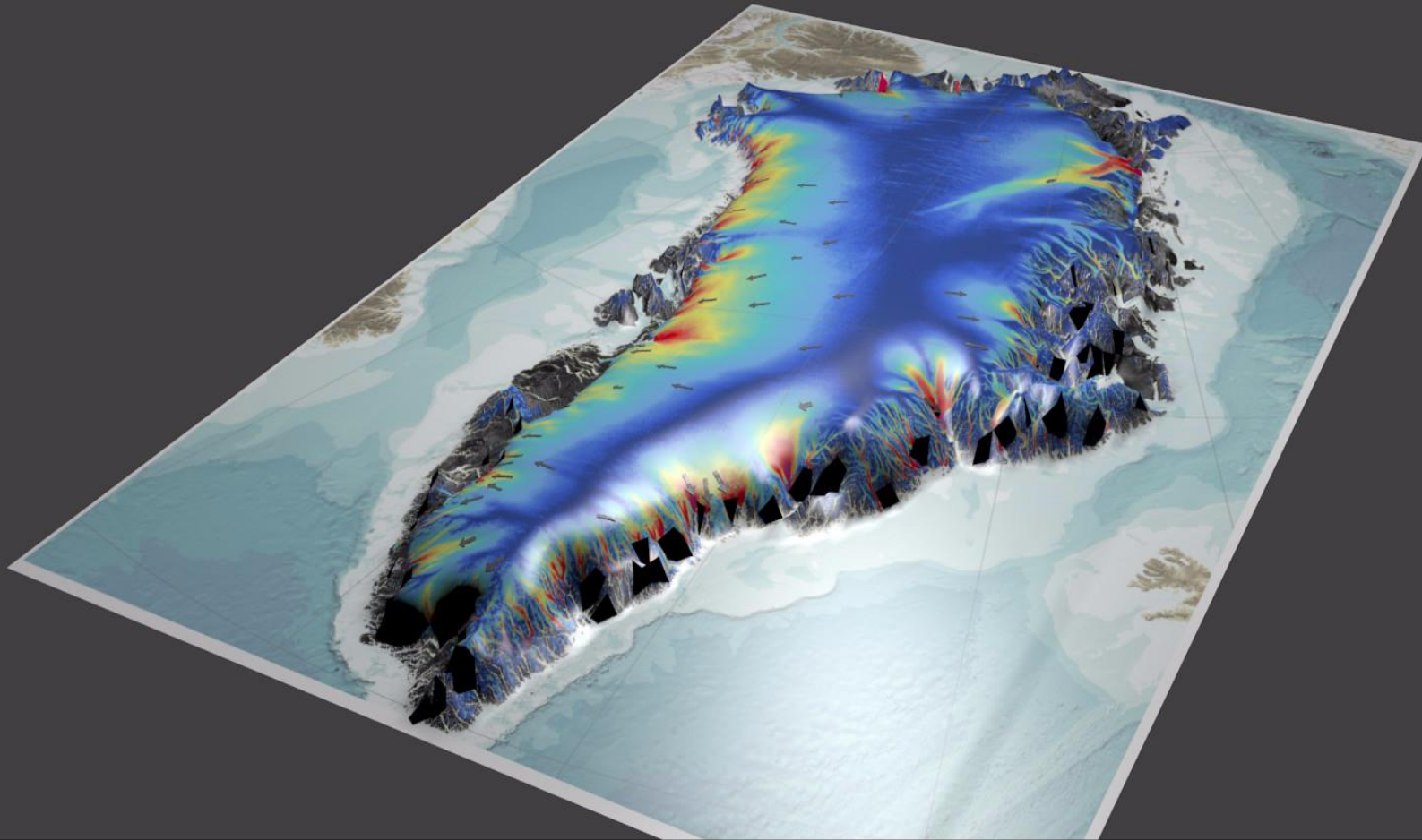
21 September 2018

distance along flowline [km]

enveo

nd Snow - Schwab

Continuous monitoring of ice motion of Greenland outlet glaciers by Sentinel-1

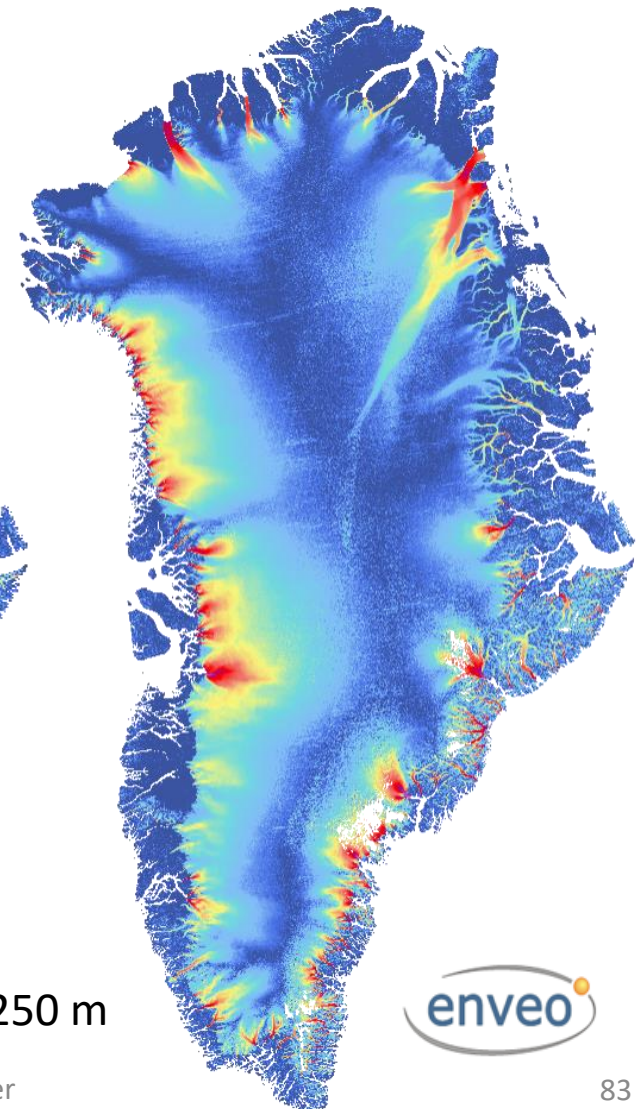
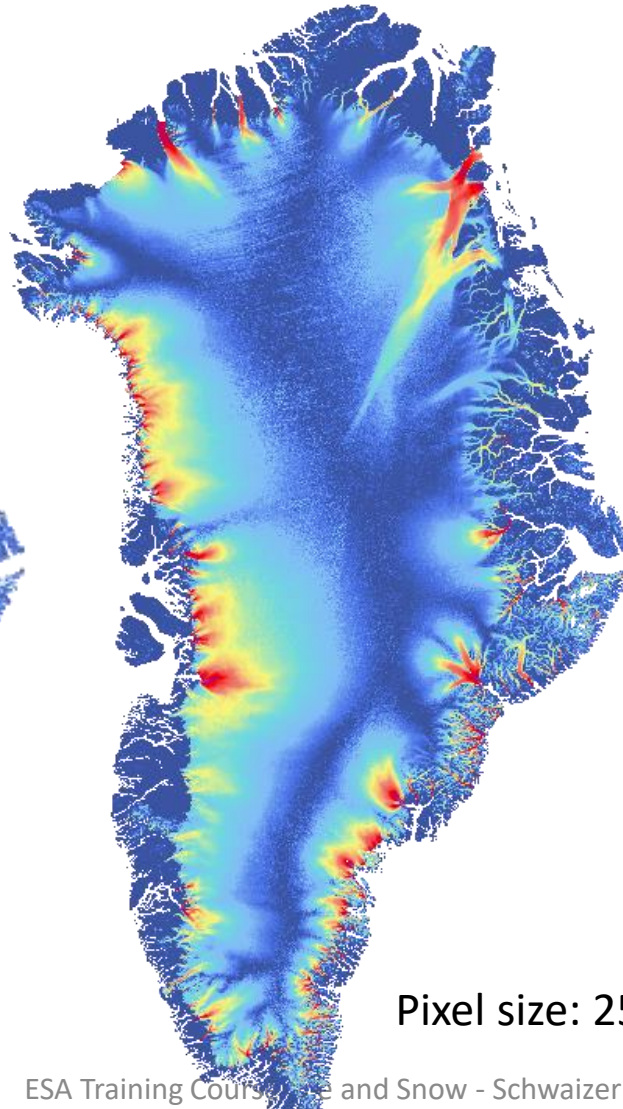
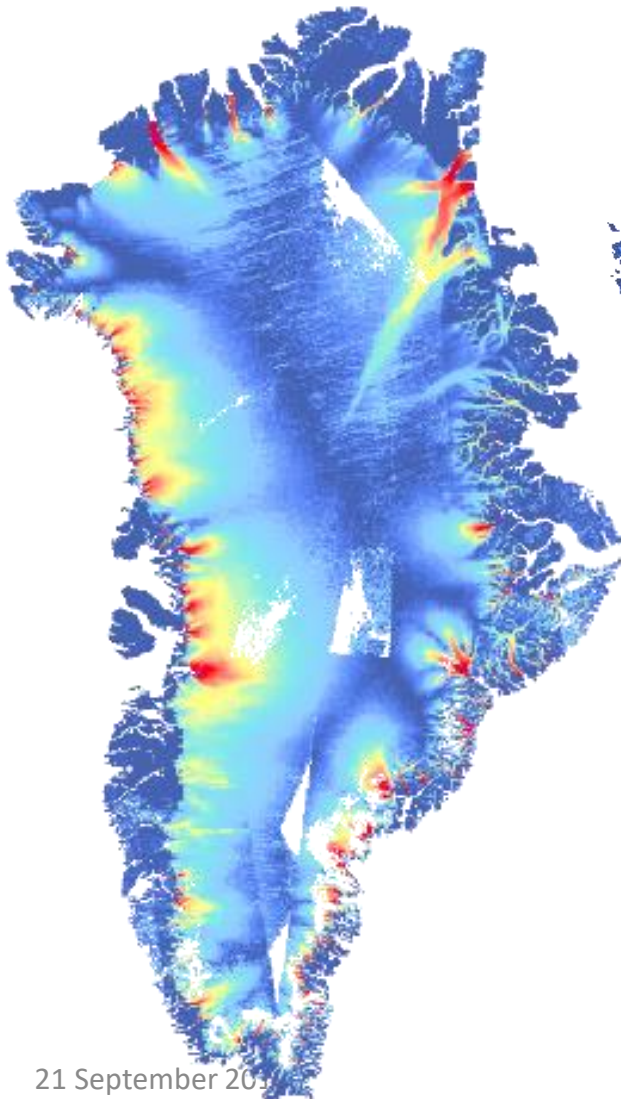


Annual Ice Velocity Maps for Greenland from Sentinel-1

2014/15

2015/16

2016/17 (23 Dec-27 Feb)



Pixel size: 250 m

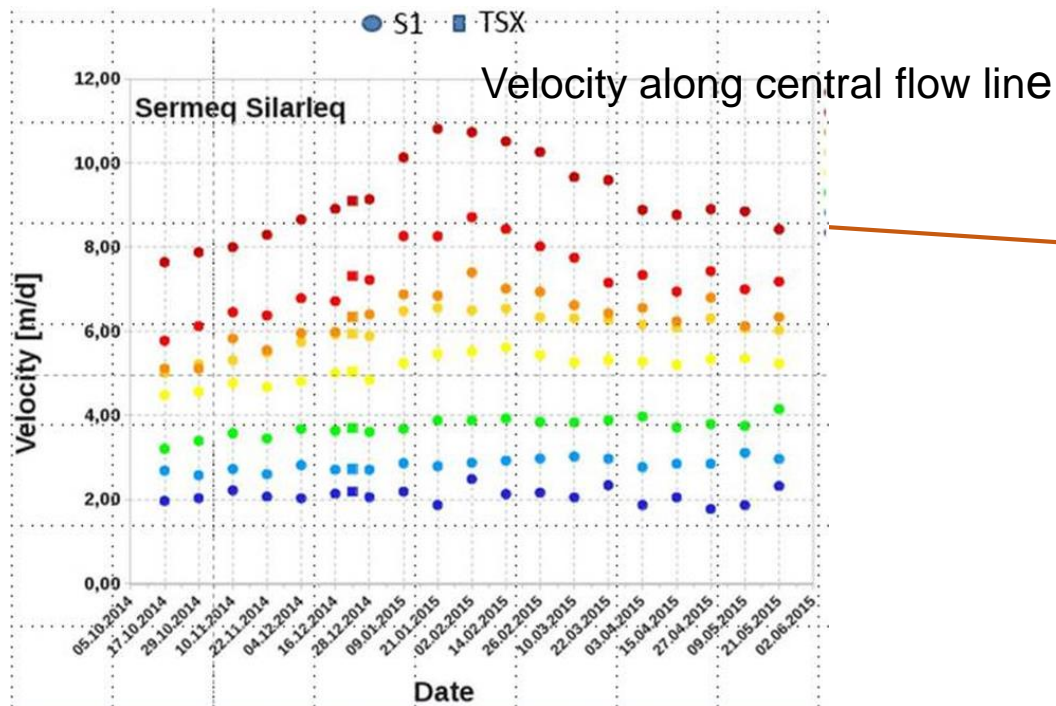


Ice Motion Map of Greenland from Sentinel-1 IW Mode Data

Grid size of velocity product:

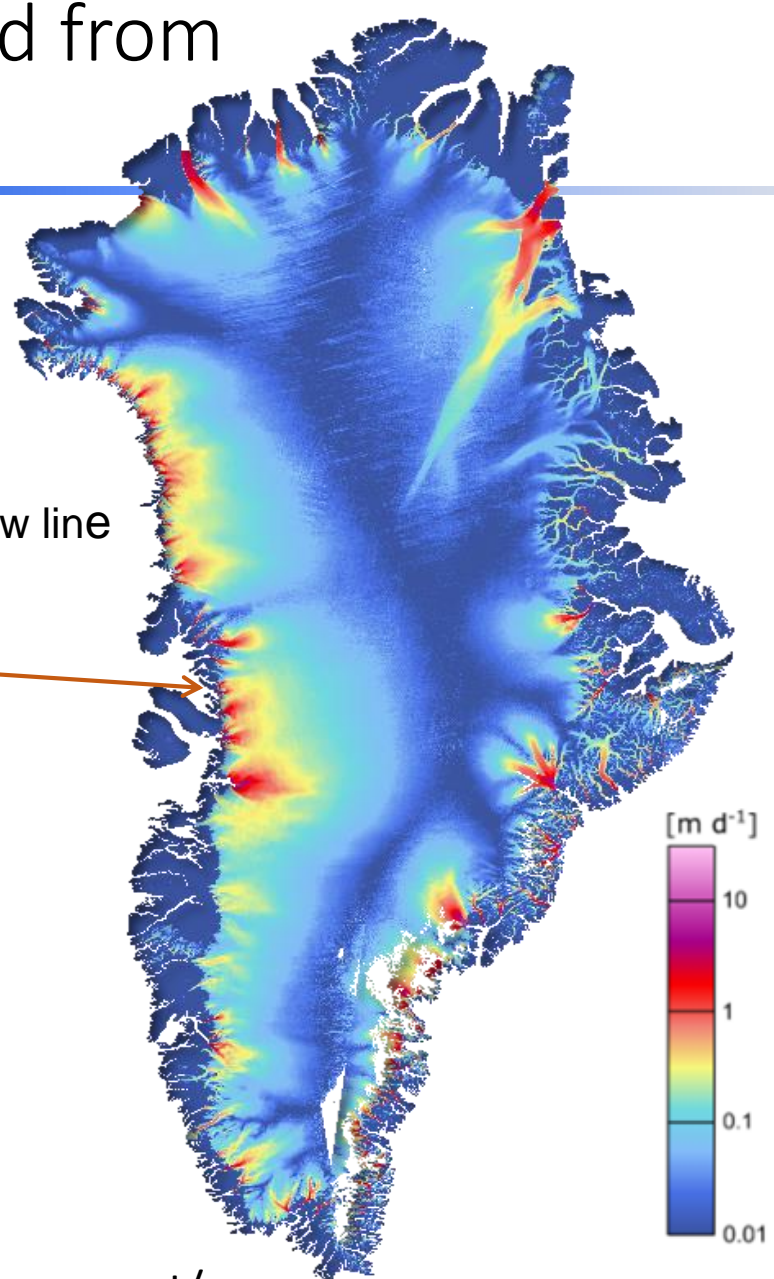
100 m regional scale, 250 m ice sheet wide

Method: Offset tracking



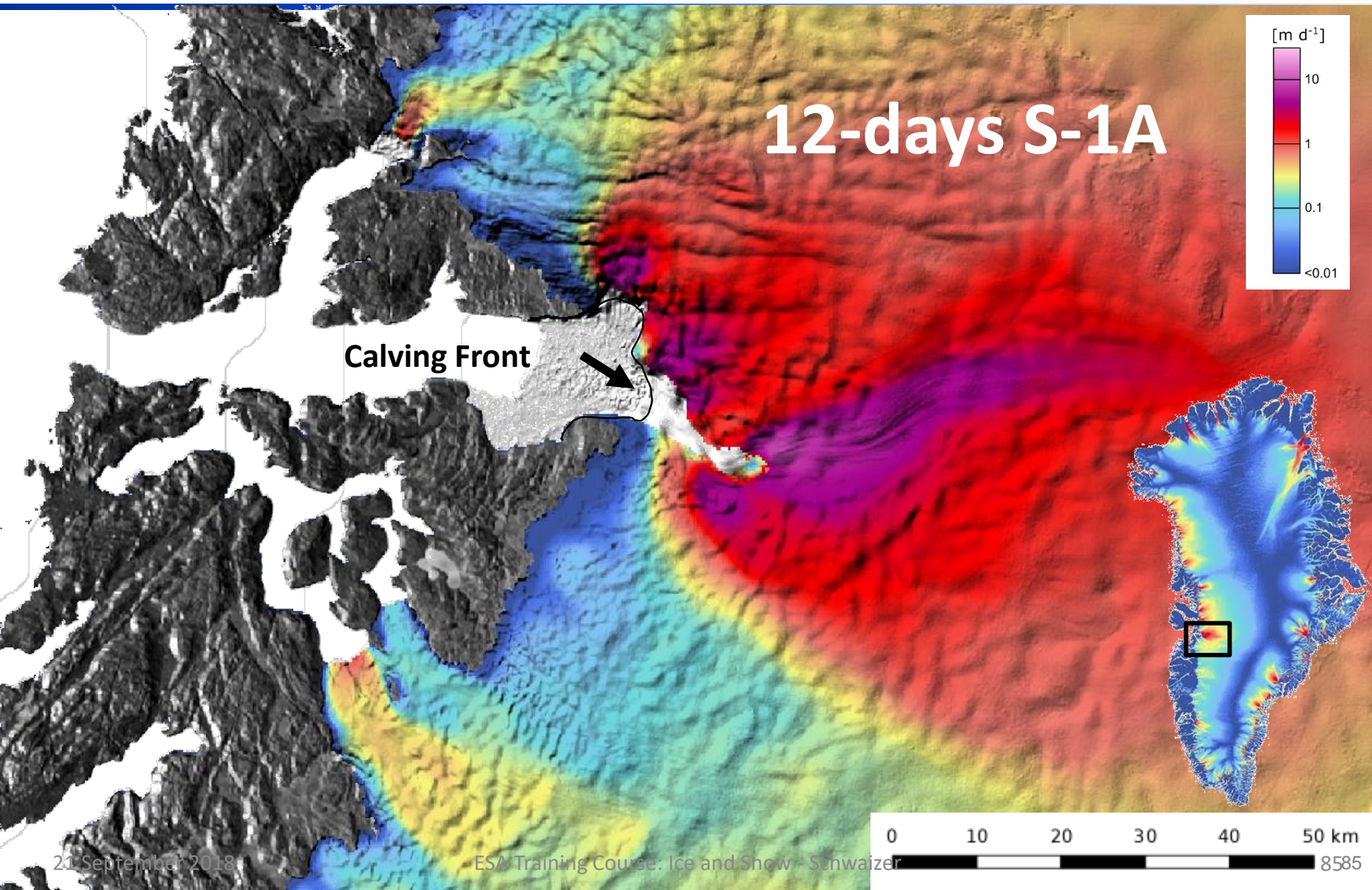
**12 day repeat mapping of
all outlet glaciers**

Data @
<http://cryoportal.enveo.at/>

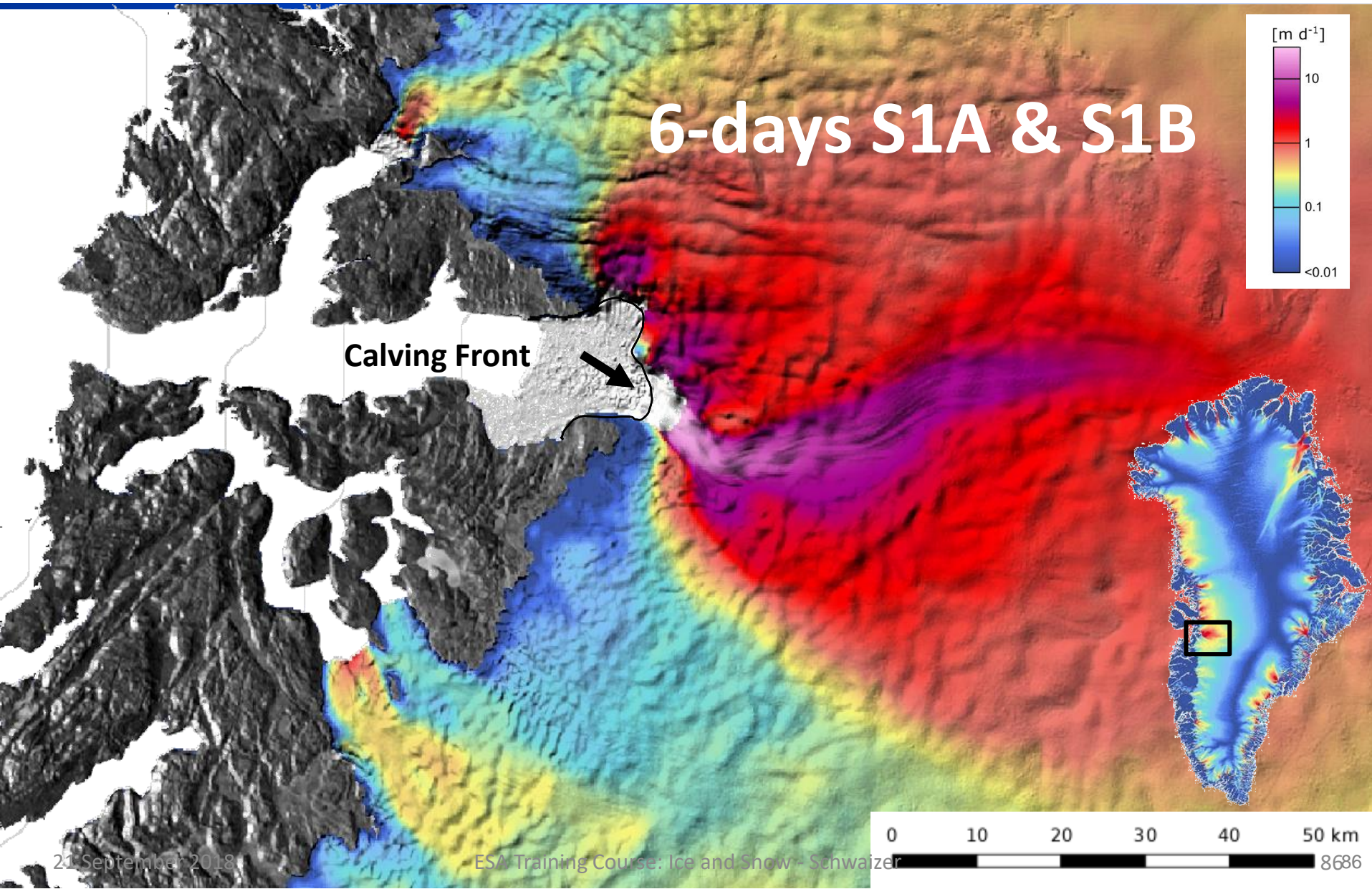


Ref: Nagler et al. 2015

Advancements of Sentinel-1A&1B Constellation – Fast Ice Streams



Advancements of Sentinel-1A&1B Constellation – Fast Ice Streams



8. InSAR Analysis of Glacier Topography & Volume Change

The change in glacier volume ΔV over time interval Δt can be converted into change of glacier mass, **net mass balance**, B_N :

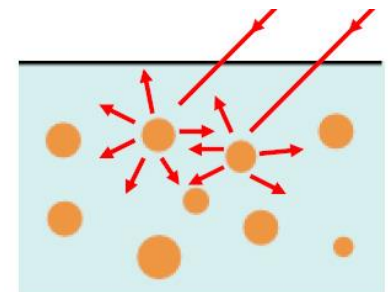
$$B_N(\Delta t) = V(\Delta t) \rho \quad ; \quad \text{for glacier ice: } \rho = 900 \text{ kg m}^{-3}$$

B_N is a key parameter for climate research and hydrology

TanDEM-X repeat observations offer excellent capabilities to reduce the uncertainty in global glacier mass balance, applying **DEM-differencing dV/dt**

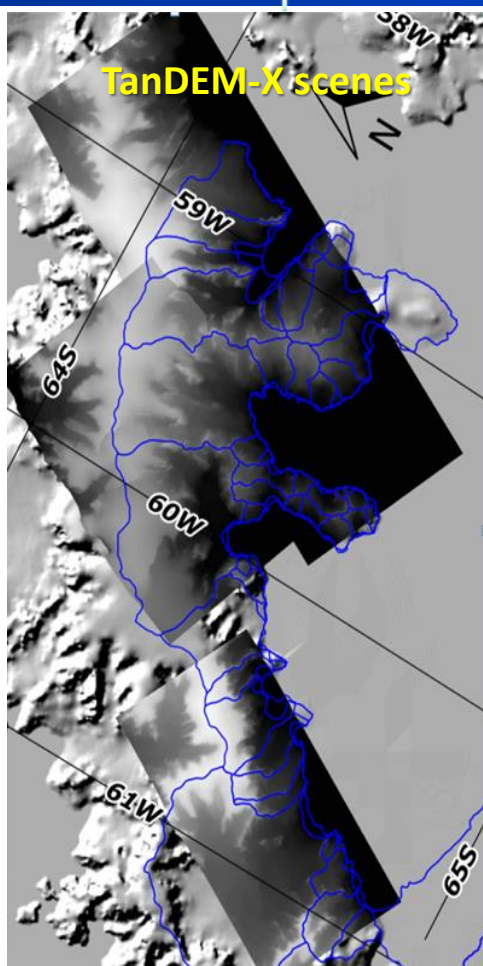
Effects of SAR signal penetration (shift of scattering phase center) need to be taken into account for DEM differencing by:

- Using repeat observations at **same radar frequency and snow state** (either dry or wet)
- Or: estimate penetration **for given snow state and radar frequency** (using model and/or empirical data)

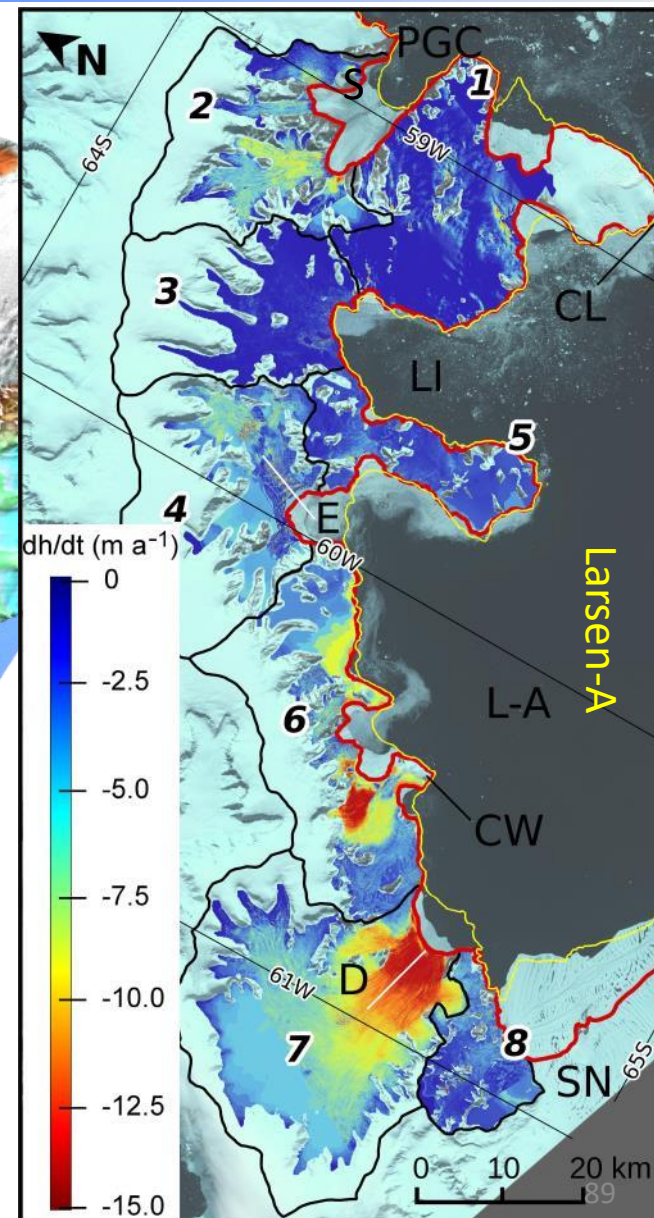
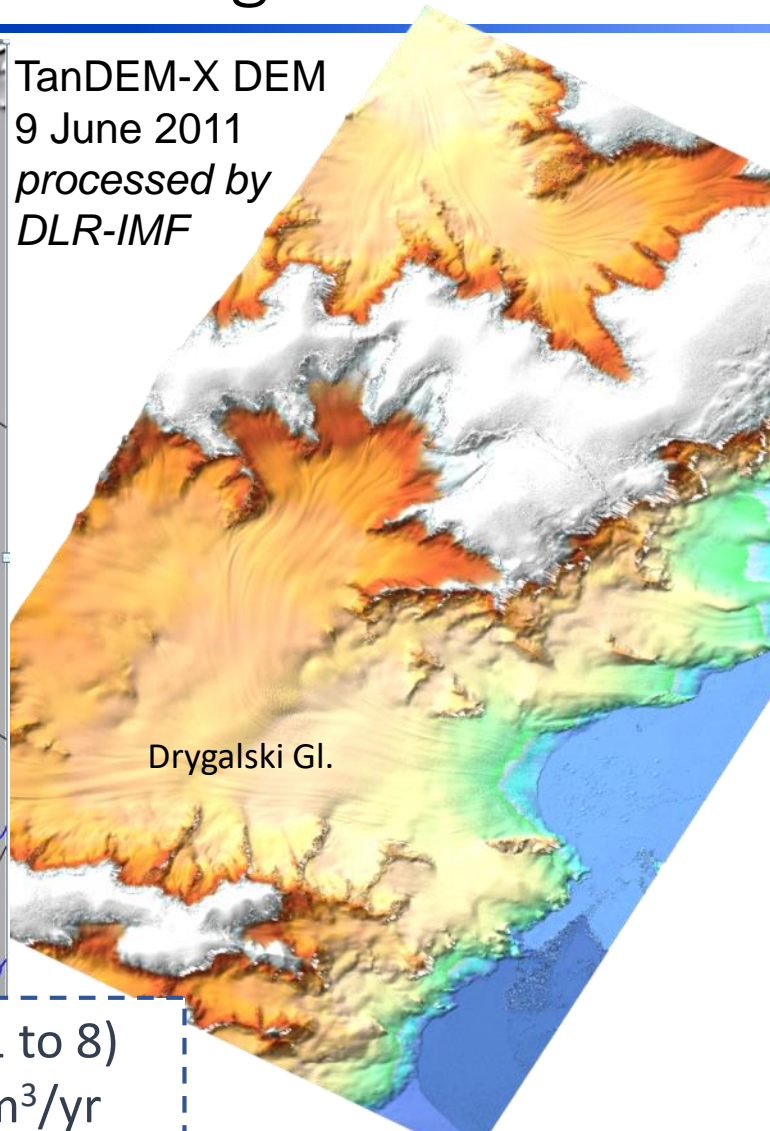


SAR signal penetration:
Slide Nr. 53 & 54

Elevation Change 2011- 2013 by TanDEM-X DEM Differencing



TanDEM-X DEM
9 June 2011
processed by
DLR-IMF



Total Change (Basin 1 to 8)

$$\Delta V = -4.54 \pm 0.39 \text{ km}^3/\text{yr}$$

$$\Delta M = -4.21 \pm 0.35 \text{ Gt/yr}$$

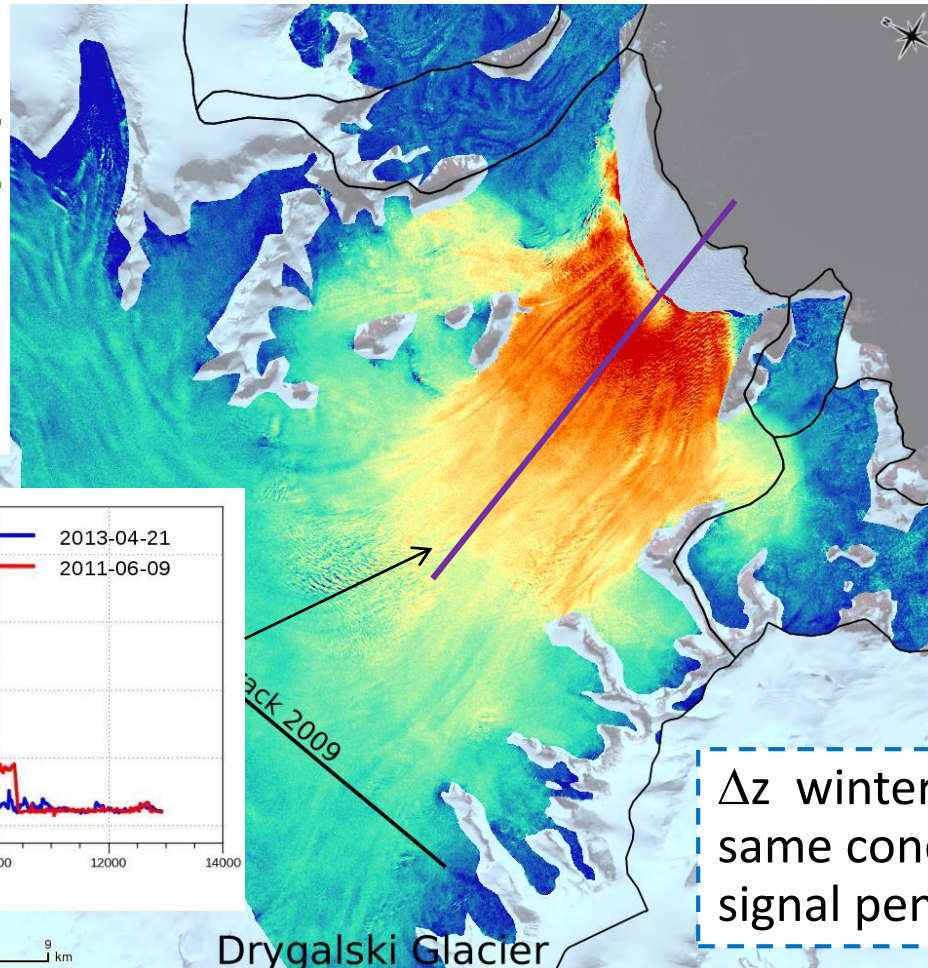
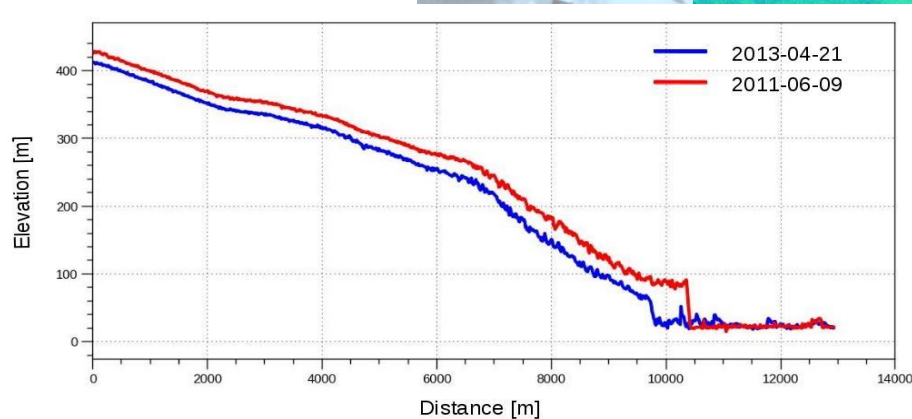
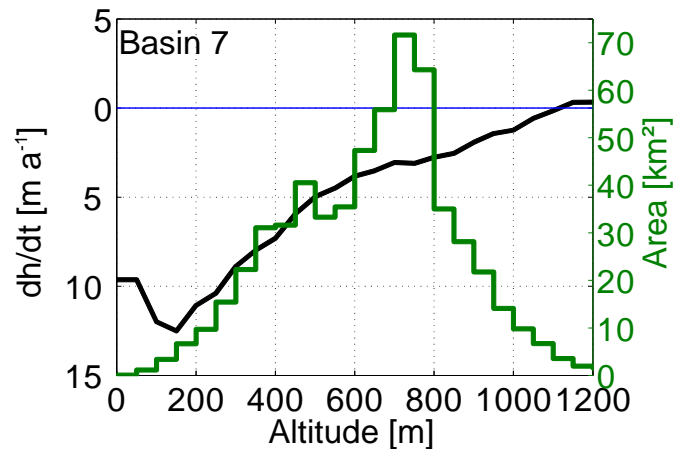
Ref: Rott et al. 2014

21 September 2018

ESA Training Course: Ice and Snow - Schwaizer

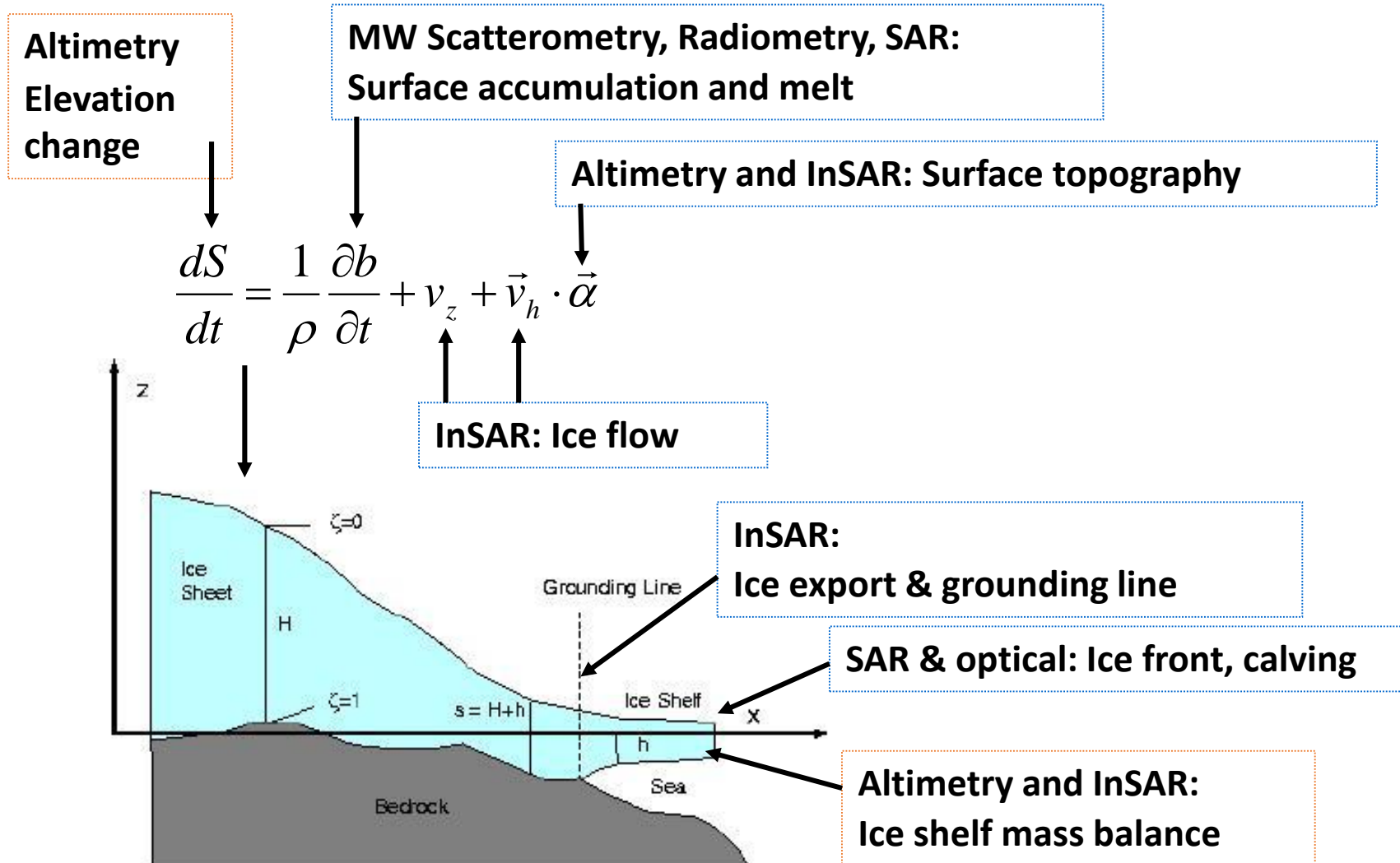
Elevation Change TanDEM-X (9 June 2011 – 21 April 2013)

dh/dt per elevation zone

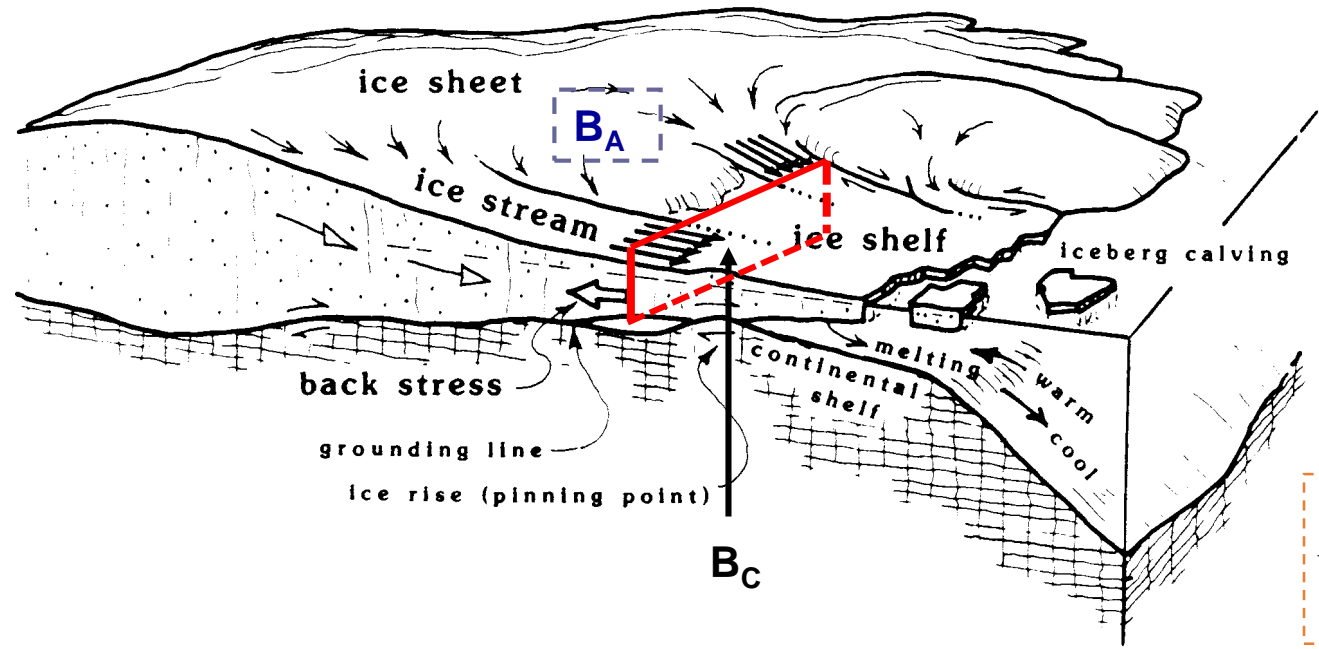


Δz winter to winter:
same conditions for
signal penetration

9. SAR Application to Monitoring Dynamics and Mass Balance of Ice Sheets



Ice Drainage of a Marine Ice Sheet



The main export of Antarctic ice is routed through ice shelves and lost by iceberg calving.

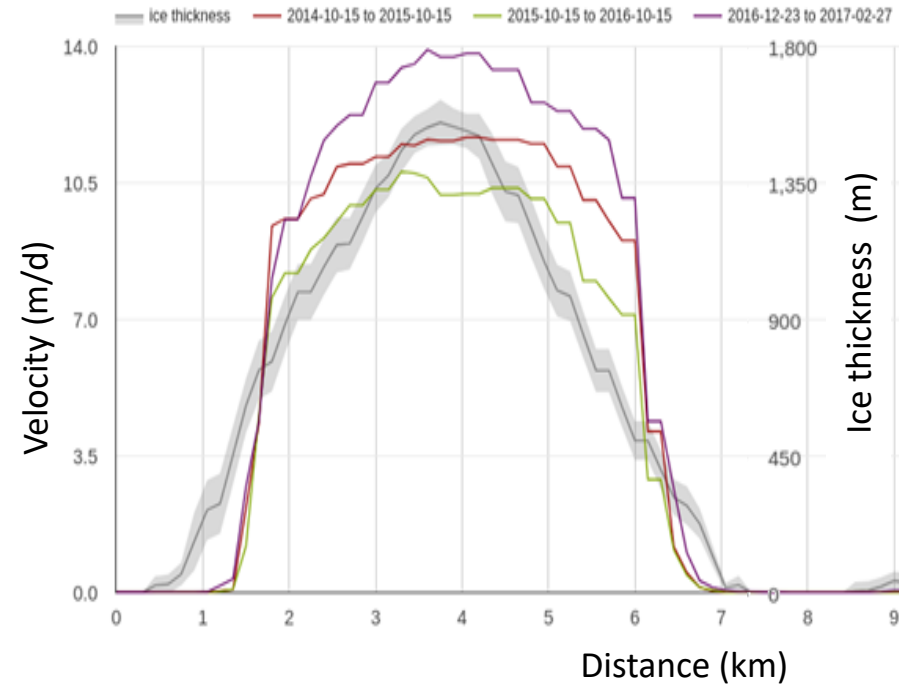
$$B_c = \int_Y [\bar{u}(y)H(y)]dy$$

The contribution to sea level rise is determined by imbalance of net accumulation, B_A , on grounded ice minus the export through a cross section at the grounding line or calving front, B_C : $B_N = B_A - B_C$

Input/Output Method IOM: Computes the net balance B_n as difference between B_A (net surface mass balance SMB) and calving flux B_C

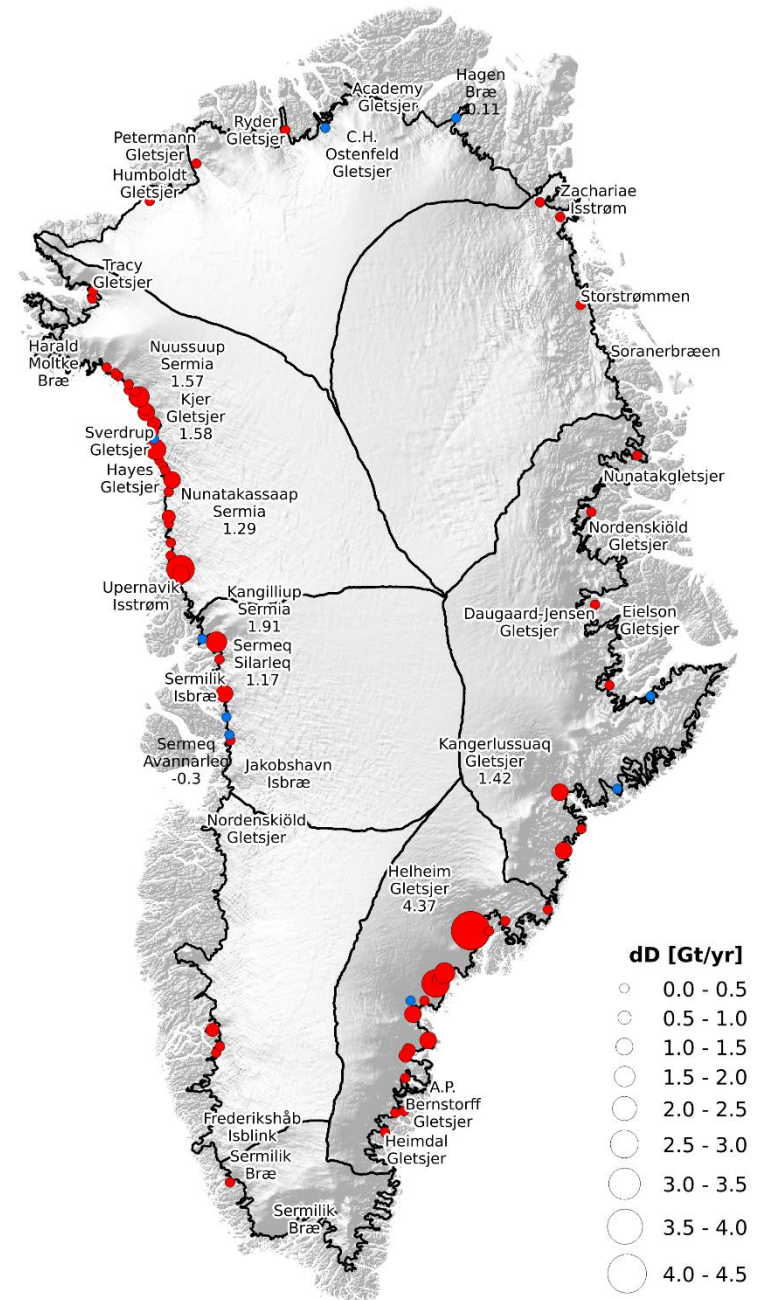
Ice fluxes for Greenland outlet glaciers 2016 – 2017

Helheim Glacier



Cross-sect. area [km ²]	2014-10-15 to 2015-10-15			2015-10-15 to 2016-10-15			2016-12-23 to 2017-02-27		
	Avg. Vel. [m/y]	Flux [Gt/y]	Flux [km ³ /y]	Avg. Vel. [m/y]	Flux [Gt/y]	Flux [km ³ /y]	Avg. Vel. [m/y]	Flux [Gt/y]	Flux [km ³ /y]
7.47 ± 0.71	1422.98 ± 42.69	17.34 ± 1.35	18.90 ± 1.47	1250.85 ± 37.53	15.34 ± 1.19	16.73 ± 1.29	1625.89 ± 48.78	19.71 ± 1.52	21.50 ± 1.6

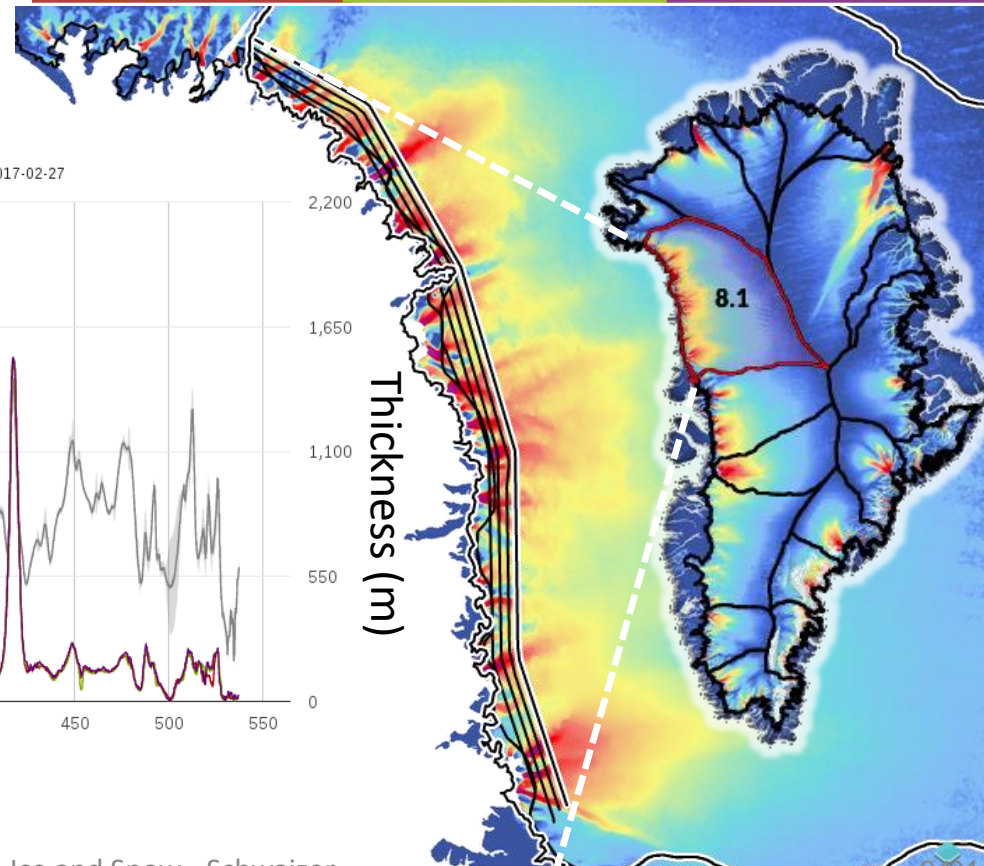
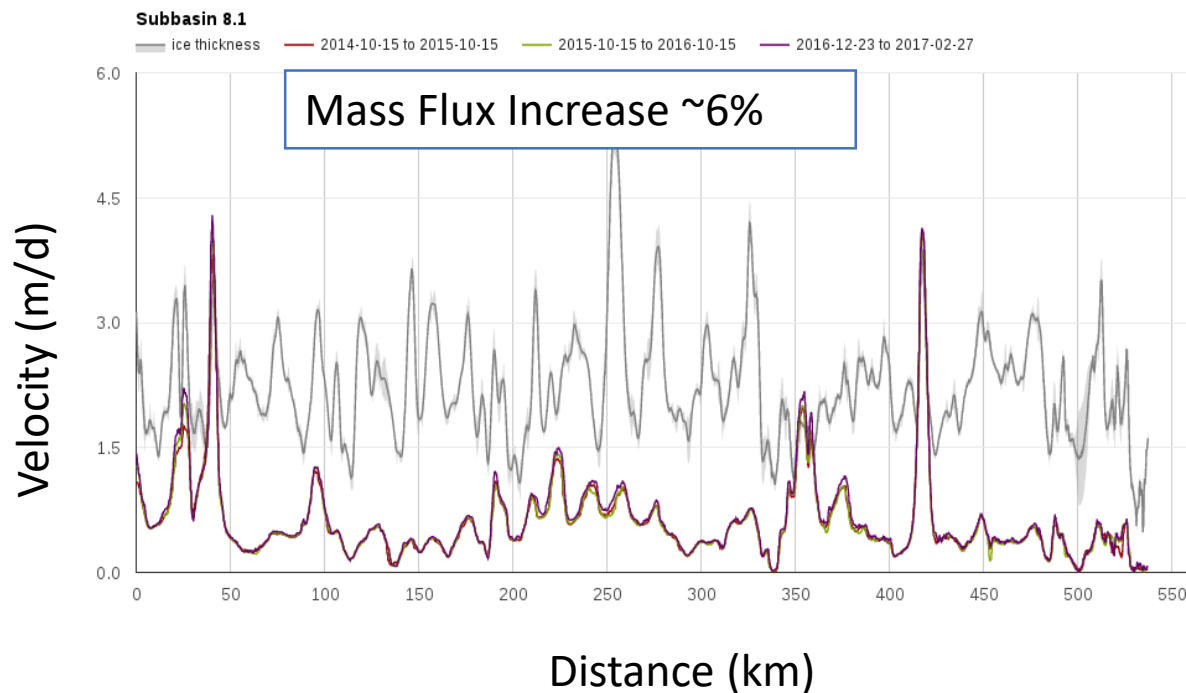
Change of ice flux – 2016 - 2017



Glacier & Ice Sheet Discharge Monitoring

Depth correction factor 0.95						2014-10-15 to 2015-10-15			2015-10-15 to 2016-10-15			2016-12-23 to 2017-02-27		
Subbasin	Gateline ID	Gateline Source	Gate Width [km]	Ice Thick.	Cross-sect. area [km ²]	Avg. Vel. [m/y]	Flux [Gt/y]	Flux [km ³ /y]	Avg. Vel. [m/y]	Flux [Gt/y]	Flux [km ³ /y]	Avg. Vel. [m/y]	Flux [Gt/y]	Flux [km ³ /y]
8.1	746	IceBridge	537.15	IDBMG4	437.18 + 24.19	220.27 + 0.00	83.70 + 4.58	91.28 + 4.99	221.06 + 0.00	84.28 + 4.62	91.91 + 5.04	233.63 + 0.00	88.98 + 4.89	97.03 + 5.33

Ice Thickness (Gogineni, 2012)
CRISIS Radar Depth Sounder Data



Ice Sheet Parameters

Ice shelf collapses at Antarctic Peninsula:

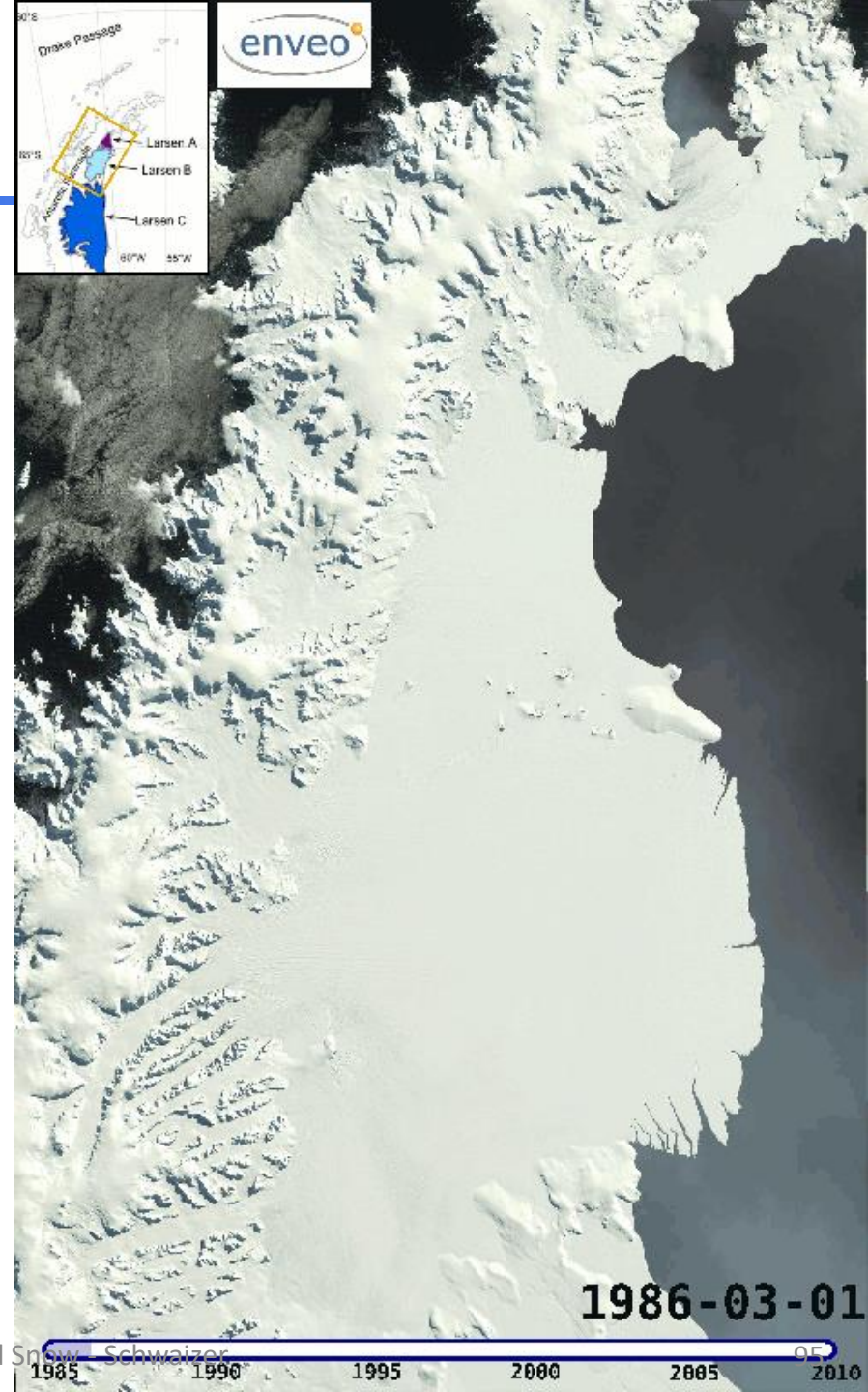
- 1995 – Larsen A
- 2002 – Larsen B

→ *Ice shelf collapse contribute directly to sea level rise*

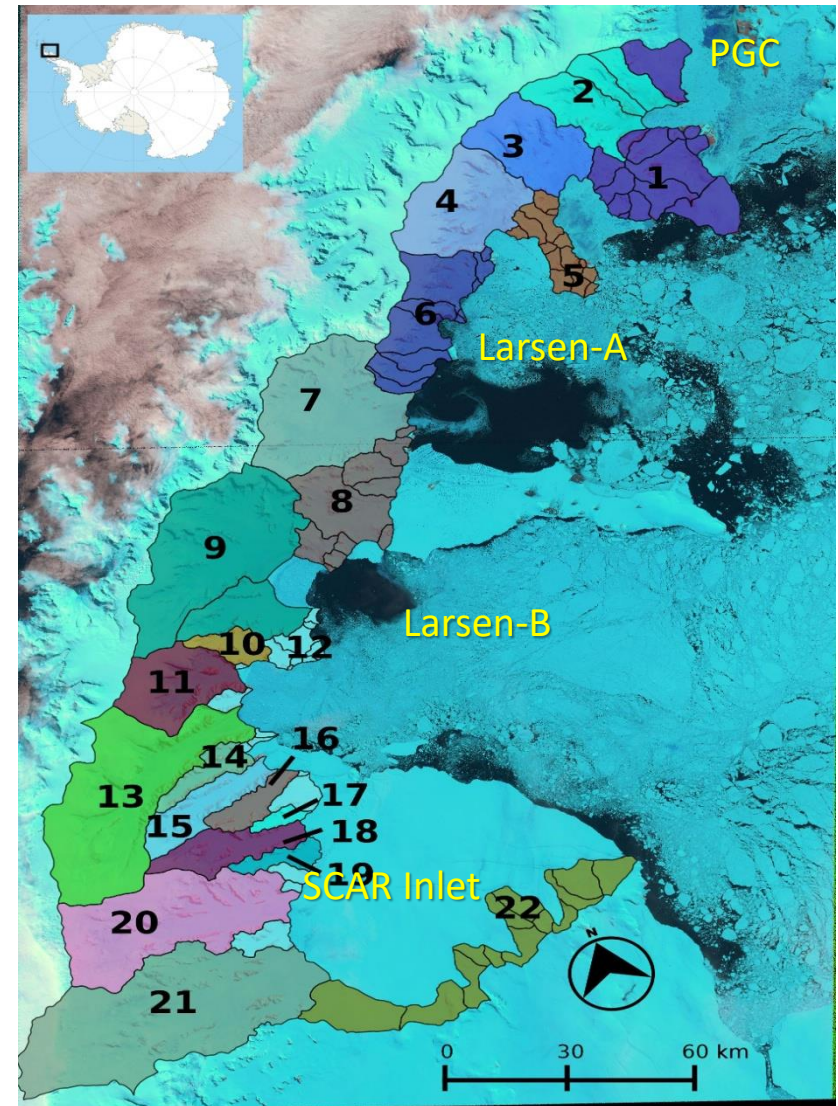
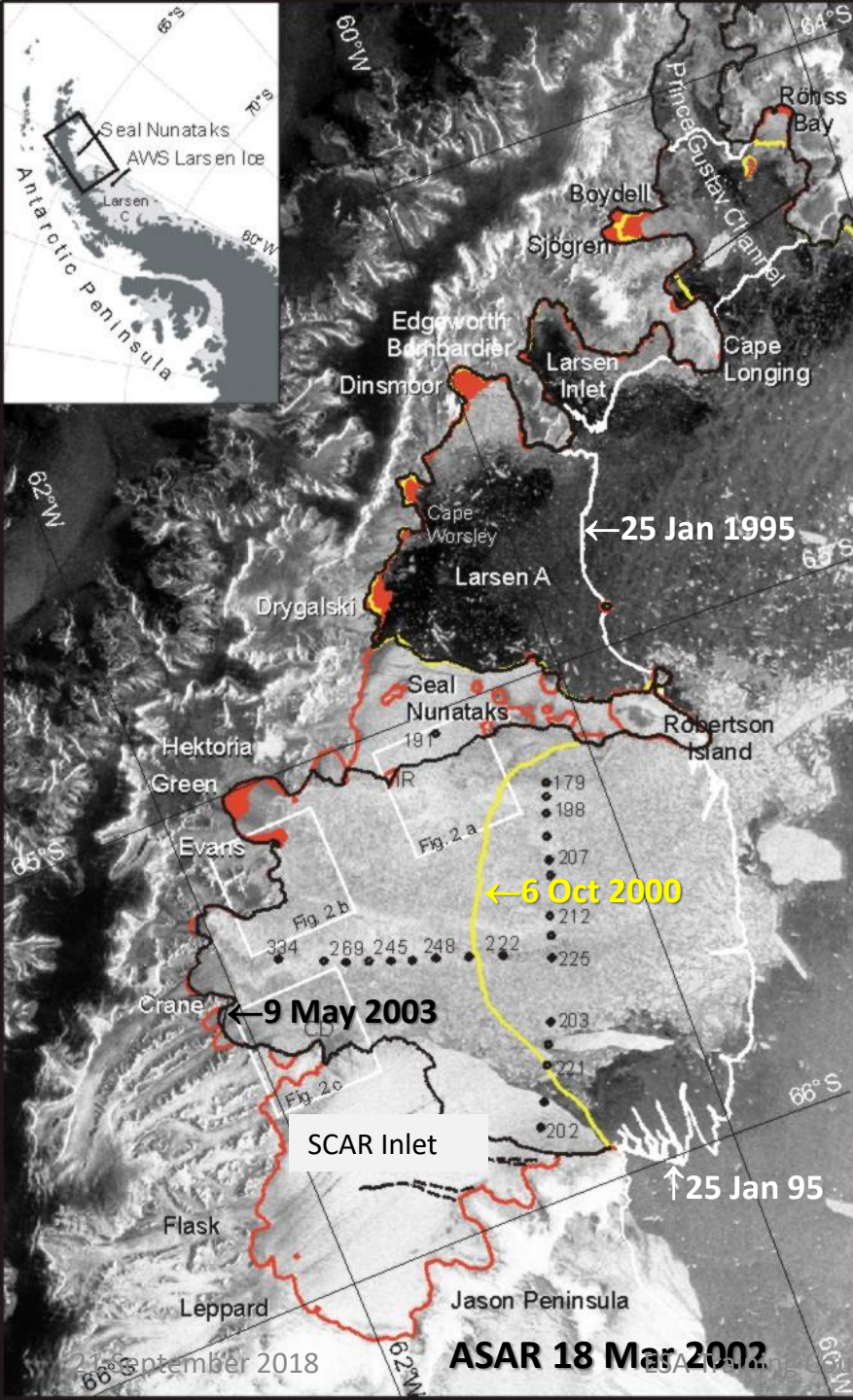
Ice shelves may collapse within very short period (LARSEN A) or retreat over long periods (several years to decades).

In order to assess stability frequent observations are needed:

- Velocity
- Rifting / crack formation
- Grounding line and migration
- Surface Melt extent
- Ice shelf thickness
- Assimilation into models

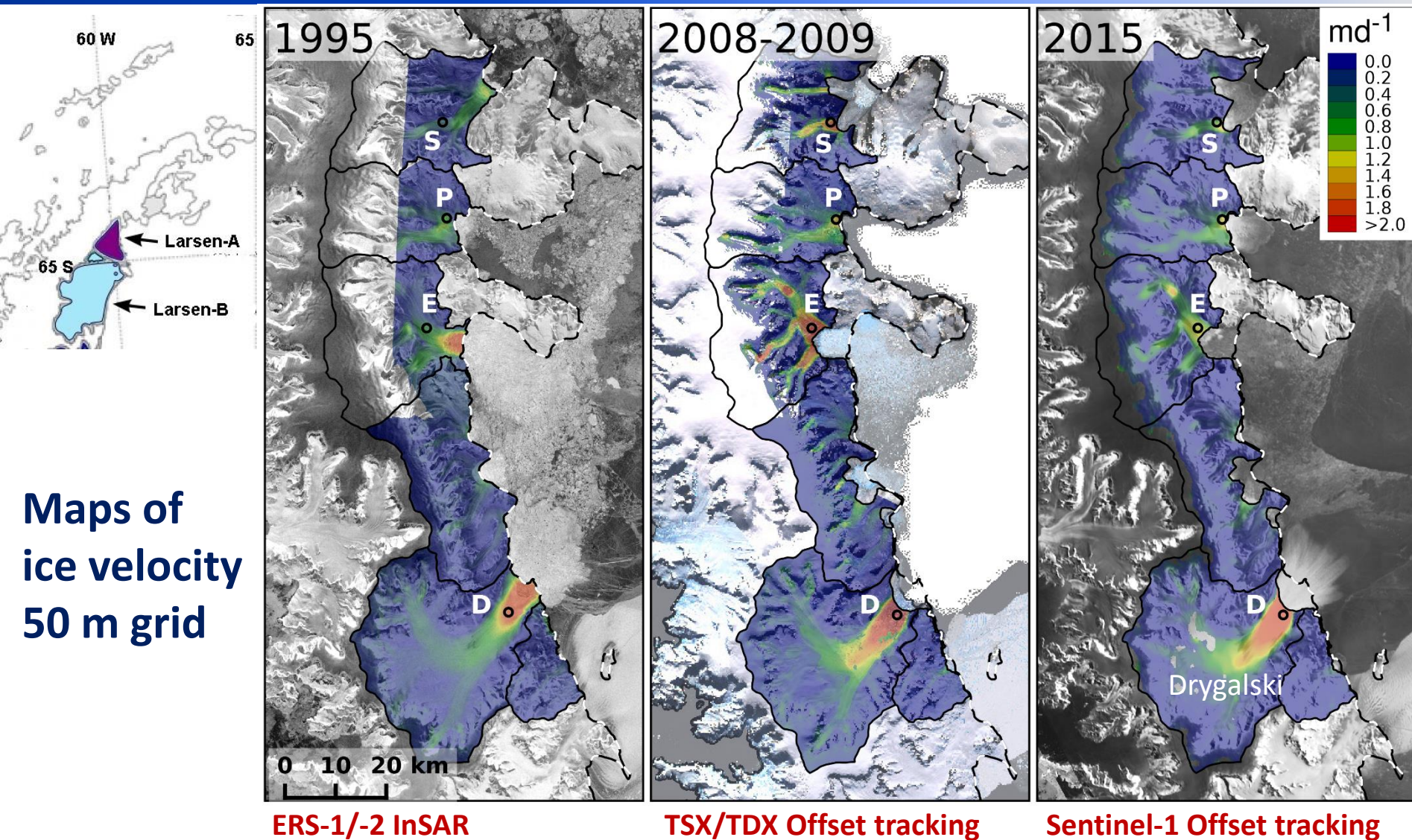


Antarctic Peninsula – Larsen Outlet Glaciers



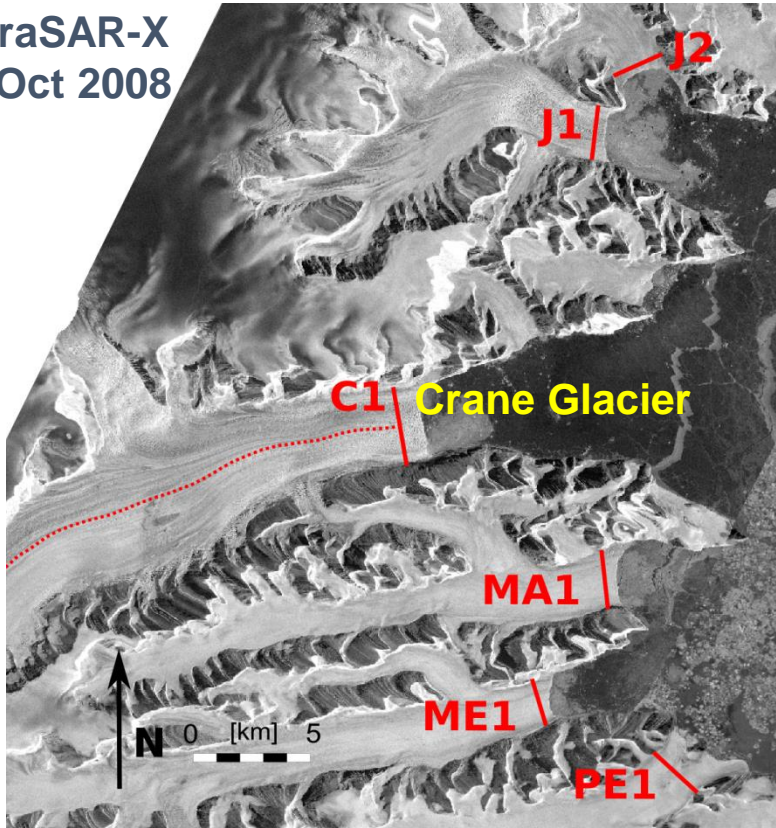
Glacier basins after A. Cook et al., 2012

Larsen A Glacier Velocities 1995 to 2015



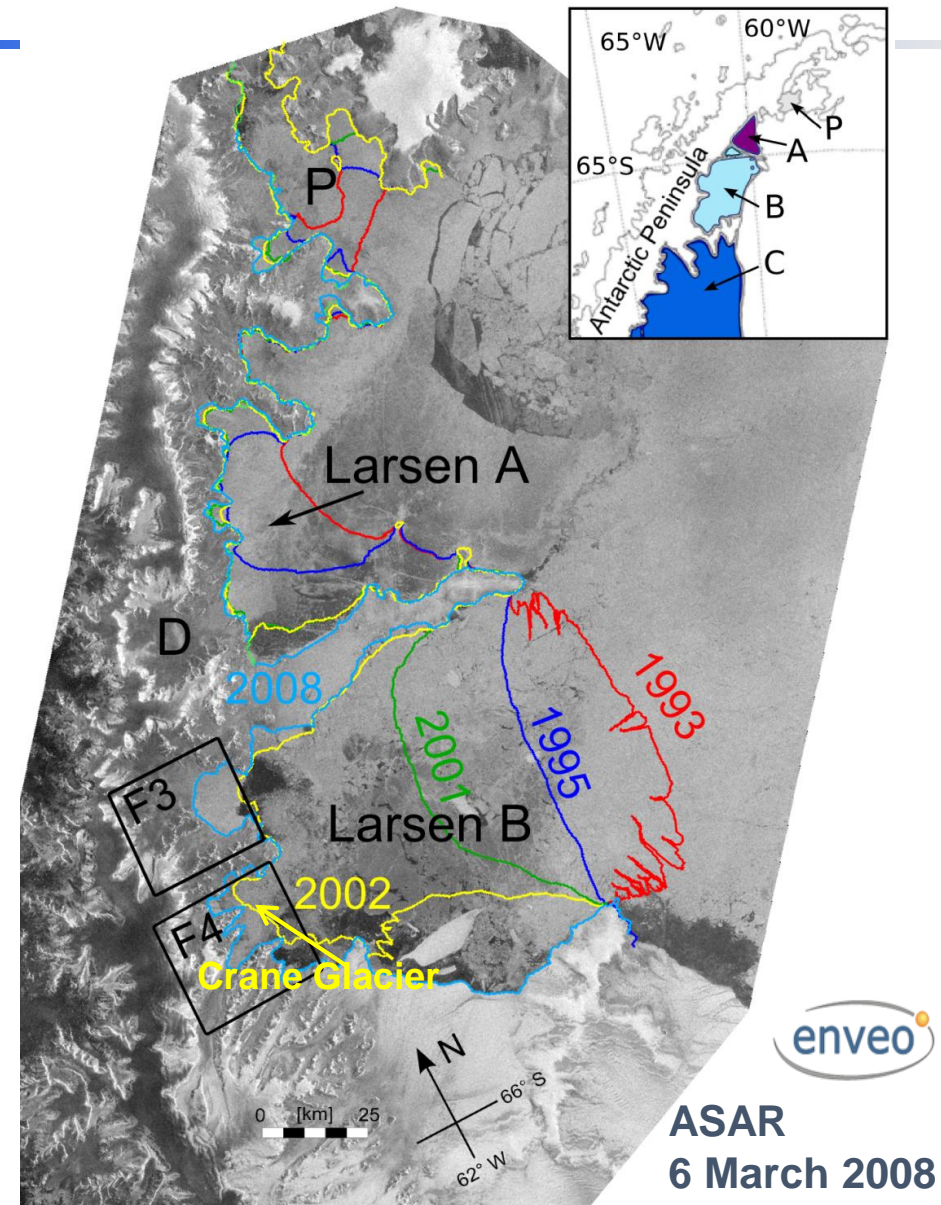
Mass Imbalance of Larsen Glaciers after Ice Shelf Collapse

TerraSAR-X
18 Oct 2008



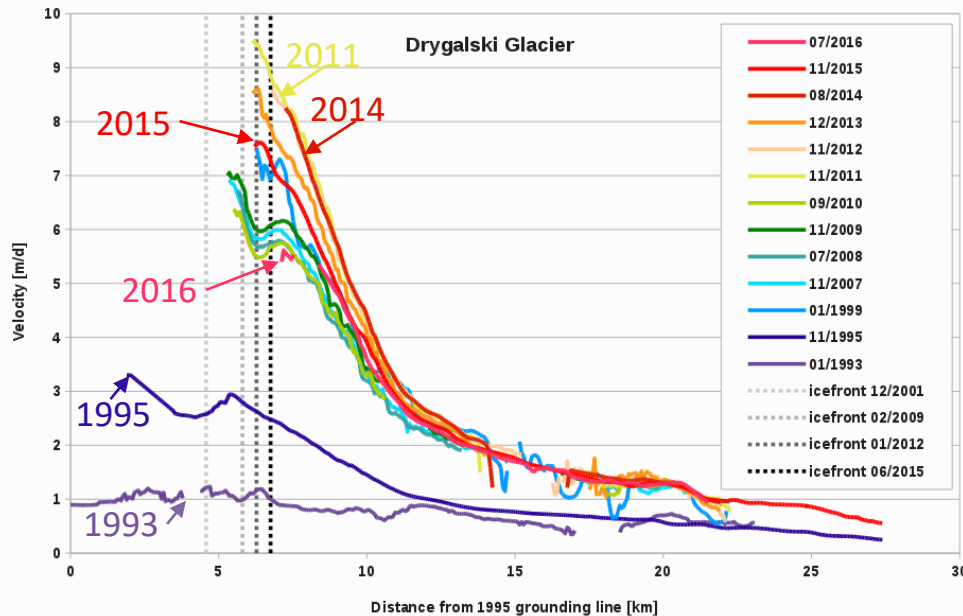
Method: IOM

Assuming $B_A - B_C$ (equilibrium state) for pre-collapse period

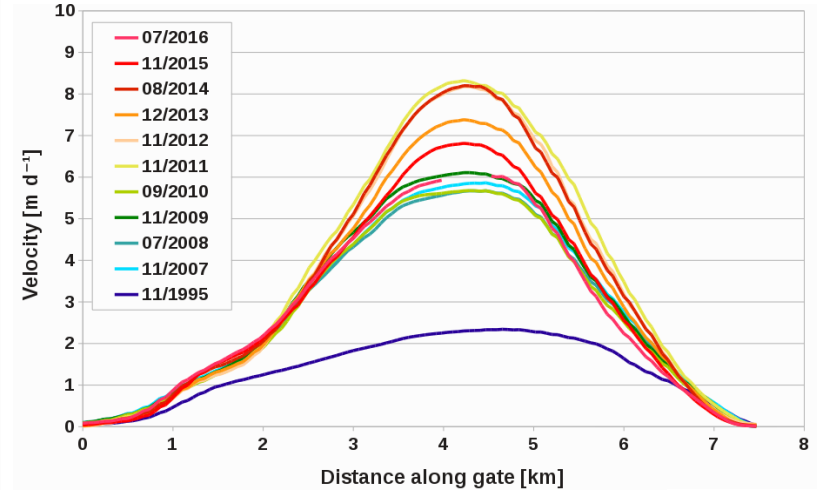


Response after Larsen-A Collapse – Drygalski Glacier

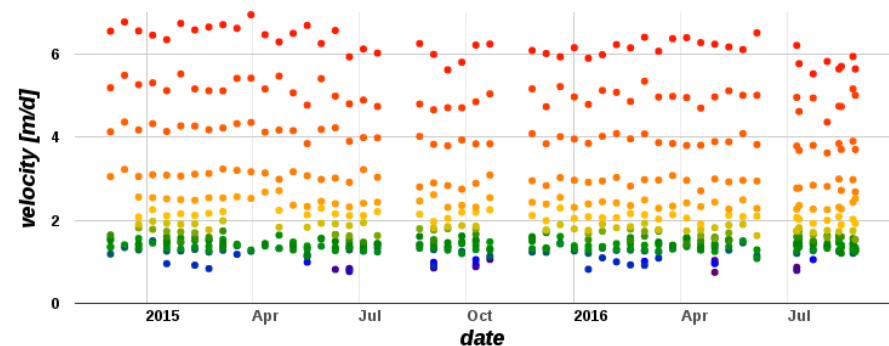
Central Flowline TSX IV time series



Gate TSX IV time series



Sentinel-1 Velocity time series Nov 2014 to July 2016 along flowline

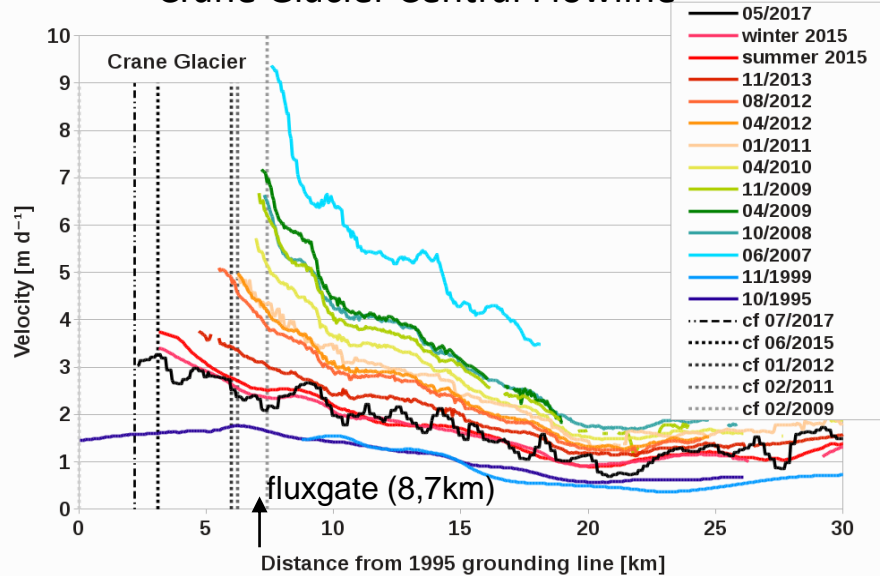


Date	Flux Gt/yr	B_n Gt/yr
Pre-Collapse	1.42 ($\rightarrow B_A$)	0 = Balance Flux
07/2008	3.40	-1.98
12/2013	3.80	-2.38
11/2015	3.00	-1.58

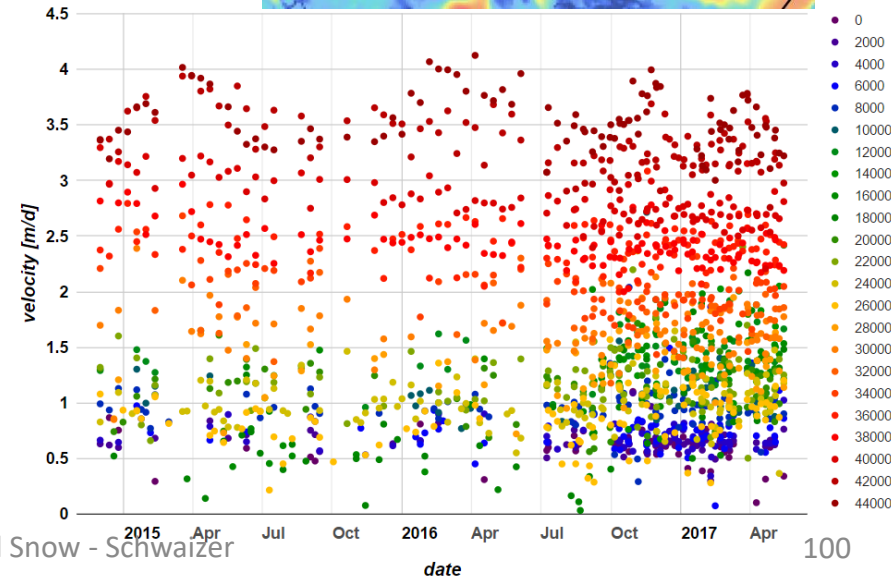
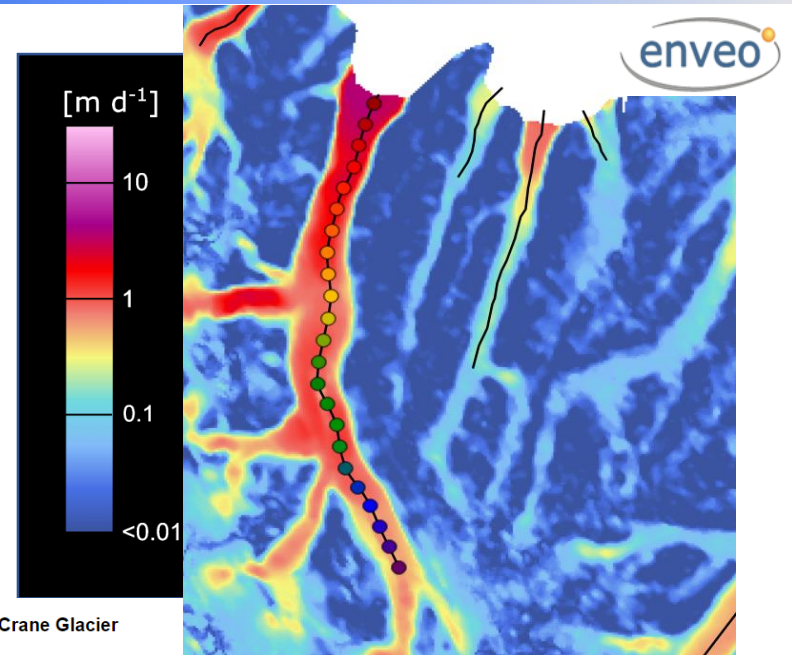
Drygalski Glacier area (2012): 1008 km²
Retreat of grounded ice 1995-2012: 41 km²

Response after Larsen B Collapse – Crane Glacier

Crane Glacier Central Flowline



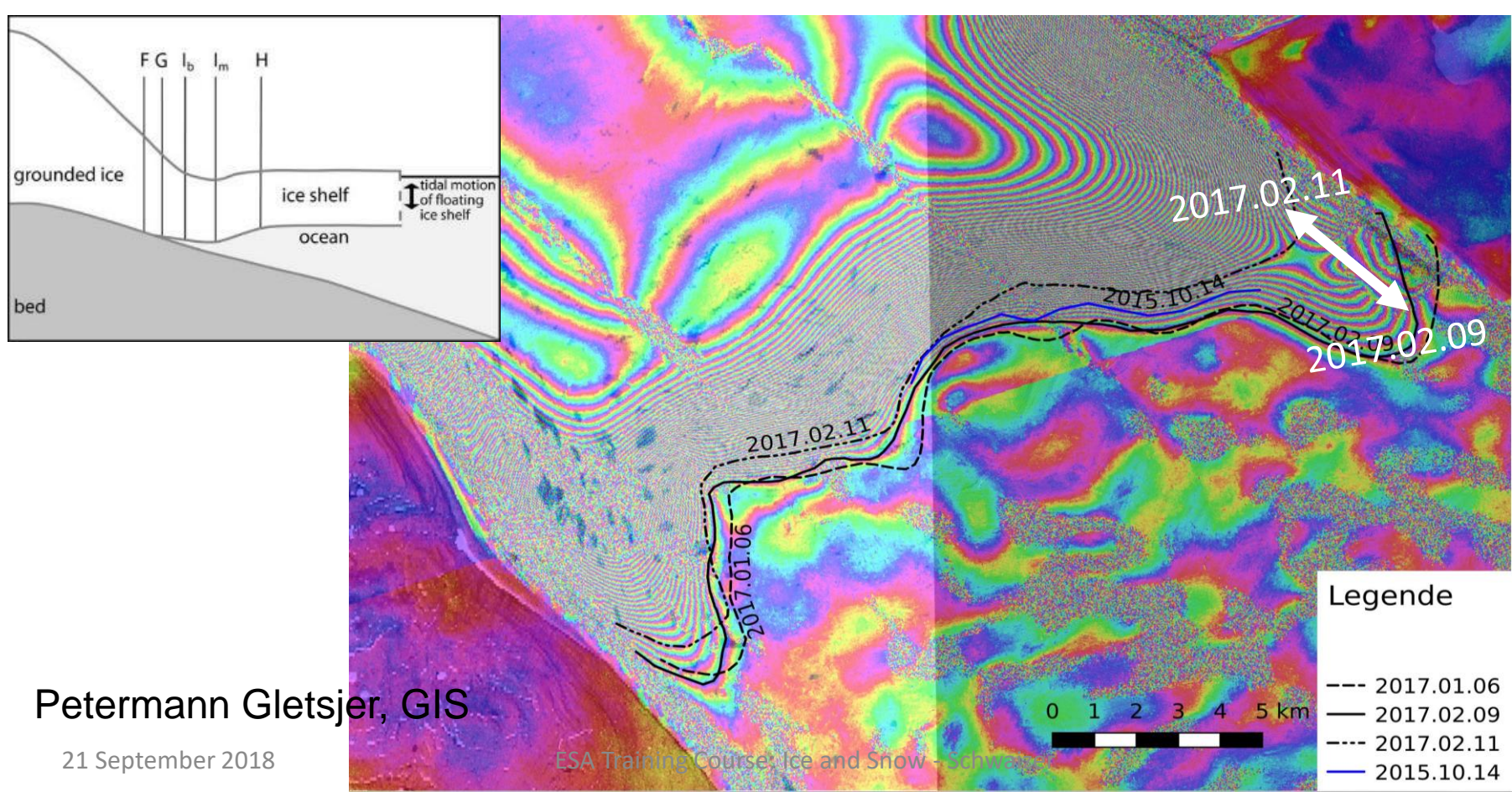
Date	Flux Gt/yr
1995-99	1.15
June 2007	5.02
2008-09	2.92
Nov. 2013	1.72
Summer Winter 2015	1.42 1.36
May 2017	1.45



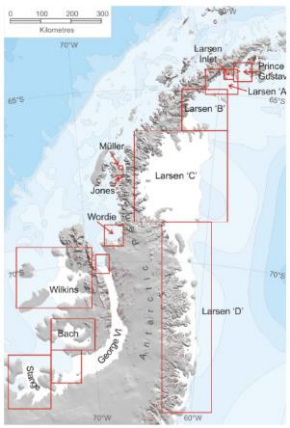
Short term variation of Grounding Line

GLL by DD-InSAR – 6 days S1A&B:

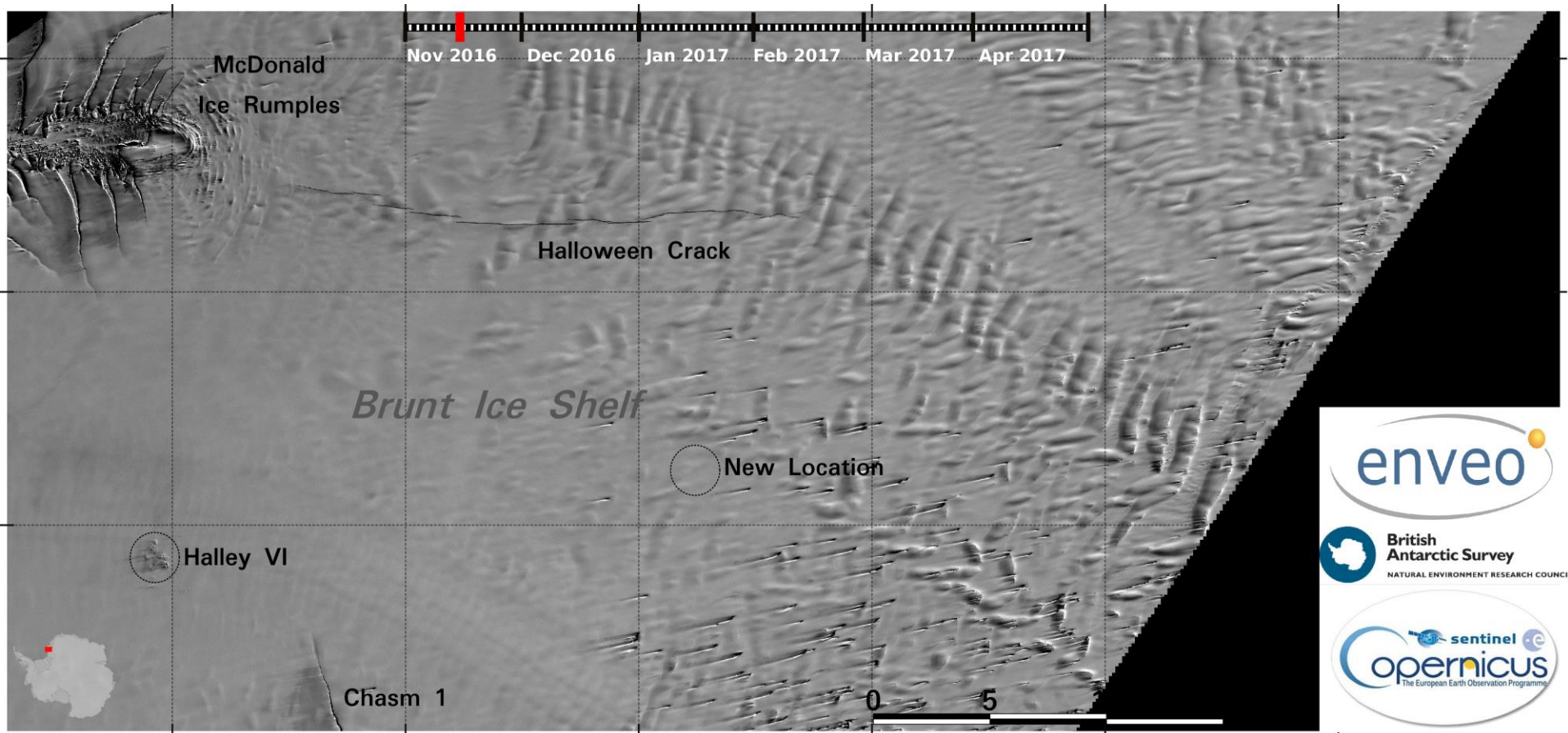
- Close time series of S1A&B enables to estimate variability of GLL due to different tidal states during SAR acquisitions,
- needed to identify GLL migrations from short term



Larsen C – Crack in Ice Shelf



Sentinel-1 Brunt Ice Shelf Rift Monitoring – 17 km from British Antarctic Research Station Halley VI

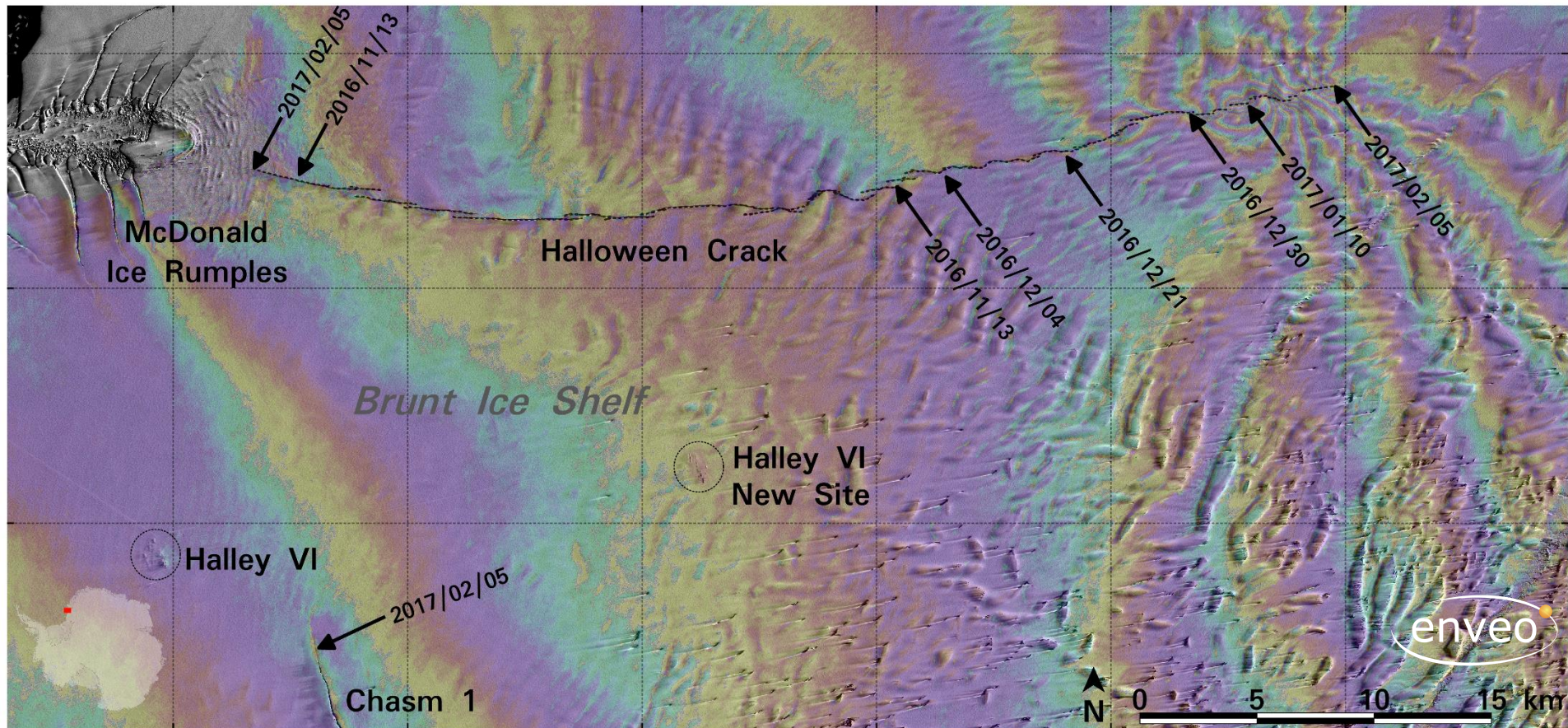


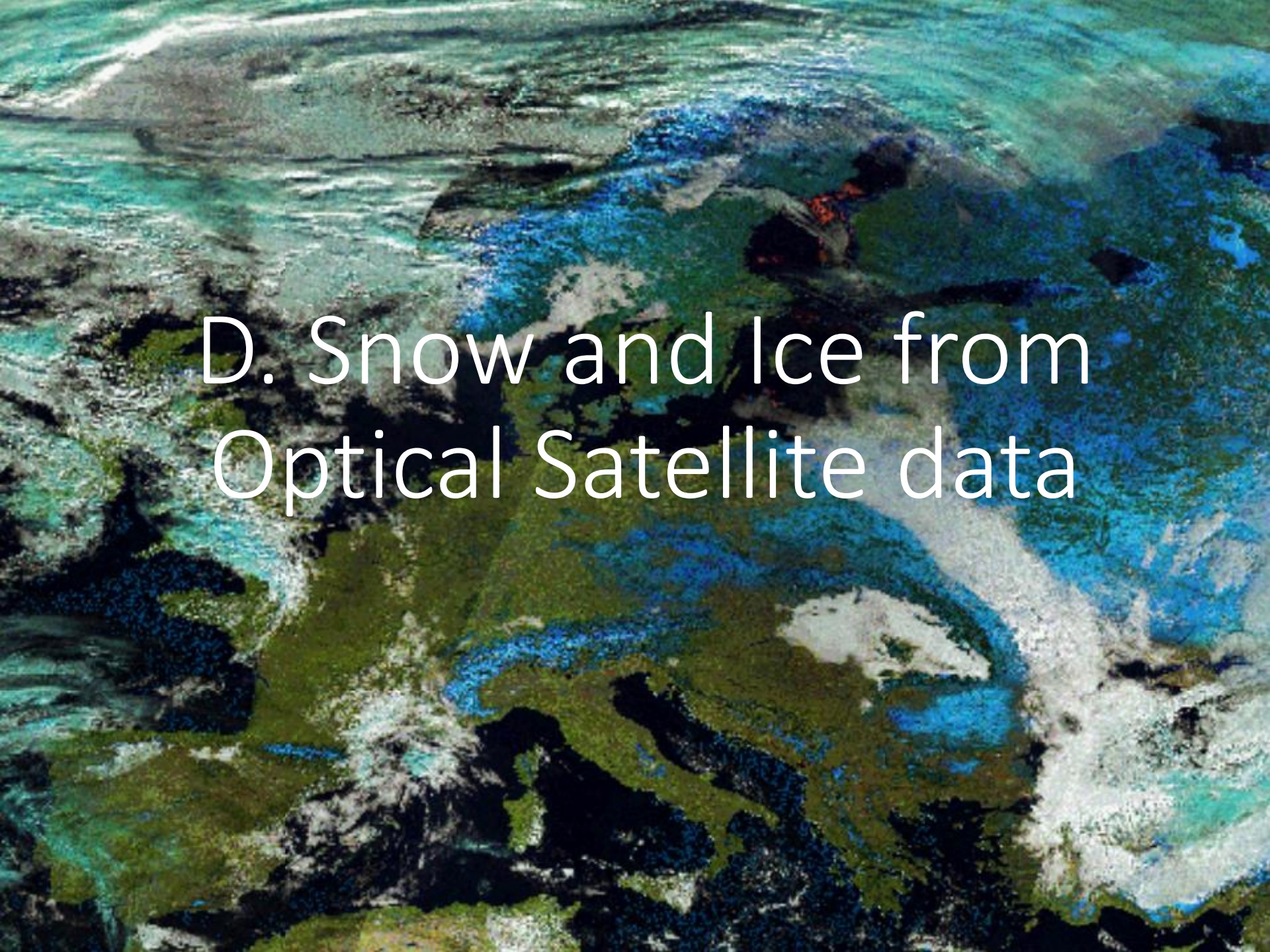
Moving Halley Station



Halloween Crack

6-day Interferogram from Sentinel-1





D. Snow and Ice from Optical Satellite data

Part D – Contents

1. Measurement Concept of Optical Satellite Data
2. Spectral Ranges of Optical Satellite Data
3. Permittivity and Reflectivity of Ice and Snow in the Visible and Infrared
4. At-Satellite Radiance and Surface Reflectance
5. Applications of Optical Satellite Data for Snow Extent Monitoring
6. Validation of Snow Extent Products
7. Glacier Parameters from Optical Satellite data

1. Measurement Concept of Optical Satellite Data

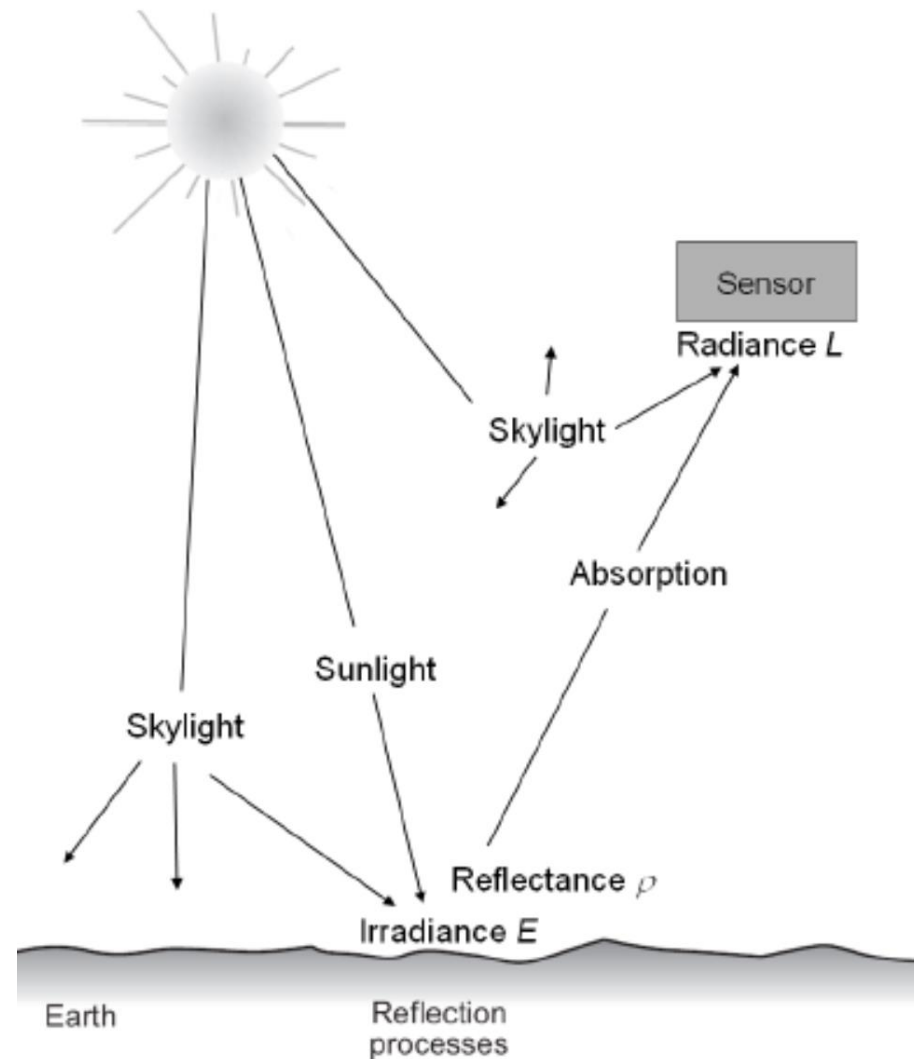
Incoming electromagnetic energy from sun ($E_I(\lambda)$) is affected by:

- Absorption ($E_A(\lambda)$)
- Scattering ($E_S(\lambda)$)
- Transmission ($E_T(\lambda)$)

Principle of energy conservation:
(energy can only be transferred, but neither be created nor destroyed)

$$E_I(\lambda) = E_A(\lambda) + E_S(\lambda) + E_T(\lambda)$$

Optical sensors measure the amount of light receiving the satellite (= at-satellite radiance L), which is often converted to reflectance at top of atmosphere.



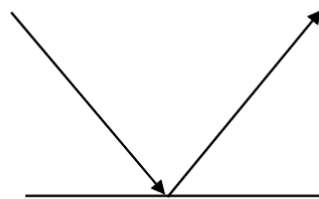
Reflectance – definitions

- *Reflectance*: Fraction of incident radiation that is reflected by a surface for a single incidence angle
- *Top of atmosphere reflectance*: spectral reflectance received by a satellite in a specific spectral band
- *Bottom of atmosphere or surface reflectance*: spectral reflectance at the surface calculated from the top of atmosphere reflectance for a specific spectral band removing all atmospheric effects from the signal
- *Surface Albedo*: Fraction of incident radiation that is reflected by a surface (all sun-view geometries considered).

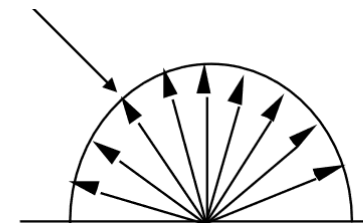
Reflectance properties

Reflectance
depends on

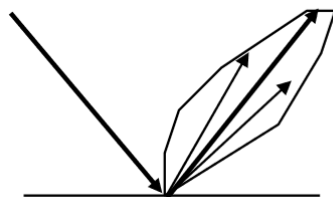
- *Wavelength energy*
- *Atmospheric attenuation*
- *Geometry of the Surface*
- *Surface Materials*



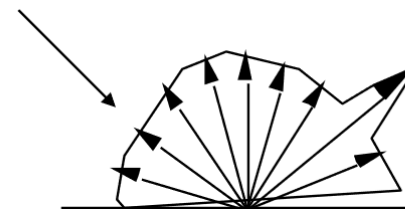
Specular reflector (mirror)



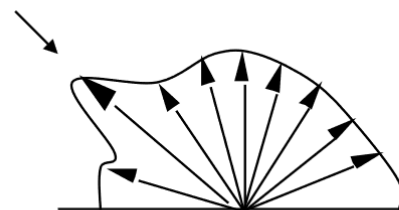
diffuse reflector (Lambertian)



Nearly Specular reflector (water)



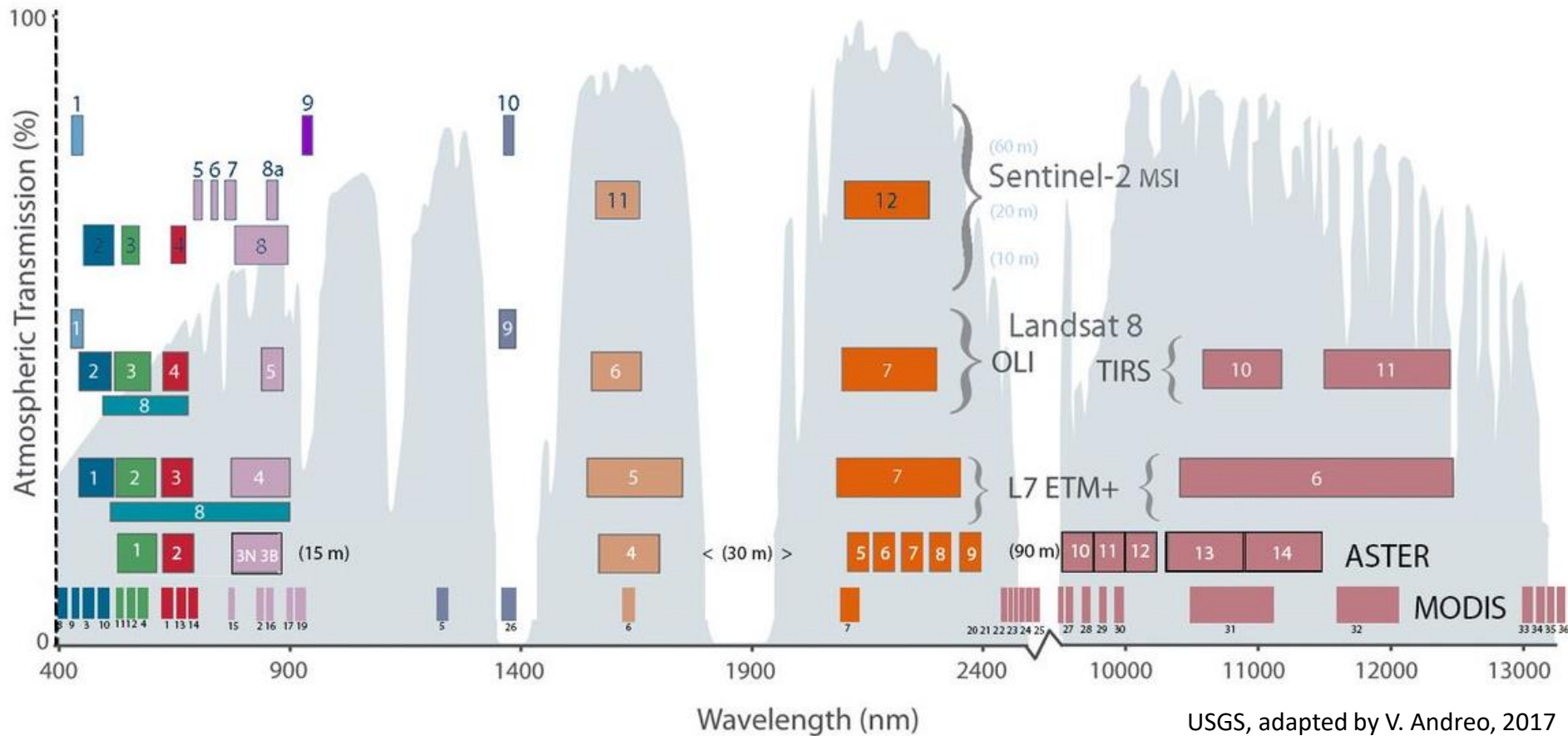
nearly diffuse reflector



Hot spot reflection

Figures from E. Vermote

2. Spectral Ranges of Optical Satellite Data



Selected Optical Sensors for Snow and Glacier Monitoring

<i>Sensor</i>	<i>Satellite</i>	<i>Bands</i>	<i>Resolution</i>
MSI	Sentinel-2	VIS, SWIR	10, 20, 60 m
OLCI, SLSTR	Sentinel-3	VIS, SWIR, TIR	300, 500, 1000 m
AVHRR	NOAA	VIS, SWIR, TIR	1 km
MODIS	TERRA, ACQUA	0.4 – 12 μm (36 Ch.)	250, 1000 m
ASTER	TERRA	VIS, SWIR, TIR, Stereo	15, 30, 90 m
TM/ETM+	LANDSAT 5,7	VIS, SWIR, TIR	15, 30, 60 m
OLI - LDCM	LANDSAT 8	VIS, SWIR, TIR	15, 30, 100 m
HRV	SPOT5	VIS, SWIR	2.5, 5, 10 m
Dig-Camera	Ikonos	VIS, NIR (4 Kan.)	1, 4 m
Dig-Camera	QuickBird	VIS, NIR (4 Kan.)	0.7, 2.5 m
Dig-Camera	PLEIADES	VIS, NIR	0.5, 2.0 m
IR Bands:	<i>NIR 0.7 – 1.2 μm; SWIR 0.7 - 2.3 μm; TIR 8 – 12 μm</i>		

3. Permittivity and Reflectivity of Snow and Ice in the Visible and Infrared

The wave velocity v and the refractive index n in a medium with electric permittivity ε and magnetic permeability μ are:

$$v = c_0 / \sqrt{\varepsilon_r \mu_r}$$

We consider non-magnetic media

$$\varepsilon_r = \varepsilon' - i\varepsilon'' = \varepsilon_r (1 - i \tan \delta)$$

$$n = n' - in'' \quad ; \quad n^2 = \varepsilon_r$$

Penetration depth in an **absorbing**
(non-scattering) medium (for $\tan \delta \ll 1$):

Penetration depth (intensity) in an
absorbing and scattering medium:
 κ_e = extinction coeff. κ_s = scattering coeff.

$$c_0 = 2.9979 \text{ E8 m/s}$$

$$\varepsilon_0 = 8.8554 \text{ E-12 [As/Vm]}$$

$$\varepsilon_r = \varepsilon / \varepsilon_0 \text{ Relative permittivity}$$

$$\delta = \varepsilon'' / \varepsilon' \text{ Loss tangent}$$

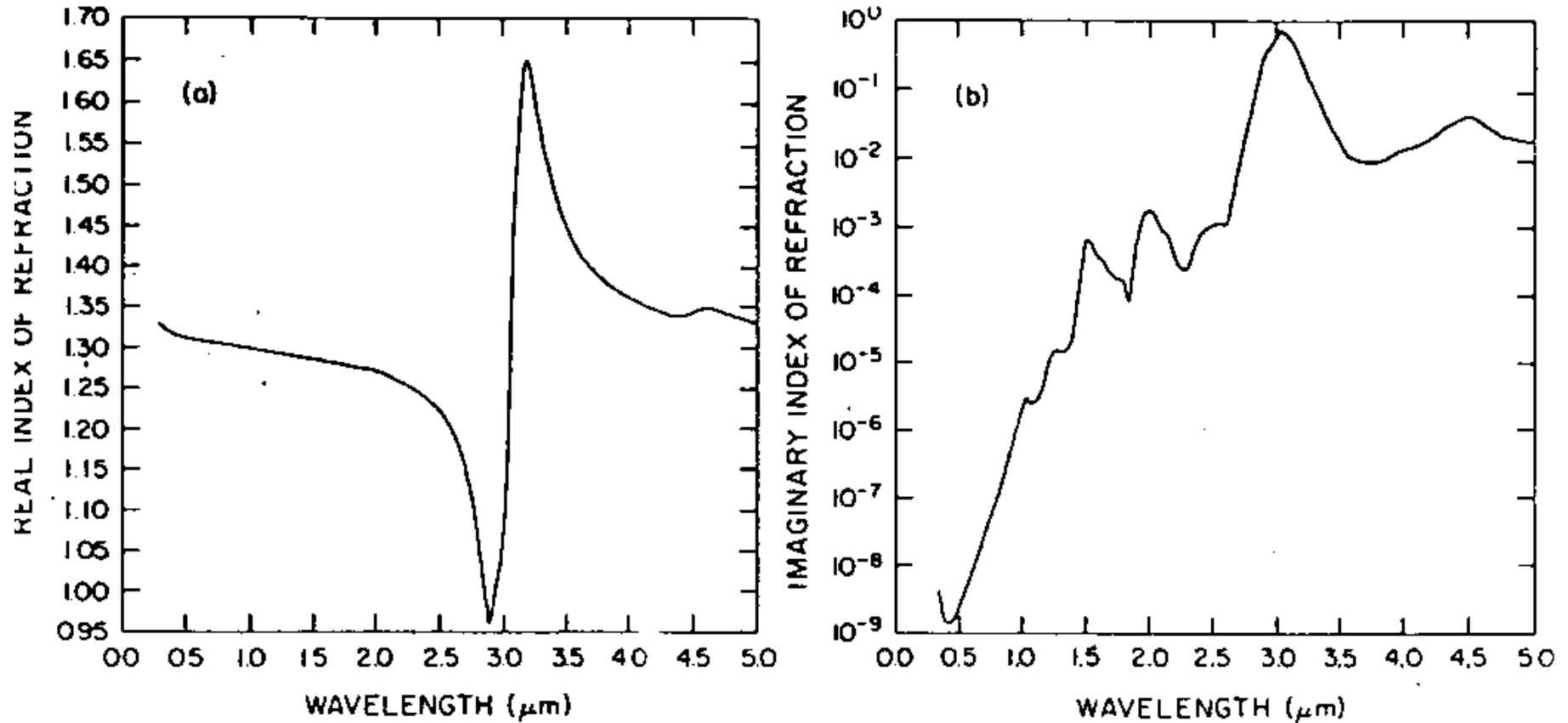
$$\kappa_a \text{ Absorption coefficient}$$

$$d_p = \frac{1}{\kappa_a} = \frac{\lambda_0}{2\pi} \frac{\sqrt{\varepsilon'}}{\varepsilon''}$$

$$d_p = \frac{1}{\kappa_e} \quad ; \quad \kappa_e = \kappa_a + \kappa_s$$

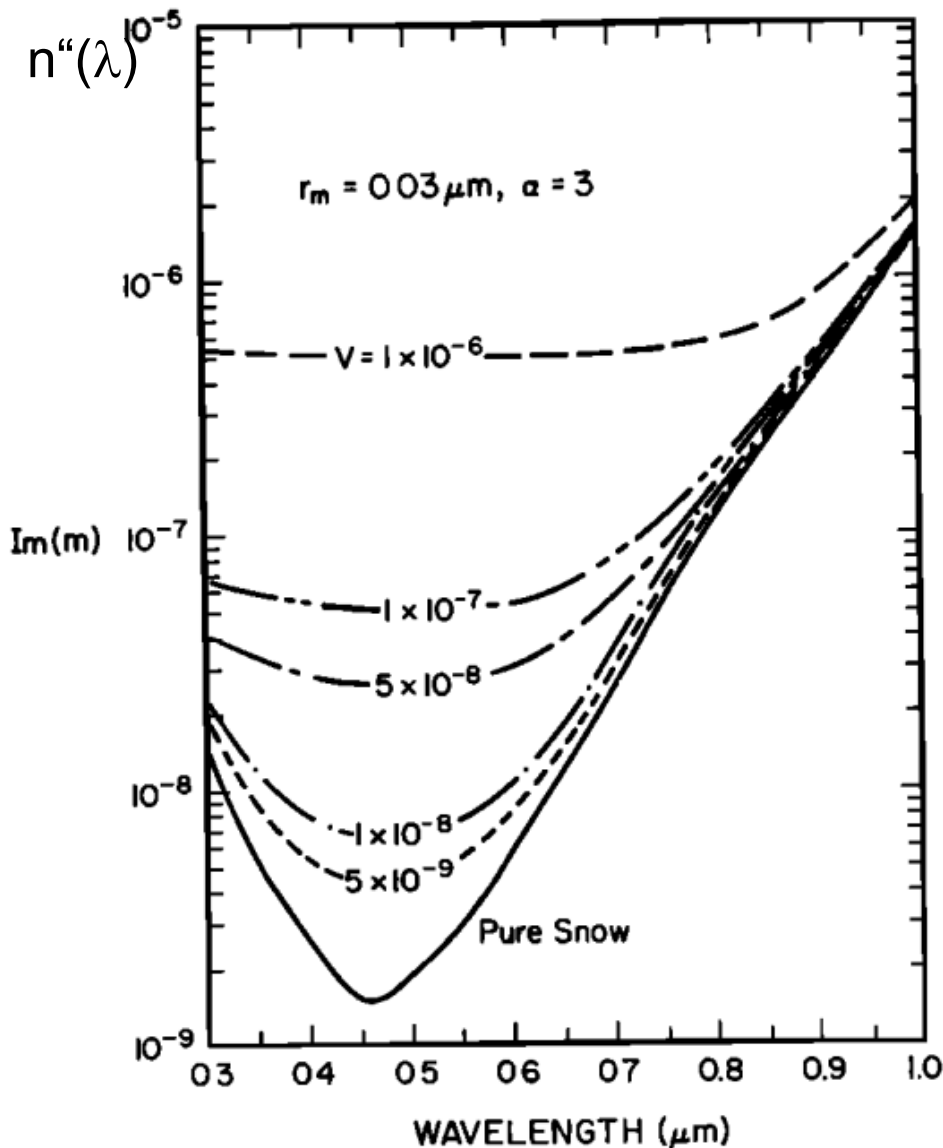
Refractive Index of Ice

$$n(\lambda) = n'(\lambda) - n''(\lambda)$$



At 2.8 μm : resonance (electron oscillation) \rightarrow maximum absorption

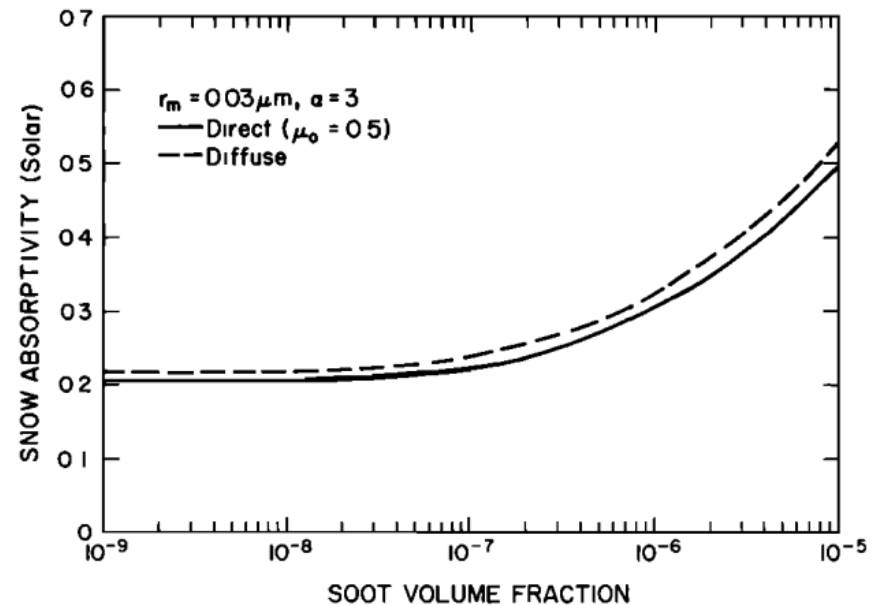
Refractive Index of Soot-contaminated Snow



Refractive index of soot
 $n = 1.8 - 0.5i$

Chylek et al., JGR 1983

**Absorptivity of new snow
 in whole range of solar spectrum
 for direct and diffuse radiation**



Extinction Coefficient of **pure ice** and sea water

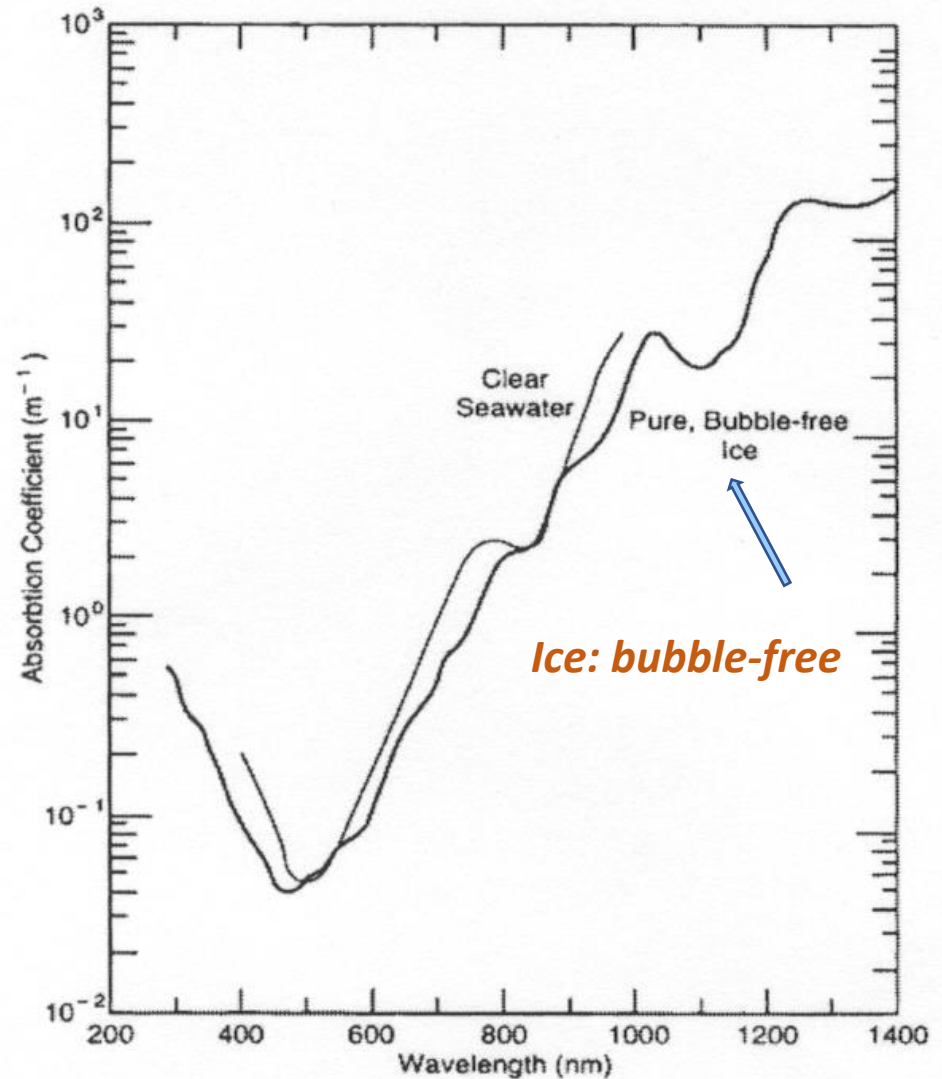
Penetration depth
(for intensity):

$$d_p = 1/\kappa_e$$

κ_e [m^{-1}] extinction coefficient

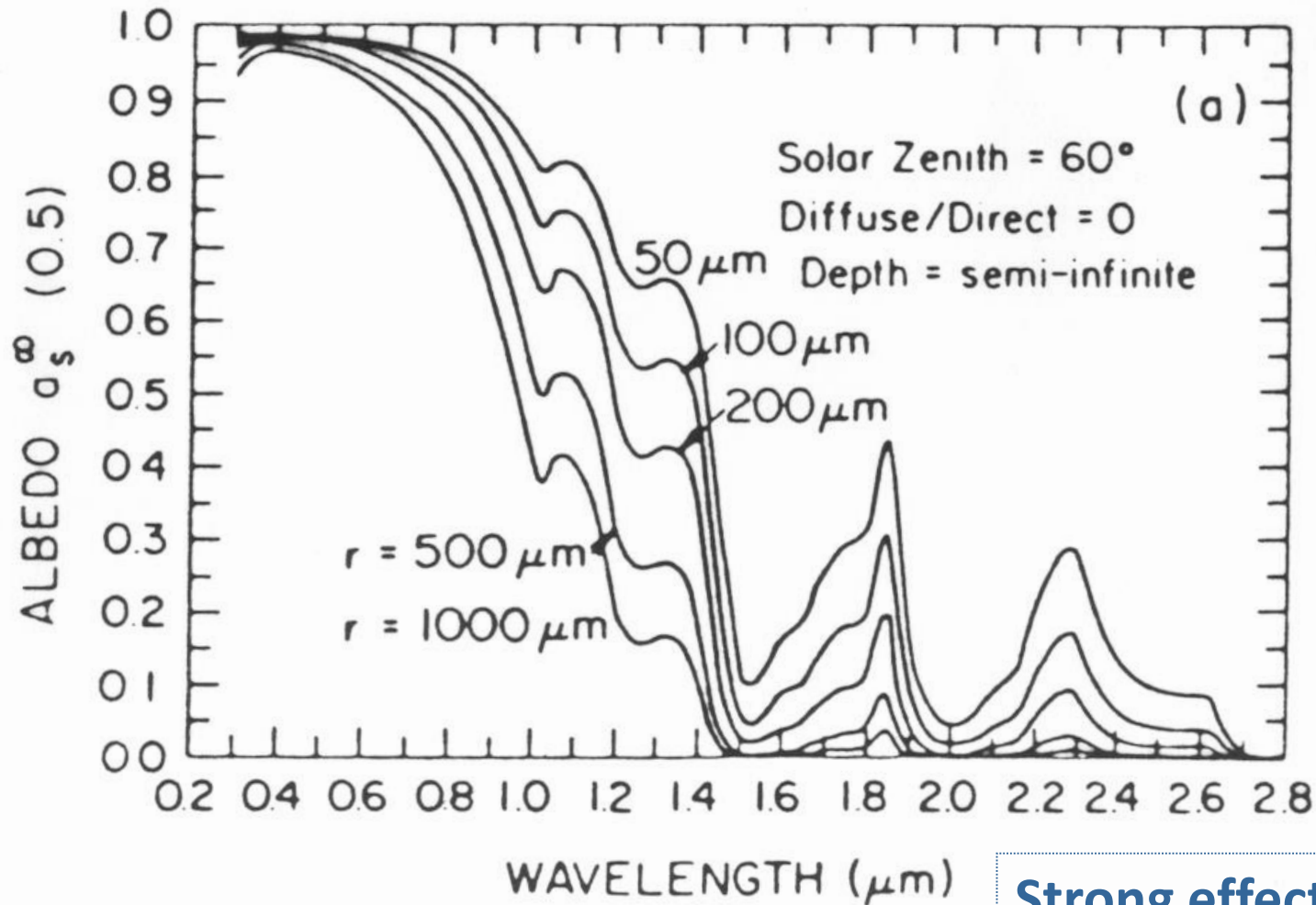
Note the spectral shift of absorption bands between water and ice.

Visible light penetration in snow is a few centimetres; scattering losses dominate!



(Perovich, 1996)

Dependencies of Spectral Reflectivity of Snow: Grain Size



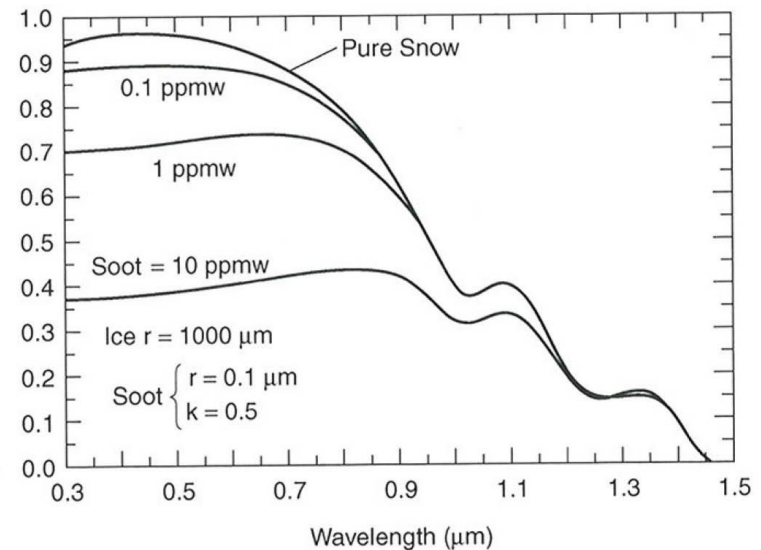
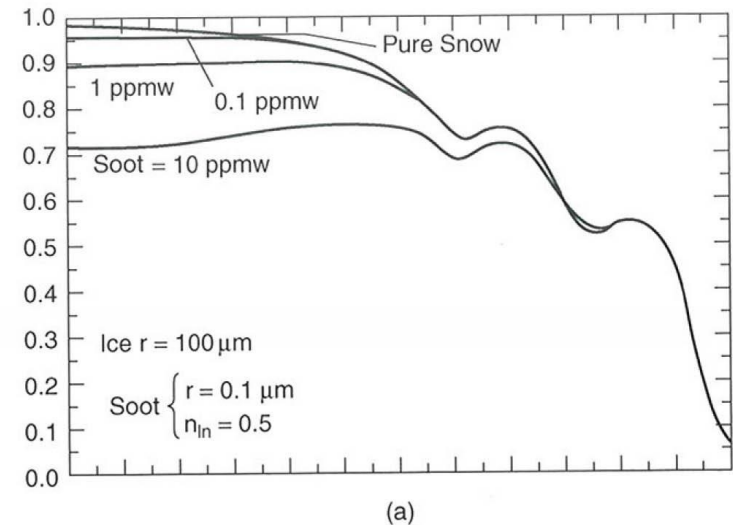
**Strong effect of
grain size in near IR**

Model Calculation by Wiscomb and Warren (1980)

Spectral Reflectivity of Polluted Snow

Decrease of albedo for snow polluted by soot, for different grain sizes.

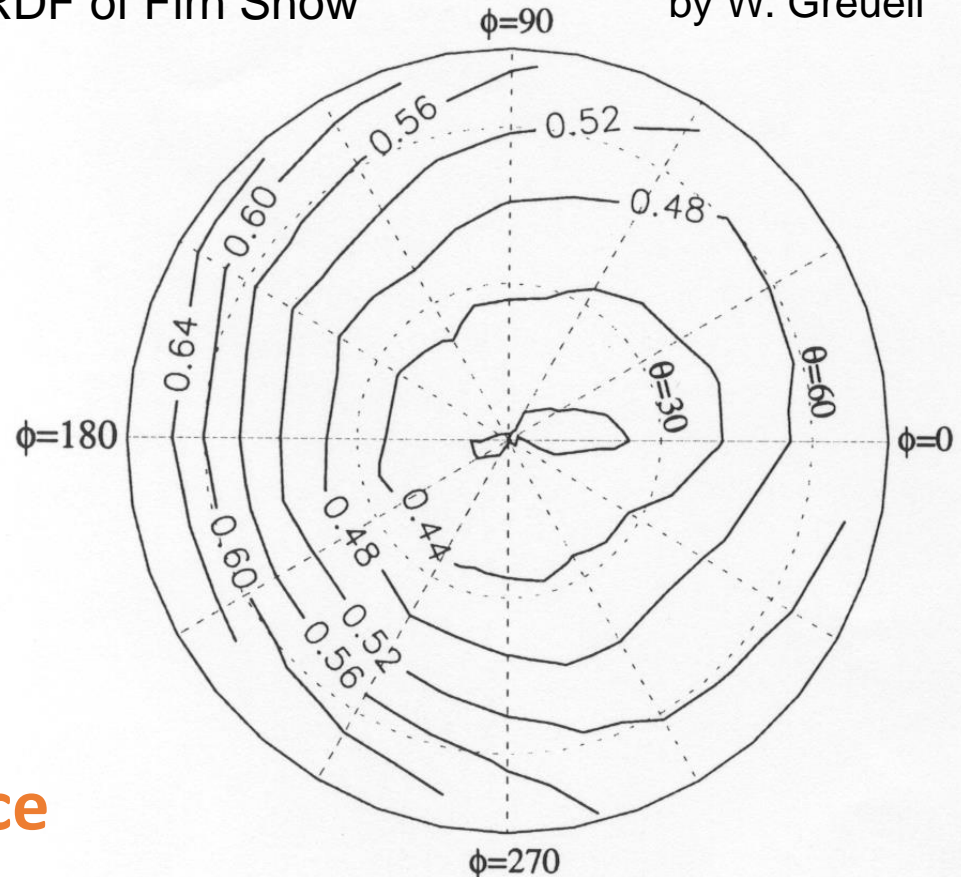
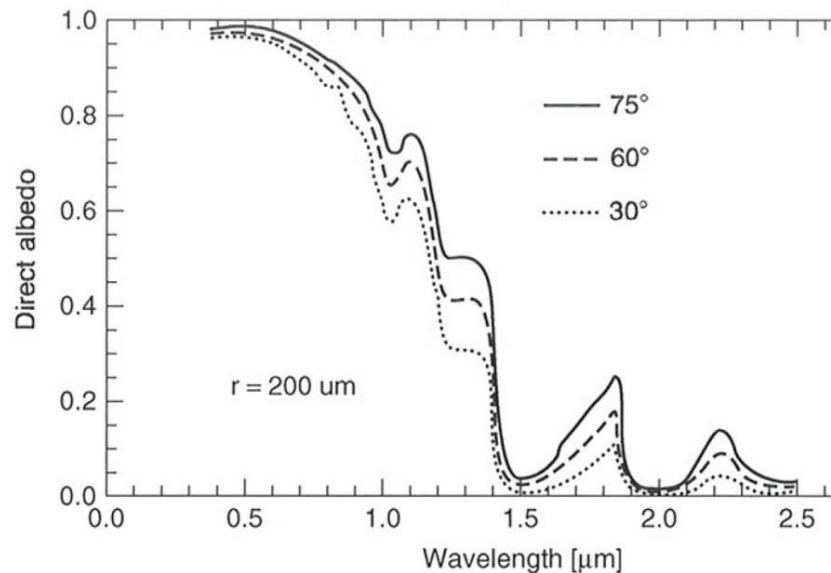
Model Calculation by
Wiscomb and Warren



Angular Dependence of Snow Reflectivity

Example:
BRDF of Firn Snow

Measurements
by W. Greuell



**Snow albedo dependence
on solar zenith angle**

Bidirectional reflectance 800 nm - 900 nm
Solar incidence: $\theta_i = 50^\circ$, $\phi_i = 0^\circ$

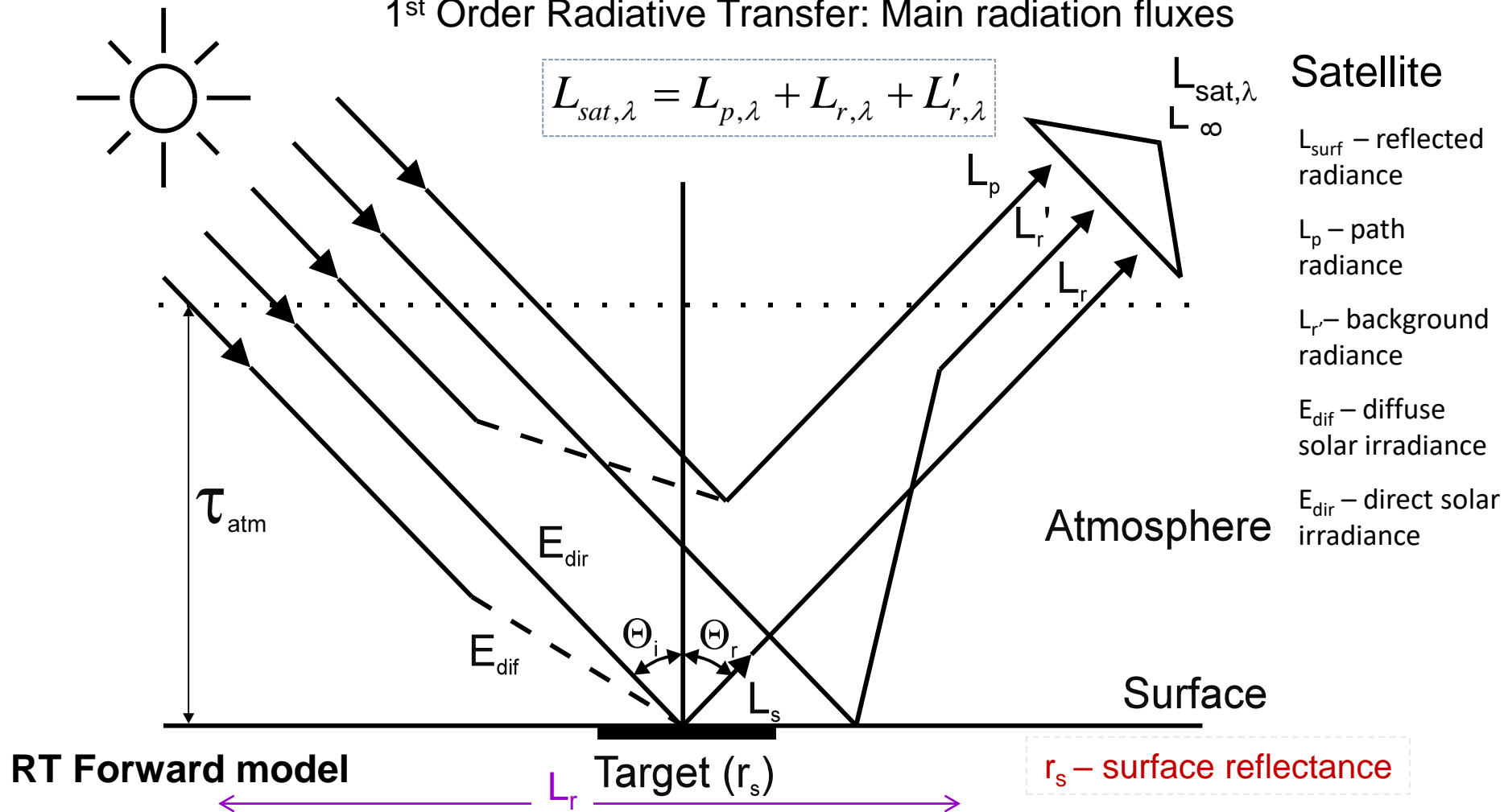
Main Factors for Spectral Reflectance of Snow in the Visible and Shortwave Infrared

- **Impurities** (Soot, Dust, ...); main factor at visible wavelengths
- **Grain size**; important at $\lambda > \sim 1 \mu\text{m}$
- **Liquid water content** (relevant in shortwave IR; primarily an indirect effect through grain size)
- **Illumination and observation geometry** (bi-directional reflectance)
- **Surface roughness**



4. At-Satellite Radiance and Surface Reflectance

1st Order Radiative Transfer: Main radiation fluxes



$$L_{sat,\lambda} = L_{p,\lambda} + L_{r,\lambda} + L'_{r,\lambda}$$

Satellite

L_{surf} – reflected radiance

L_p – path radiance

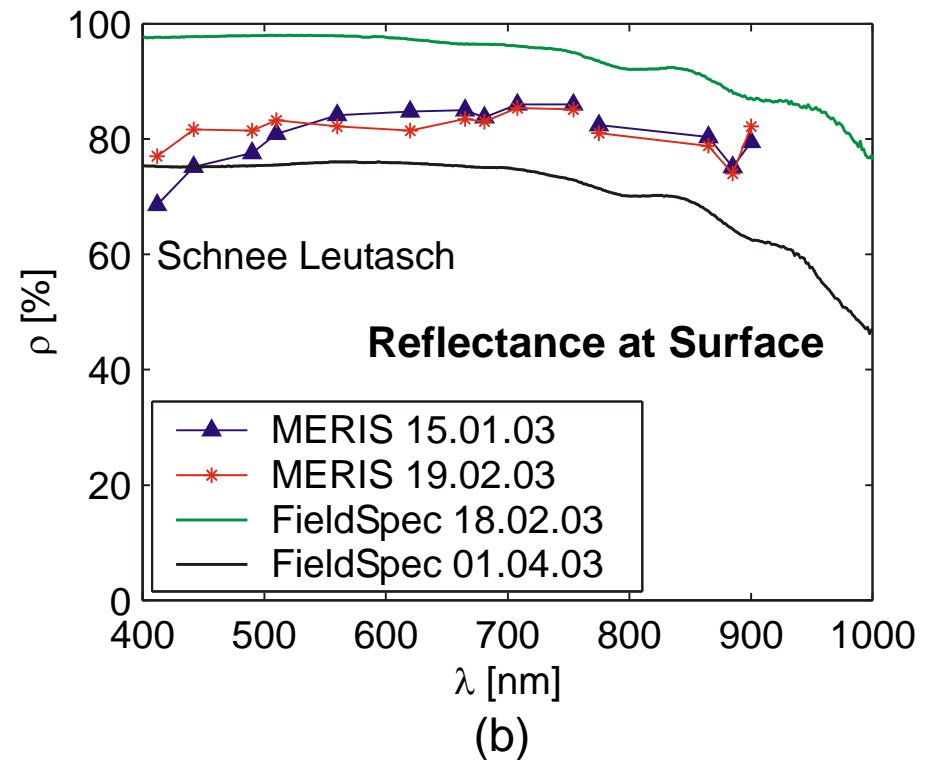
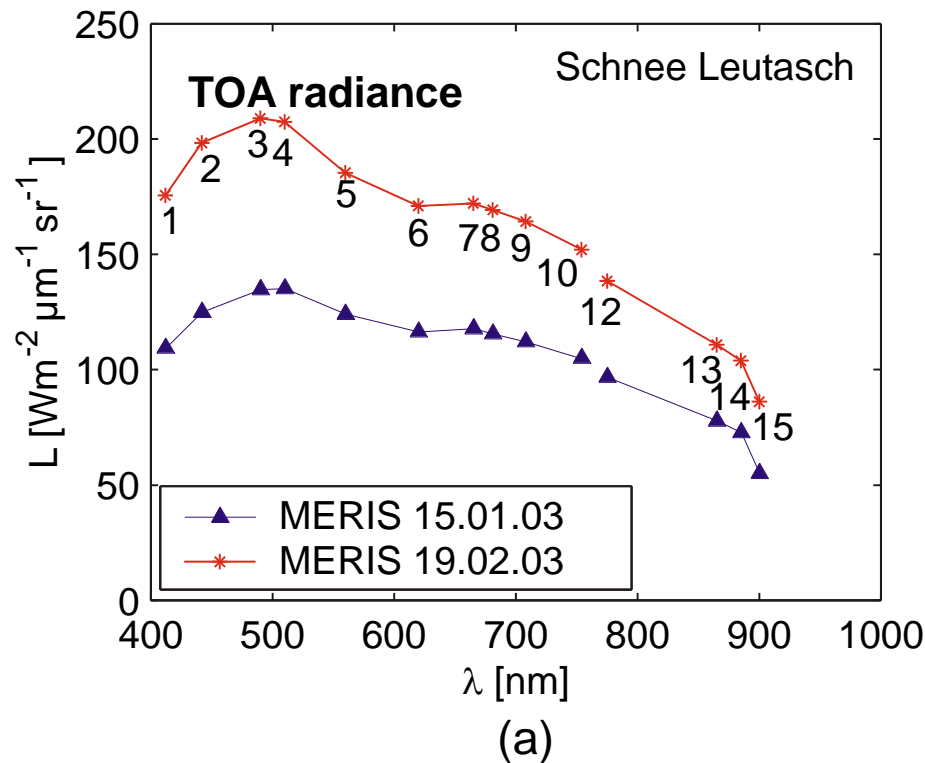
L_r – background radiance

E_{dif} – diffuse solar irradiance

E_{dir} – direct solar irradiance

$$L_{sat,\lambda} = r_{surf} (E_{dir} \cos \theta_i + E_{dif}) (1/\pi) \exp(-\tau_{atm}/\cos \theta_r) + L_p + L'_r \quad [\text{W m}^{-2} \text{ sr}^{-1} \mu\text{m}^{-1}]$$

Snow Surface Reflectance retrieved from at-Satellite Radiance (TOA)



(a) At-satellite radiance (b) At-surface reflectance of snow derived from MERIS data (band 1 to 10 and 12 to 15) compared to field spectrometer measurements.

[Envisat project #164, Floricioiu & Rott, 2005]

Radiative Transfer Code used for computing surface reflectance:

6S (Second Simulation of a Satellite Signal in the Solar Spectrum, <http://6s.ltdri.org/>)

Surface reflectance in complex terrain

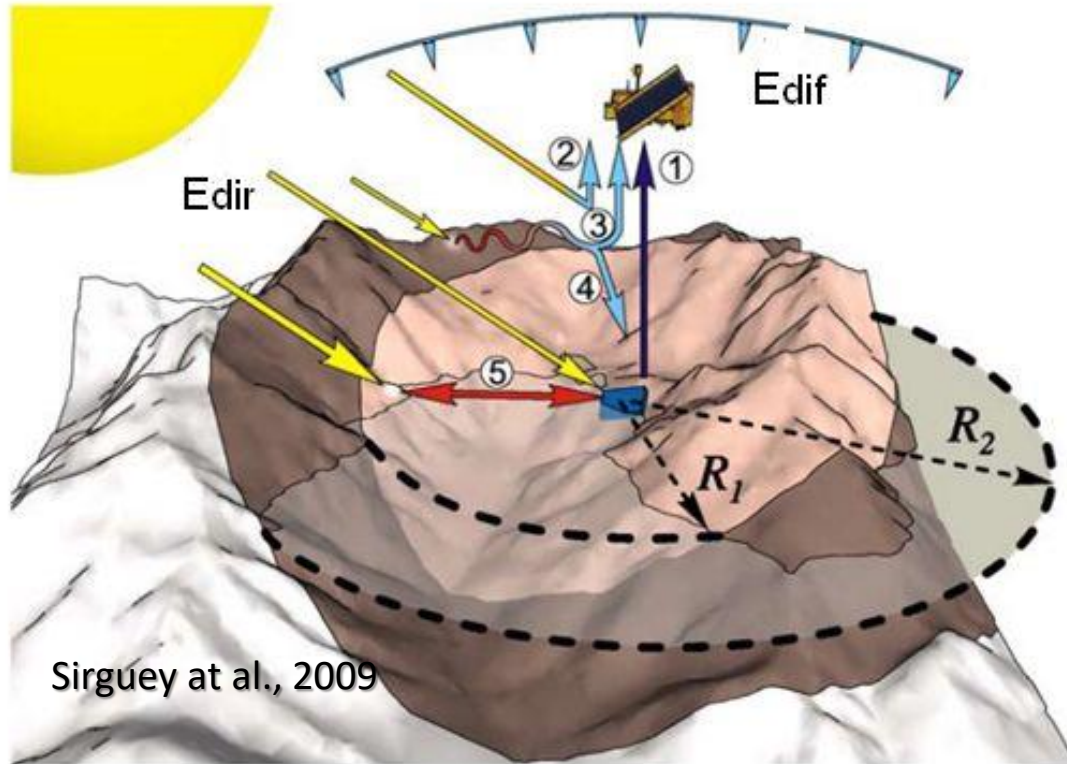
... depends additionally on local topography ...



A bright sun with a prominent lens flare is positioned in the upper center of the frame against a clear, deep blue sky. Below the sun, a vast, snow-covered landscape unfolds, featuring rolling hills and ridges. The snow appears textured, with some areas showing darker patches or tracks. The overall scene conveys a sense of a cold, high-altitude environment.

... and seasonal surface conditions

Radiation fluxes in complex terrain



- 1 L_{surf} – reflected radiance
- 2 L_p – path radiance
- 3 L_r – background radiance
- 4 E_{dif} – diffuse irradiance
- 5 E_{ter} – reflected terrain irradiance

b – coefficient for shading

γ – angle between solar ray and surface normal

E_{dif}^* – total diff irradiance on slope

RT forward model: Reflected radiance on slope

$$L_{\text{surf}} = (1/\pi) r_s [b E_{\text{dir}} \cos \gamma + E_{\text{dif}}^* + E_{\text{ter}}]$$

Inversion of RT model to get broadband surface reflectance

(1) Bidirectional spectral surface reflectance

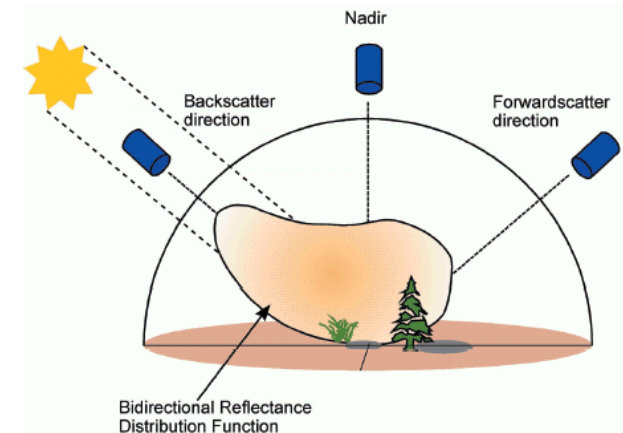
Iterative procedure (diffuse irradiance depends on surface albedo)

$$r_s^{(i)}(\theta_s, \varphi_s; \theta_v, \varphi_v) = \frac{\pi [L_{sat} - L_p - L_r'^{(i)}]}{t_v [bE_{dir} \cos \gamma + E_{dif}^{*(i)} + E_{ter}^{(i)}]}$$

t_v – atmospheric transmission for sensor view

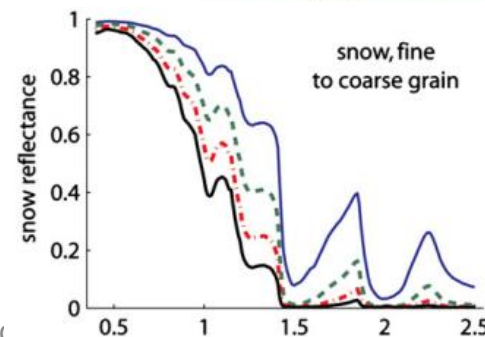
(2) Hemispheric spectral surface reflectance

Correct for angular reflectivity, using BRDF

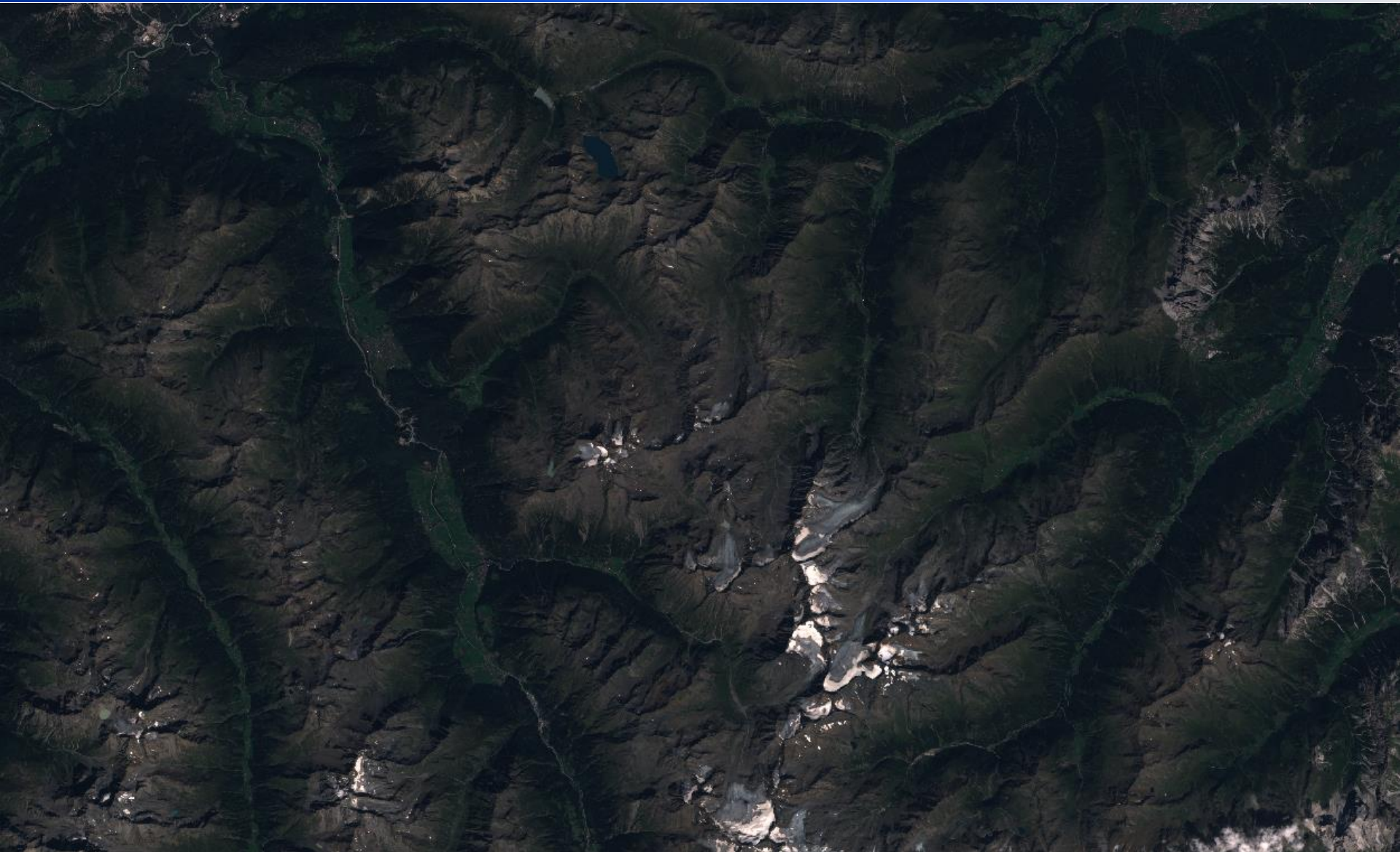


(3) Broadband surface reflectance

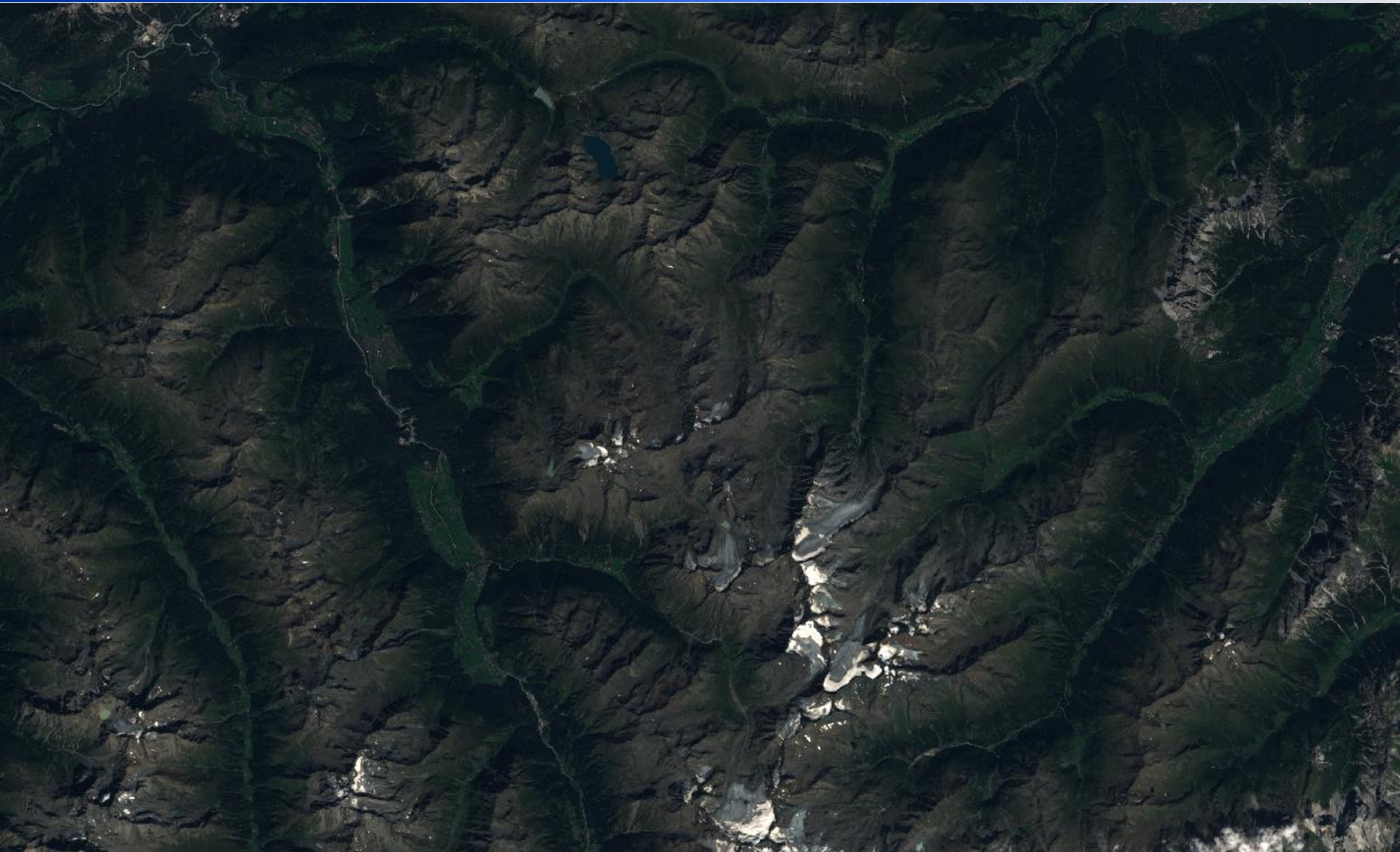
Apply spectral reflectance function



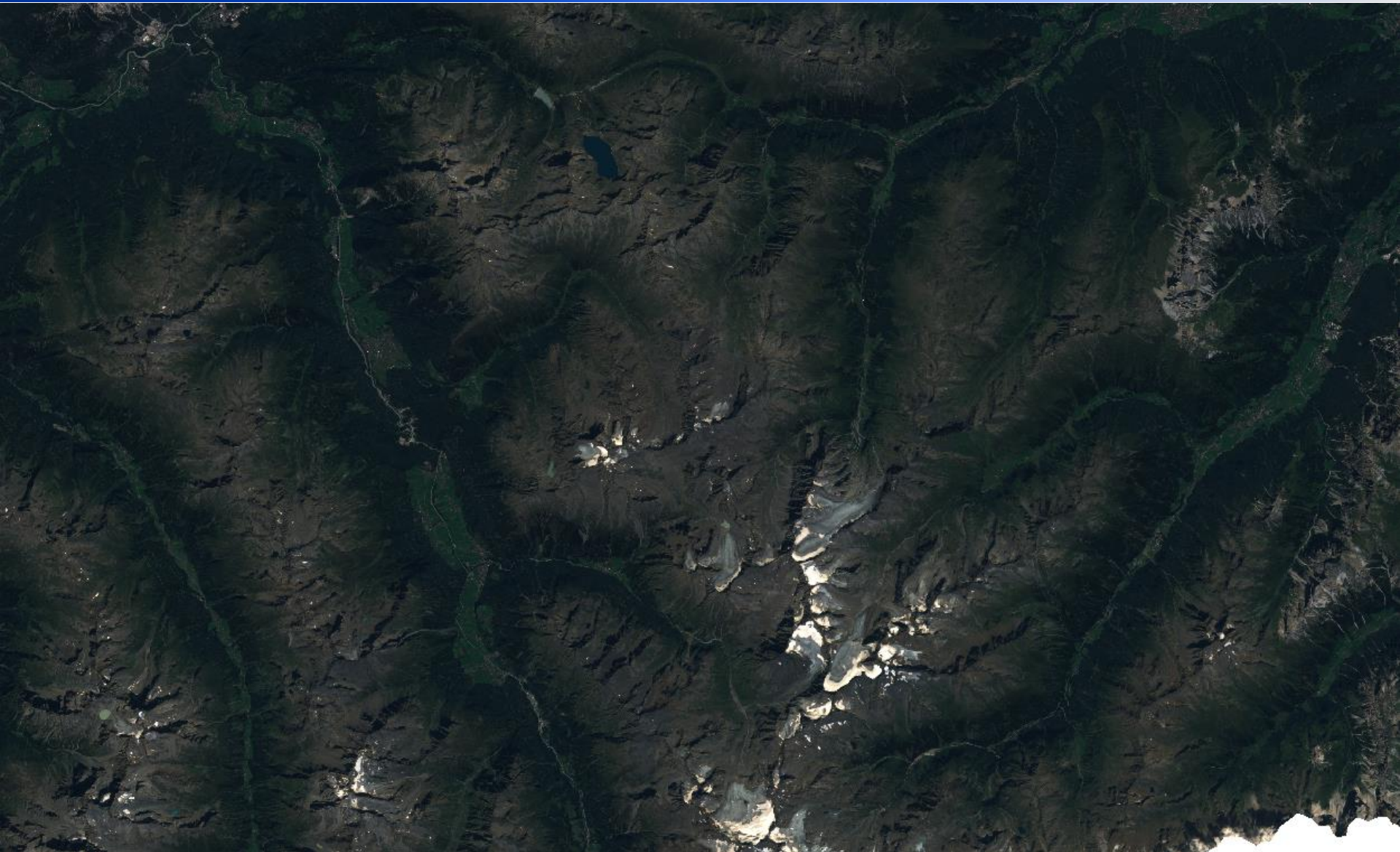
Effects of atmospheric and topographic corrections – Top Of Atmosphere Reflectance



Effects of atmospheric and topographic corrections – Atmospheric Correction (SMAC)



Effects of atmospheric and topographic corrections – Atmospheric Correction (SMAC) & Topographic Correction (Ekstrand)



Effects of atmospheric and topographic corrections – Atmospheric Correction (6S)



Effects of atmospheric and topographic corrections – Atmospheric Correction (6S) & Topographic Correction (Ekstrand)



Requirements for accurate atmospheric and topographic corrections

- Solar and viewing angles for satellite image
- Atmospheric parameters at time of satellite image acquisition (e.g. from radiosonde measurements or from reanalysis data of numerical weather prediction models)
- Basic knowledge about the general climate conditions
- Digital Elevation Model (DEM) in the same resolution as the satellite image
- Exact geolocation match of DEM and satellite image
- Computing power!!!

5. Applications of Optical Satellite Data for Snow Extent Monitoring

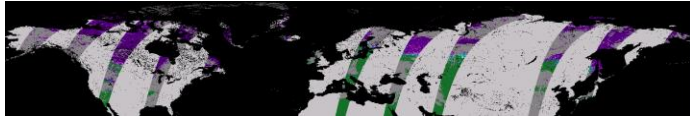
- Snow extent per pixel:
 - Binary (snow / snow free)
 - Fractional (0 – 100%)
- Thematic information in forested areas:
 - Snow on ground
 - Viewable snow (snow on top of forest canopy)

Limitations and challenges in snow cover monitoring:

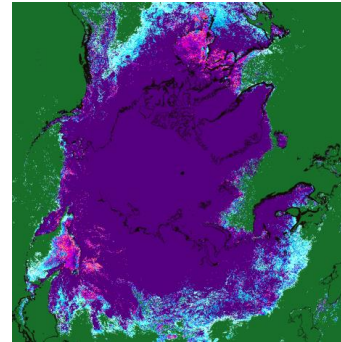
- Discrimination of snow and clouds
- Polar darkness (reduced light in high latitudes)

Currently Available Hemispheric and Global Snow Products from Optical Satellite data

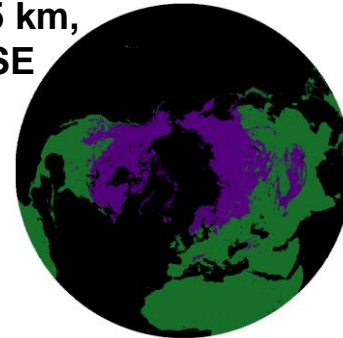
GlobSnow, 1 km, Fractional SE



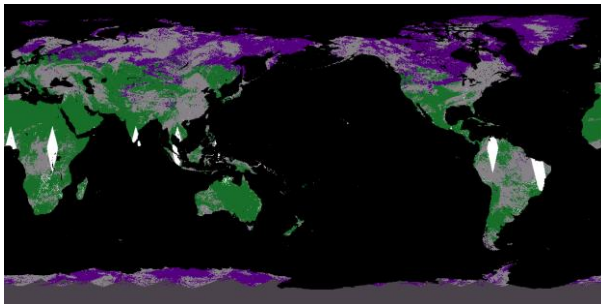
**Pathfinder,
5 km,
Fractional
SE**



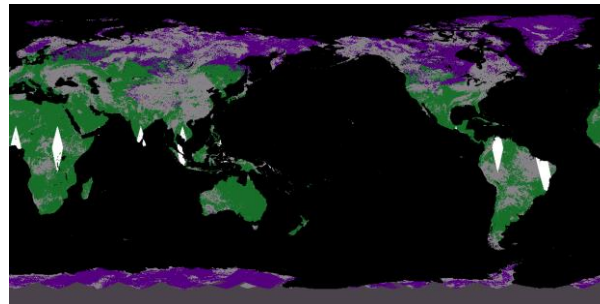
**CryoClim, 5 km,
Fractional SE**



JAXA MDS10C, 5 km, Binary SE



JAXA GHRM5C, 5 km, Binary SE



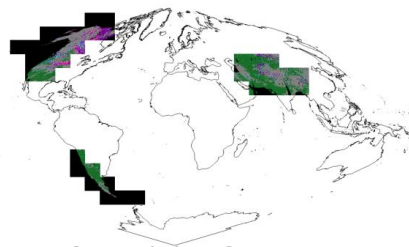
AutoSnow, 4 km, Binary SE



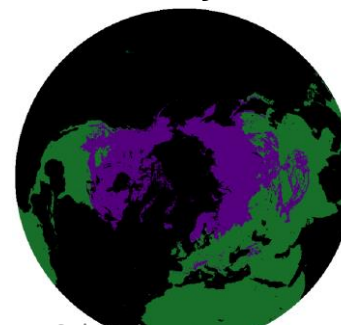
**MOD10_C5, 0.5 km,
Fractional SE**



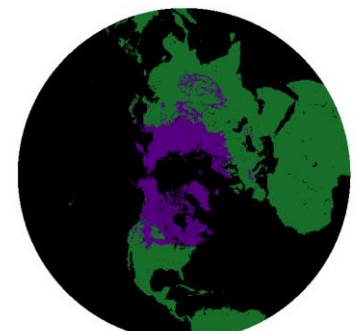
**MODSCAG, 0.5 km,
Fractional SE**



**MEaSURES, 25 km,
Binary SE**

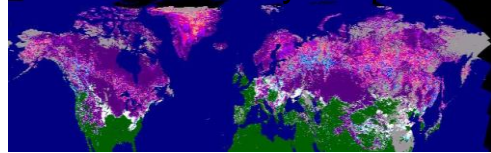


IMS, 4 km, Binary SE

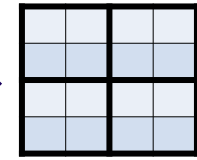
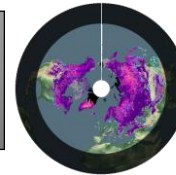


Intercomparison of Hemispheric Snow Products

Data stack of daily SE products



Transformation to common projection (EASE-GRID 2.0)



Aggregate SE to intercomparison grid sizes 5 km & 25 km



Generate weekly / monthly maximum, minimum and average SE map

Generate valid pixel mask by applying common mask of non-valid areas (e.g. sea)

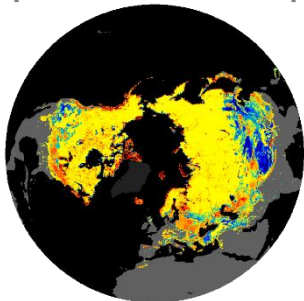
Weekly / monthly SE data

Deviation of SE products from climatological mean SE map

Intercomparison of valid pixels of SE products

- Pixel by pixel (daily)
- Spatial difference maps (monthly)

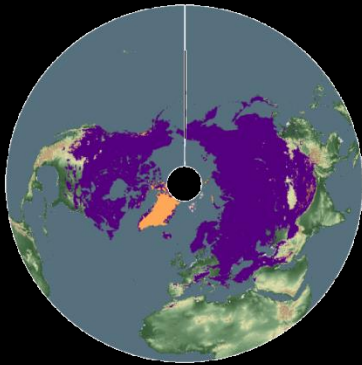
Spatial Difference Map



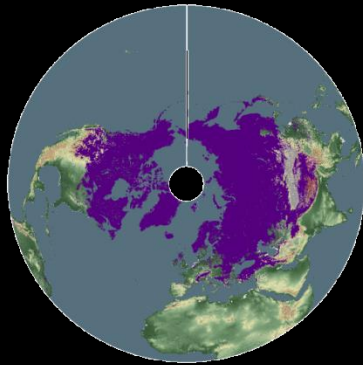
- Statistical parameters (fractional: Bias, RMSE, Correlation Coefficient, Number of used pixels; binary: F-Score, Recall, Precision, Accuracy)
- Fraction of total SE
- Time series of parameters
- Separate statistic analysis for forest / non-forest / plain areas / mountains / SCF classes, Sturm's climate classes of seasonal snow

Hemispheric snow products reprojected in EASE-GRID 2.0

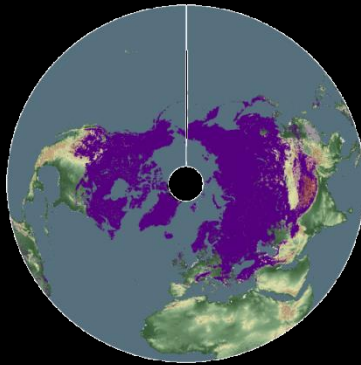
MEaSURES



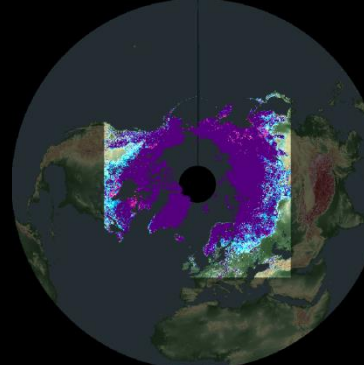
**JASMES
MDS10C**



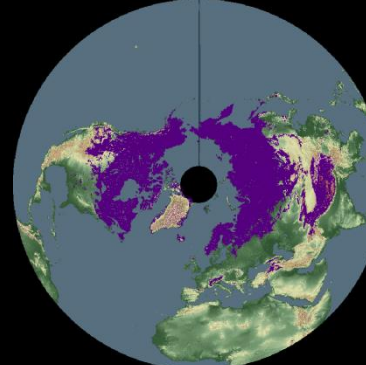
**JASMES
GHRM5C**



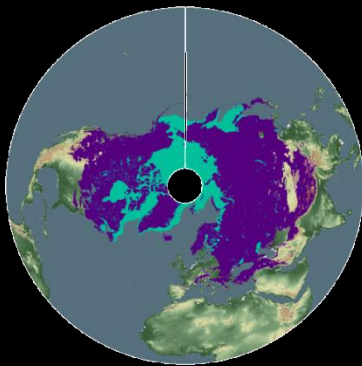
**AVHRR
Pathfinder**



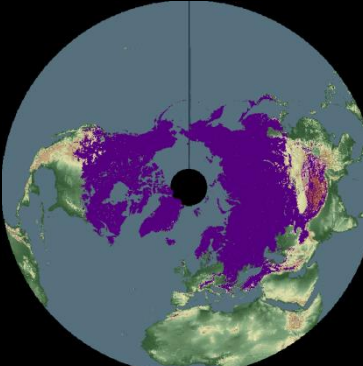
CryoClim



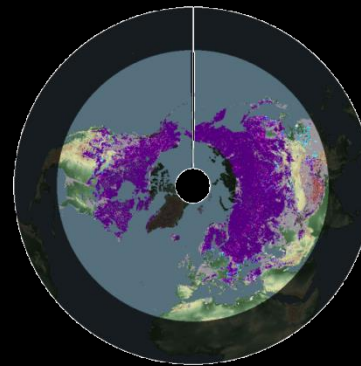
NOAA IMS



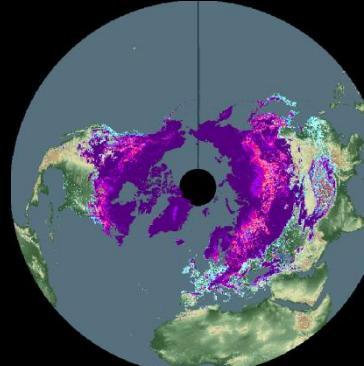
AutoSnow



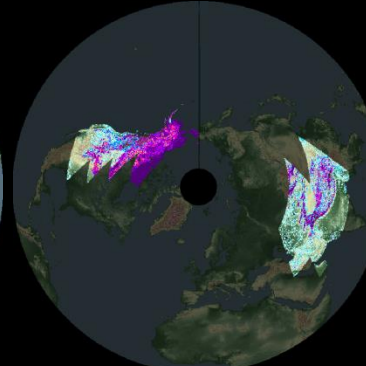
GlobSnow



MOD10_C5



SCAG



6. Validation of Snow Extent Products

In-situ observations: *Often requested, little understood...*



In-situ snow observations

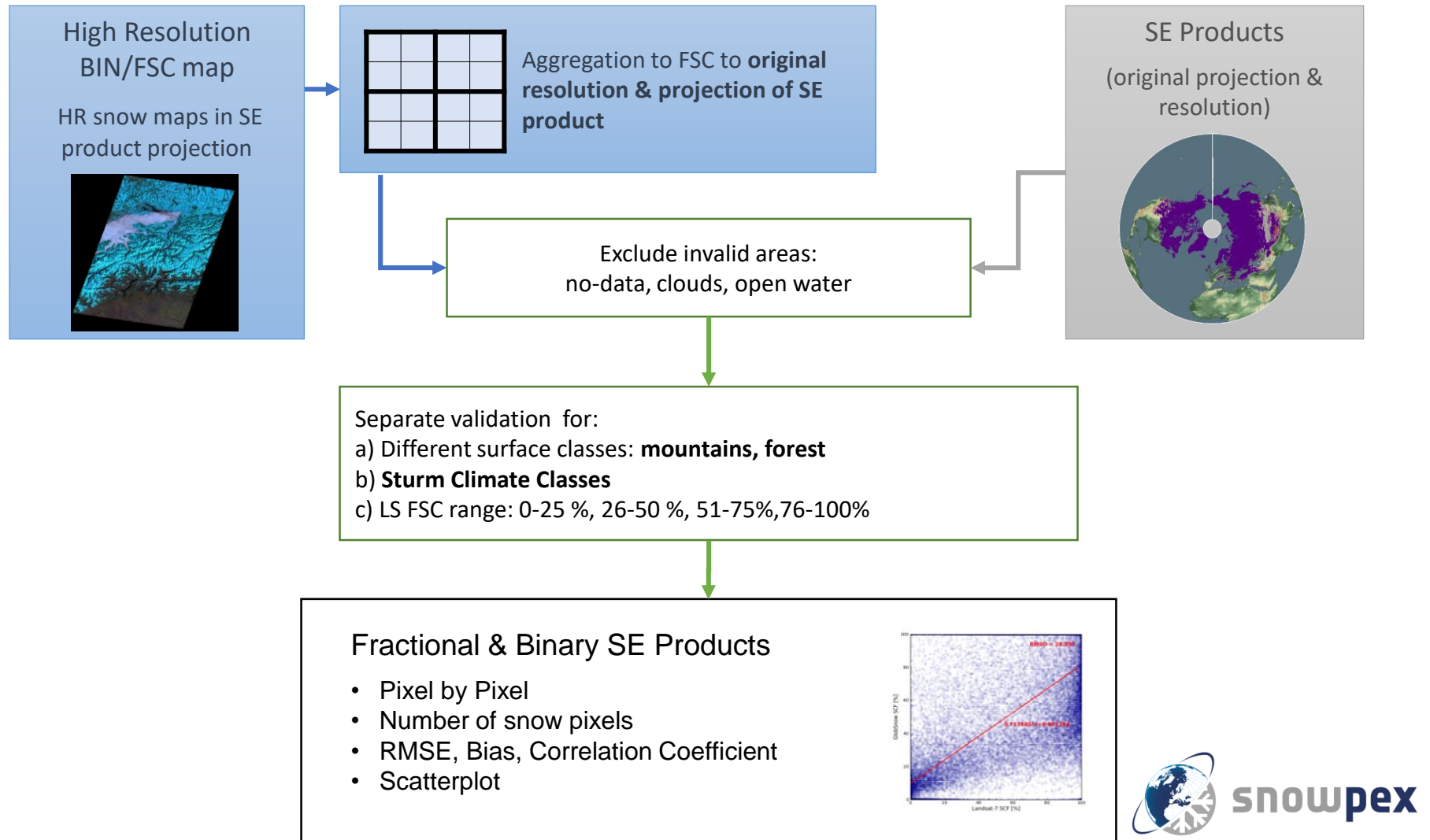
- Very accurate point measurement
- Measured snow depth measured must be converted into binary snow information for the corresponding pixel (snow / snow free):
- Often used thresholds to classify snow:
 - Snow depth > 0 cm
 - Snow depth ≥ 2 cm
 - Snow depth ≥ 15 cm
- In-situ snow measurements do often NOT report zero snow
- In-situ measurements only available in open land (not in forests!)
- Only limited in-situ measurements available globally (high effort and costs)

Validation of Snow Products – In-situ observations

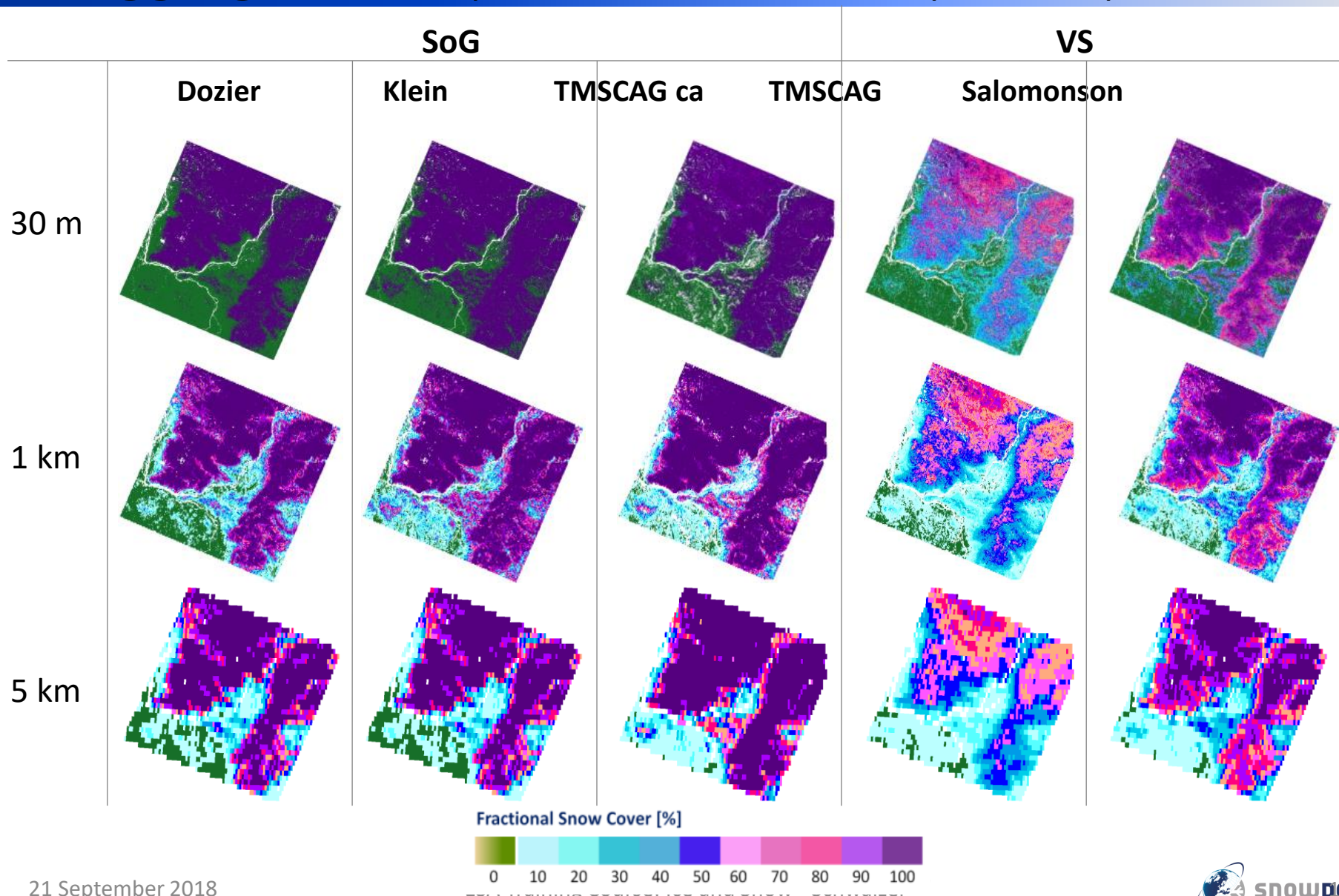
How would YOU interpret this case???



Validation of snow products – Reference snow maps from higher resolution optical satellite data



High resolution reference snow maps – aggregation to pixel size of hemispheric products



Snow maps from high resolution optical satellite data

- Spatial extent of several tens to hundreds of square kilometres
- Coverage of multiple surface classes
- Repeat time frequencies between 5 and 26 days
- Data from Sentinel-2 and Landsat with pixel sizes between 10 m and 30 m are available free of charge
- Very high resolution data (0.30 m – 2.5 m) are only available at high costs (commercial data providers)
- Cloud cover limits usable data set
- Snow algorithms need further development

7. Glacier Parameters from Optical Satellite Data

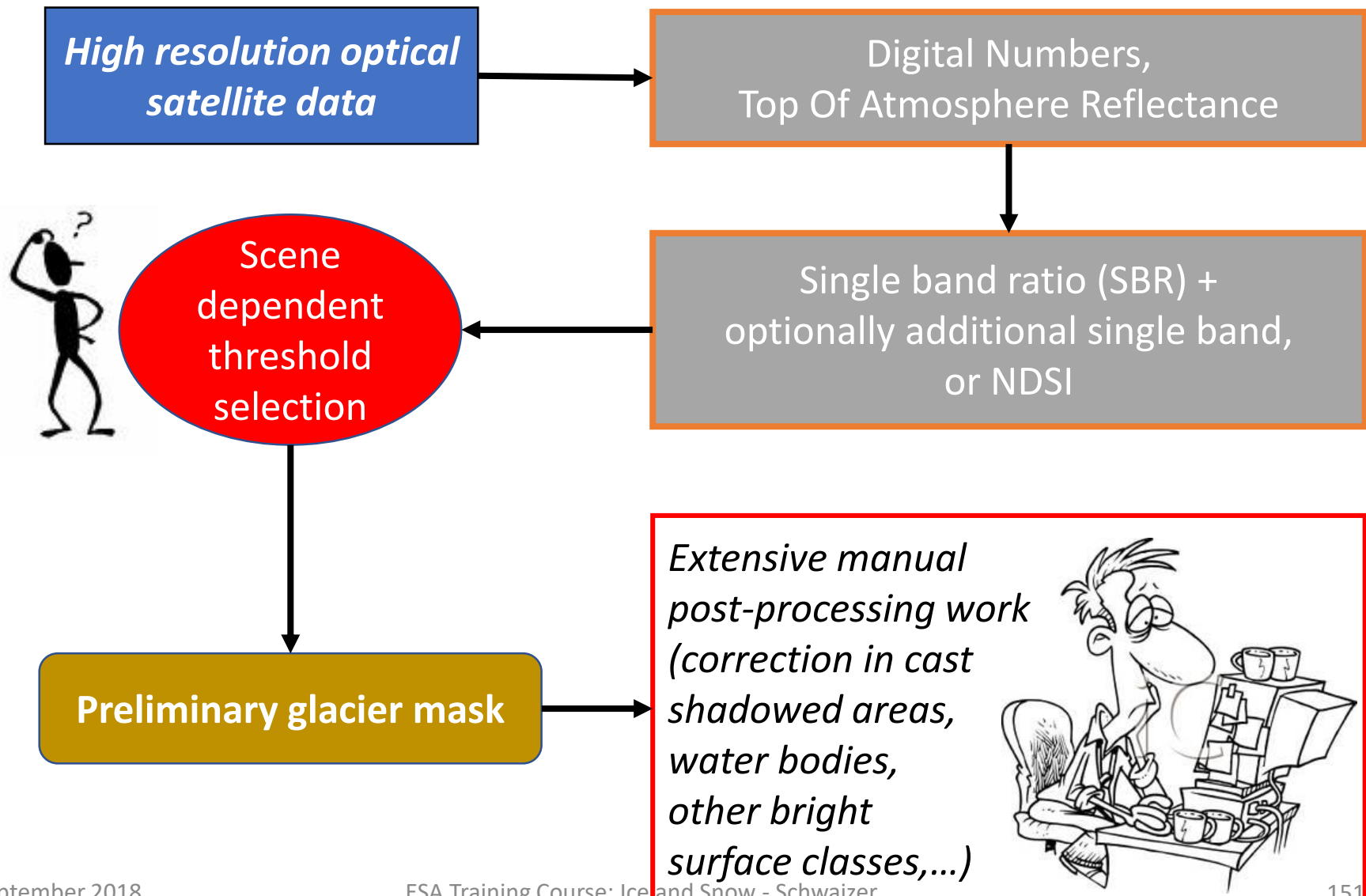
- *Glacier outlines (= area)*
- *Snow and ice areas on glaciers*
- *Glacier facies (snow, firn, ice, debris, supraglacial lakes, etc.)*
- Glacier front mapping
- *Ice motion (offset tracking)*
- Glacier topography



© Schwaizer

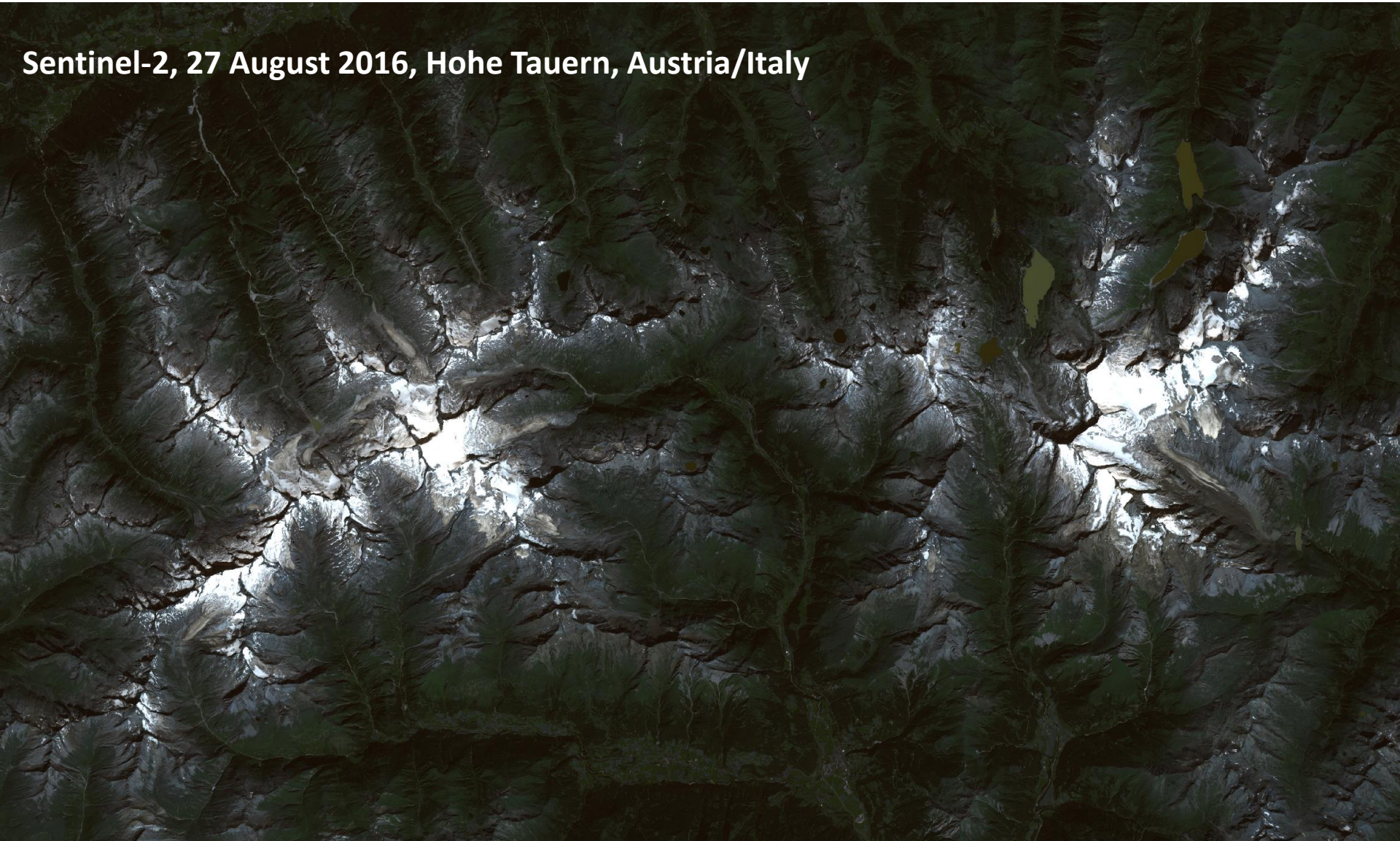
For most of these glacier parameters, high resolution optical satellite data acquired close to the date with maximum ablation on glaciers are mandatory!!!

Commonly used methods for mapping glacier areas in the past years

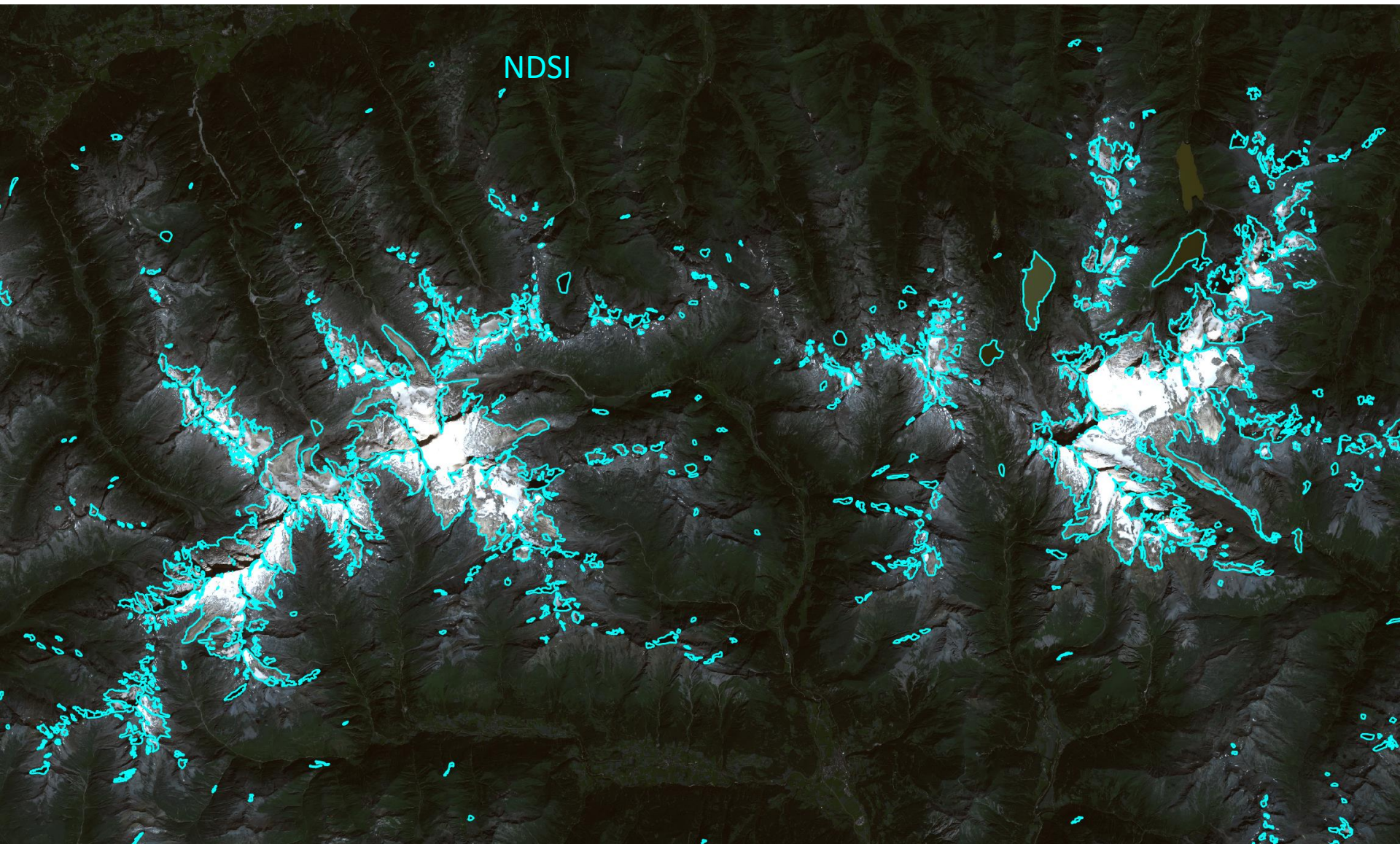


Some preliminary glacier areas resulting from the standard methods

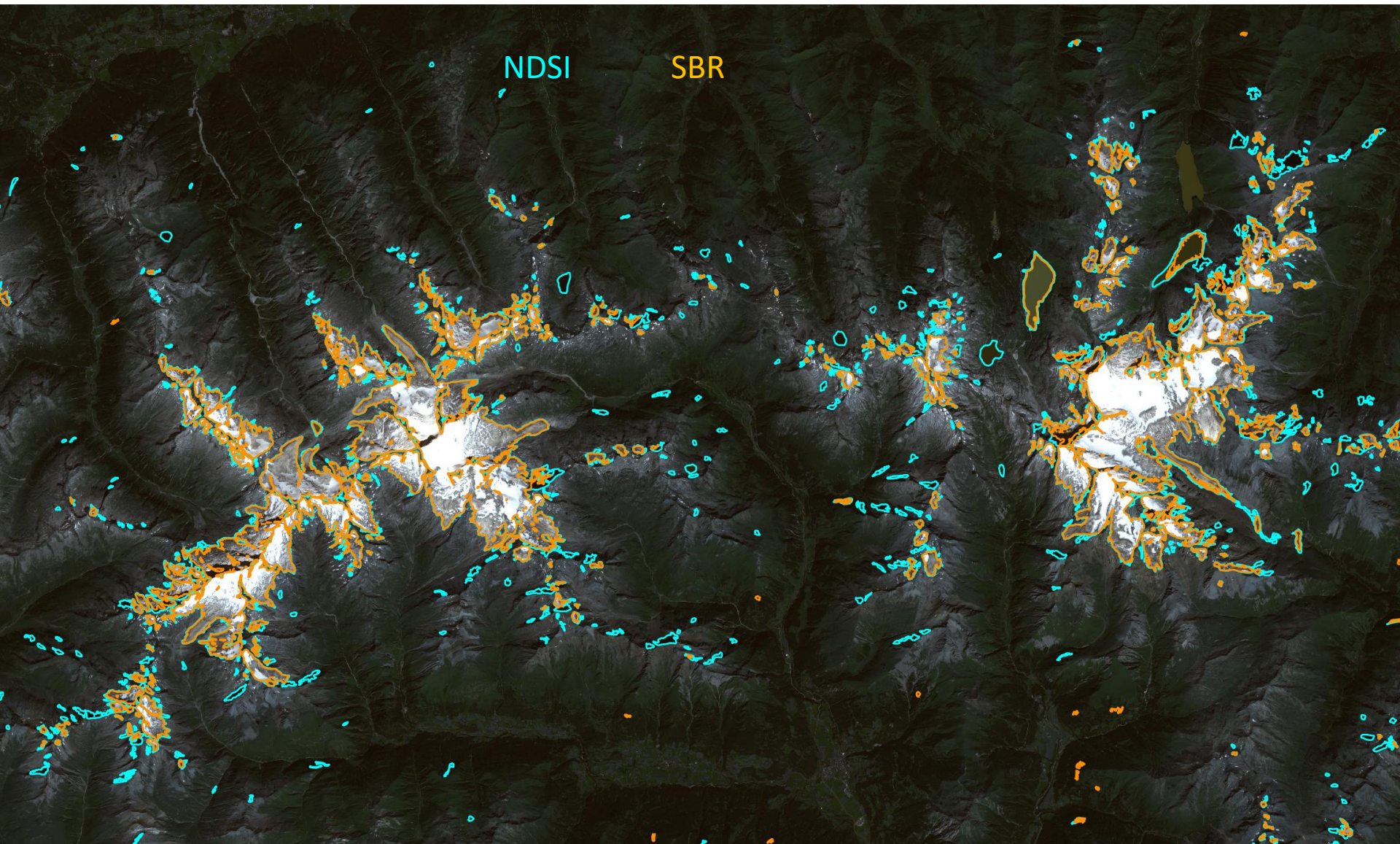
Sentinel-2, 27 August 2016, Hohe Tauern, Austria/Italy



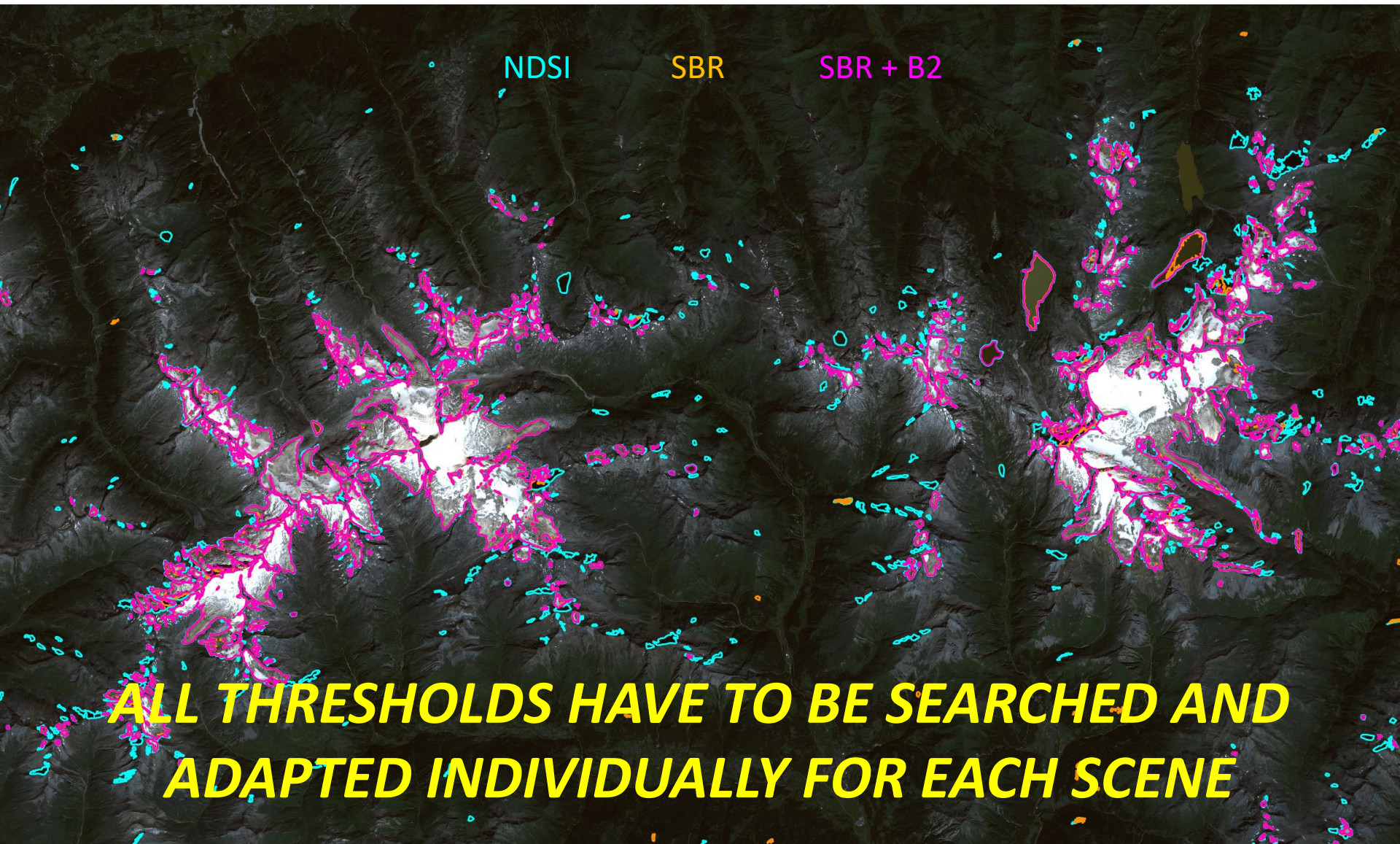
Some preliminary glacier areas resulting from the standard methods



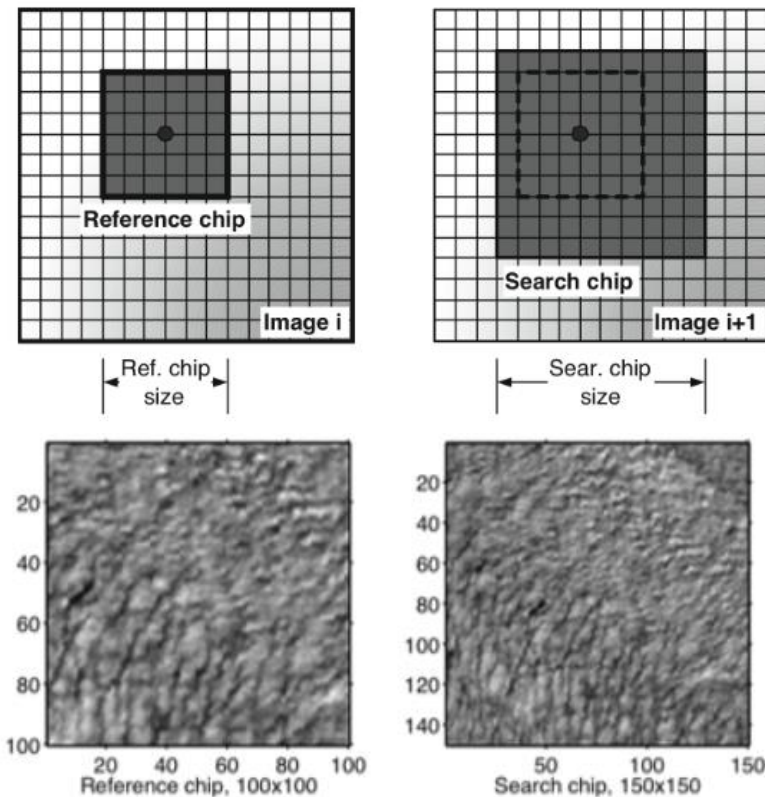
Some preliminary glacier areas resulting from the standard methods



Some preliminary glacier areas resulting from the standard methods

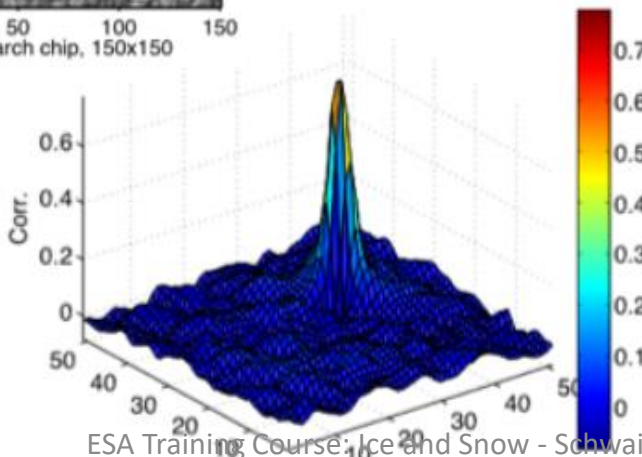


Ice Motion from Repeat Pass Optical Satellite Images

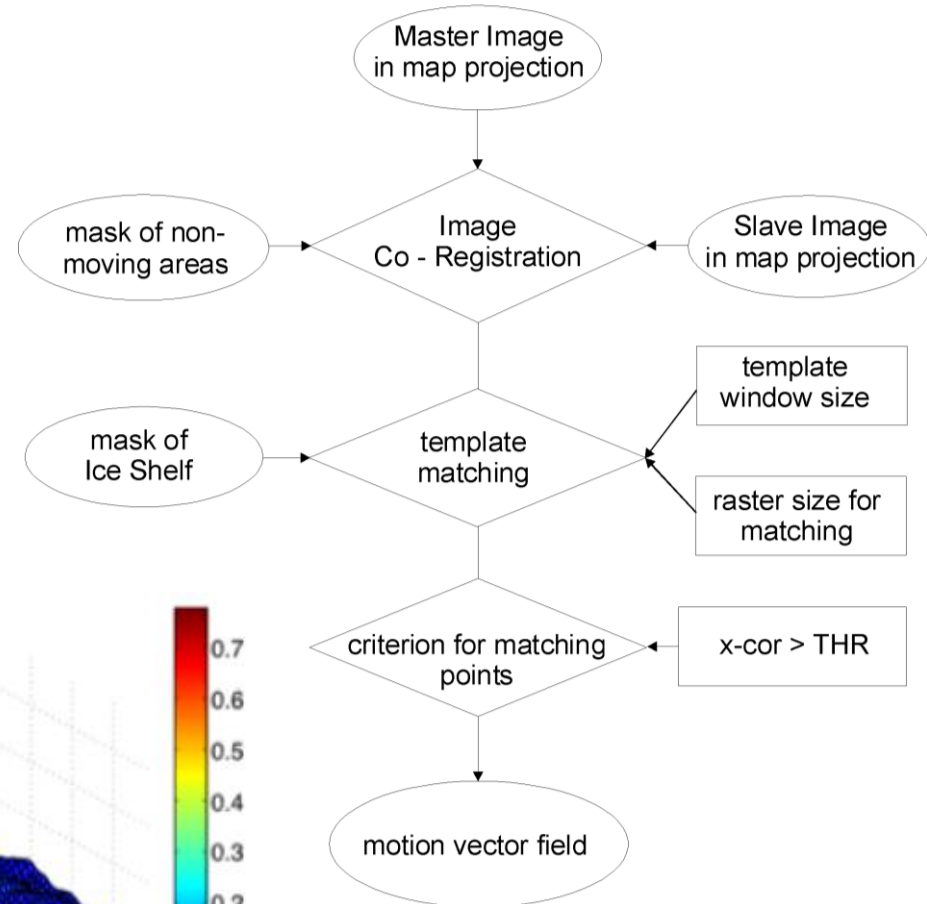


Technique:

Template matching in repeat pass imagery
Conservative features are tracked

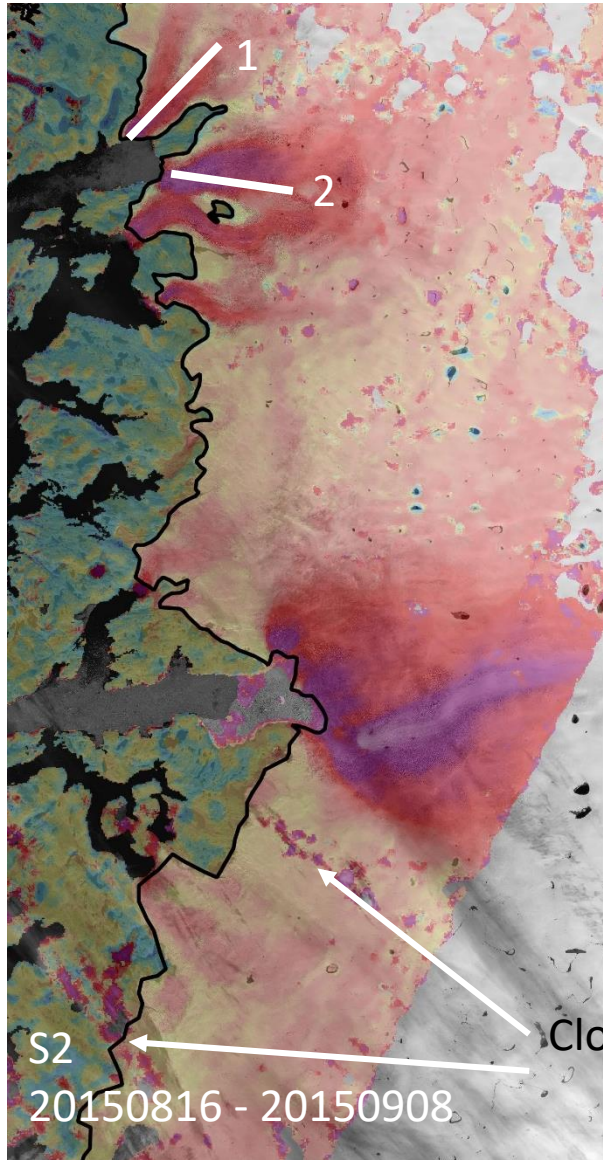


Processing Flowchart

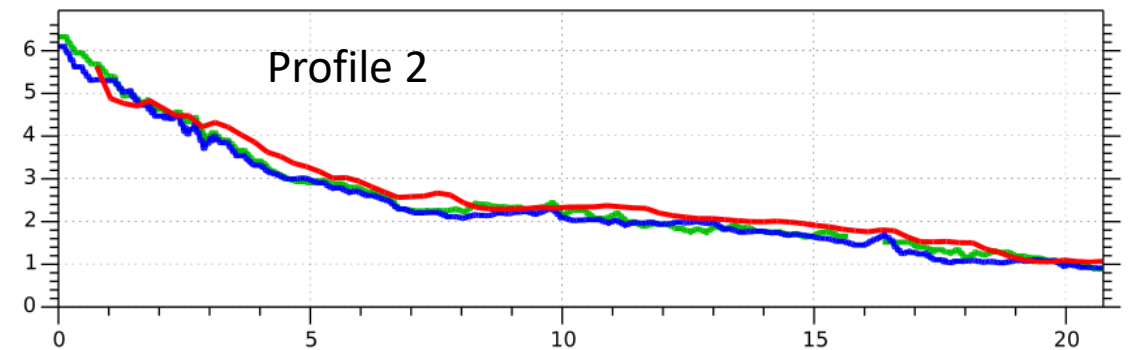
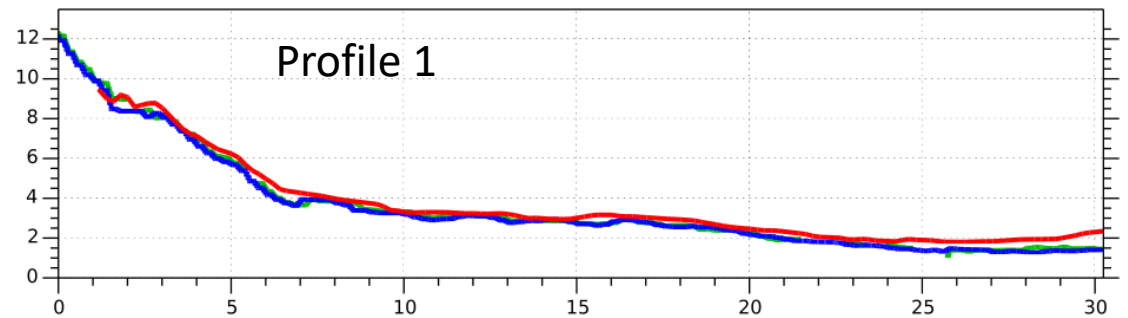


Ahn & Howat TGRS, 2010

Ice velocity in Greenland from Sentinel-2



Ice velocity map from Sentinel-2 L1C data: Feature tracking applied on S2A data of 2015/08/16 – 2015/09/08 over West Greenland



- S2 FT IV: 20150816 - 20150908
- S1 FT IV: 20150819 - 20150831
- S1 FT IV: 20150831 - 20150912

E. Concluding Remarks

- Snow and ice are highly dynamic parameters in space and time
- Continuous monitoring of cryospheric parameters is needed for multiple applications
- Many (research) groups are already working on different cryospheric parameters from Optical and Radar satellite data, and are providing these data
- Most cryospheric products are designed for a specific application or usage, and have thus limitations for other applications

... and there is still a lot of work to do ...

- New sensors require the adaptation or new development of algorithms and methods
- The amount of data increase significantly with data from the new Copernicus Sentinel satellites
→ new challenge to store and process all these data
- Combination of radar and optical satellite data is still work in progress
- Continuous monitoring of cryospheric parameters and understanding all the results retrieved from satellite data is work in progress...

Practical Training – Schedule

2 Groups: execute each one main exercise:

- *Mapping snow from Sentinel-2 optical data over Alps*
- *Mapping wet snow from Sentinel-1 SAR data over Alps*

Timing:

13:30 – 15:00 & 15:15 – 16:30:

Process the data following the instructions of the exercises

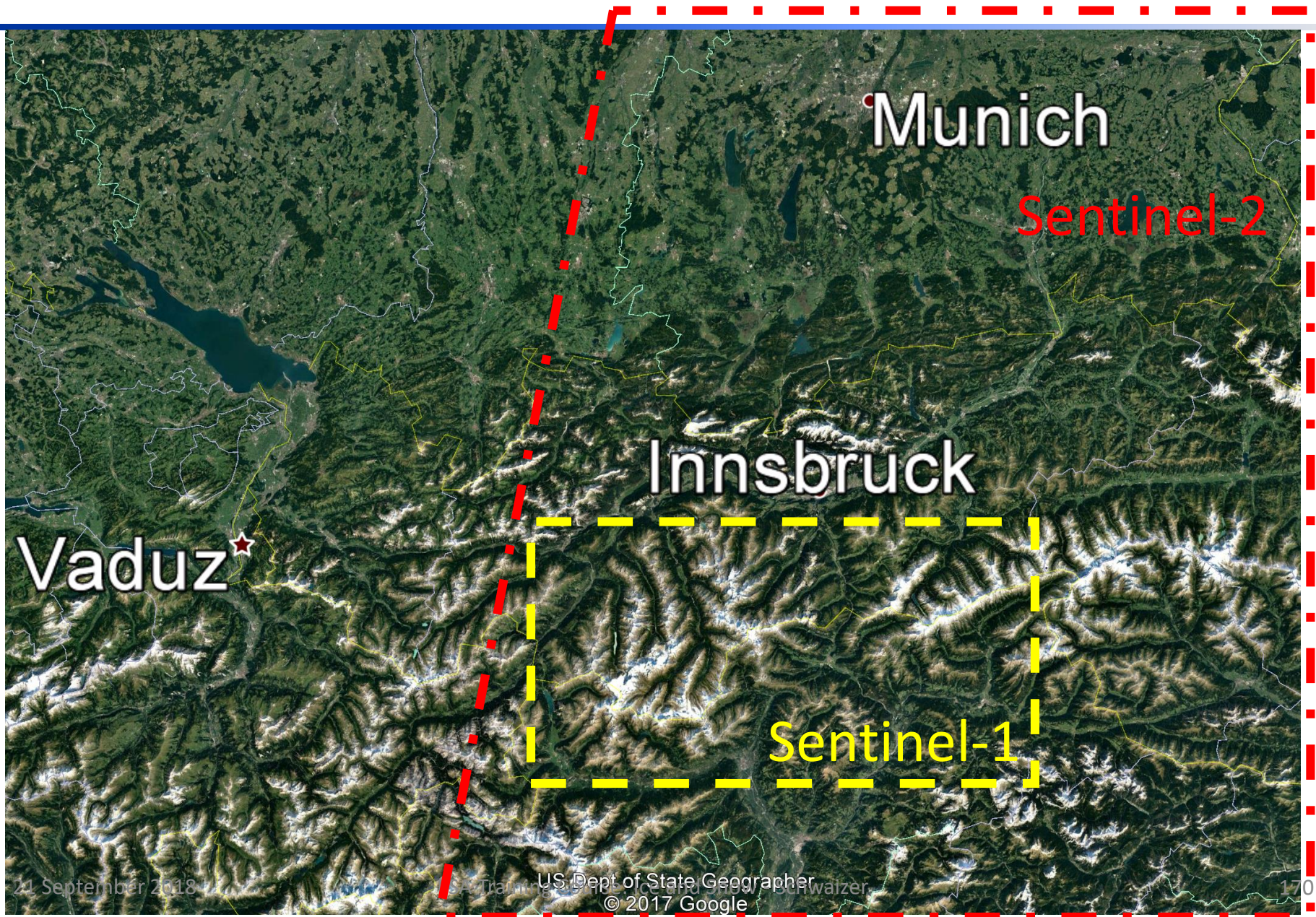
You can either work alone or together with a colleague.

In case of any problems or questions, feel free to communicate with your colleagues, or just ask me!

16:30 – 17:00:

Interpretation of results (together)

Test site: Alps



Alps – Dominant landscapes

Full data set: Lakes, urban areas, cultivated areas, mountains, forest

Subset: Mountains, glaciers, forest



Main data base for snow mapping:

*Sentinel-1 and Sentinel-2 images of **29 April 2016**: snow on mountains, snow free in the valleys, melting conditions*

*Sentinel-1 image of **30 January 2017**: dry snow conditions everywhere*